APOLLO LEM ADAPTER STRUCTURAL ANALYSIS

by

J. Padlog, W. Luberacki, R. H. Gallagher

Report No. 2286-950001

April 1966

Final Report

NASA Contract NAS 9-3970

Prepared for

The National Aeronautics and Space Administration
Manned Spacecraft Center
Houston, Texas

BELL AEROSYSTEMS - A textron COMPANY

FOREWORD

This report was prepared by Bell Aerosystems, a Textron Company, under NASA Contract NAS9-3970 and covers work performed for the NASA Manned Spacecraft Center, Houston, Texas during the period January 1965 to April 1966. The contract was administered under the direction of Mr. P. D. Smith of Structures and Mechanics Division, NASA Manned Spacecraft Center. Mr. J. Padlog acted as Principal Investigator.

The authors wish to acknowledge the assistance and contributions provided this project by Messrs. F. Braun and D. M. Dupree.

ABSTRACT

29079

Results of a stress and deformation analysis performed on the Apollo LEM Adapter for various design conditions are presented. Effects of both mechanical and thermal loads are included in the analysis. Particular attention is given to the determination of the reactions at the attachment points between the LEM and LEM Adapter of the Apollo Vehicle.

Author

CONTENTS

ILLUSTRATIONS

ILLUSTRATIONS (CONT)

TABLES

I. INTRODUCTION

This report presents the results of a stress and displacement analysis performed on the Apollo LEM Adapter for various applied mechanical and thermal load conditions (Ref. 1). The method of analysis employed is the matrix displacement method, which is based on the use of discrete elements for idealization of the structure. Numerical results were obtained with use of the Bell General Purpose Structural Analysis Computer Program, a program for matrix displacement analyses of complex structures.

One of the major objectives of the analysis performed was the determination of the interaction loads between the LEM and LEM Adapter of the Apollo vehicle for the various design conditions of interest. This task was accomplished in part by considering the LEM as a discrete element with known stiffness properties.

Section II of this report presents in detail the various conditions of analysis investigated and the assumptions made regarding such items as structural characteristics and support conditions. A description of the methods employed to determine the structural and load idealization required for the analysis is contained in Section III. Numerical results obtained from the stress and deformation analyses are then summarized in Section IV. Conclusions deduced from the results obtained for the various analyses performed are briefly summarized in Section V. This Section also contains recommendations for future analyses.

For completeness of presentation of the work performed, a brief description of the Bell General Purpose Structural Analysis Computer Program is presented in Appendix A.

In order to treat the LEM as a discrete structural element in the displacement analysis approach employed, it was necessary to transform available LEM flexibility matrices to symmetrical stiffness matrices. The procedure used to accomplish these transformations is outlined in Appendix B.

II. ANALYSIS CONDITIONS

A. GENERAL ARRANGEMENT

The general arrangement of the Apollo vehicle is illustrated in Figure 1. The work described in this report is specifically directed towards the determination of the structural behavior of the LEM Adapter, which extends between Stations 502.0 and 838.0, and of the loads acting at the interface between the LEM Adapter and the LEM (Station 583.0).

Because of the extreme complexity of the LEM Adapter, it was necessary to treat the structure as symmetric about one plane with the subsequent consideration of one-half of the structure. The LEM Adapter is basically a stiffened sandwich shell which is composed of aluminum alloy, type 2024. The properties of this material, as a function of temperature are shown in Figure 2.

The loading conditions concern two orientations of the entire vehicle with respect to airload direction. Actually, neither condition can be identified exactly with an axis of symmetry. Satisfactory approximations can be formed, however, and for this reason each of the load conditions is associated with a different symmetrized idealization of the structure.

B. STRUCTURAL CHARACTERISTICS

Idealization of the LEM Adapter structure into discrete structural elements for two separate orientations with regard to air loadings is shown in Figures 3 and 4. The coordinates of the node points in each idealization appear in Tables 1 and 2. The sandwich panels of which the Adapter is fabricated are represented by equivalent flat plate elements in plane stress and flexure. The characteristics of the sandwich element and LEM stiffness are defined in Section IIIB. The stiffeners, both circumferential and longitudinal, are represented by means of axial-flexural elements whose stiffness properties are in the form of areas and moments of inertia. These properties are summarized in Table 3. Element I essentially represents a ring element at the SM-LEM Adapter interface. To account for the large inplane stiffness of the SM aft bulkhead also located at this station, the moment of inertia, I_{yy}, of this element was assumed as 1000 $in.^4$. The LEM stiffness properties for both orientations are derived in Appendix B.

C. SUPPORT CONDITIONS

Because of symmetry, certain displacements and rotations are completely restrained on the plane of symmetry and are so designated in the input to the program.

Normally, any point in a stiffened shell structure can have six degrees of freedom (three translations and three rotations). When considering a flat plate in flexure,

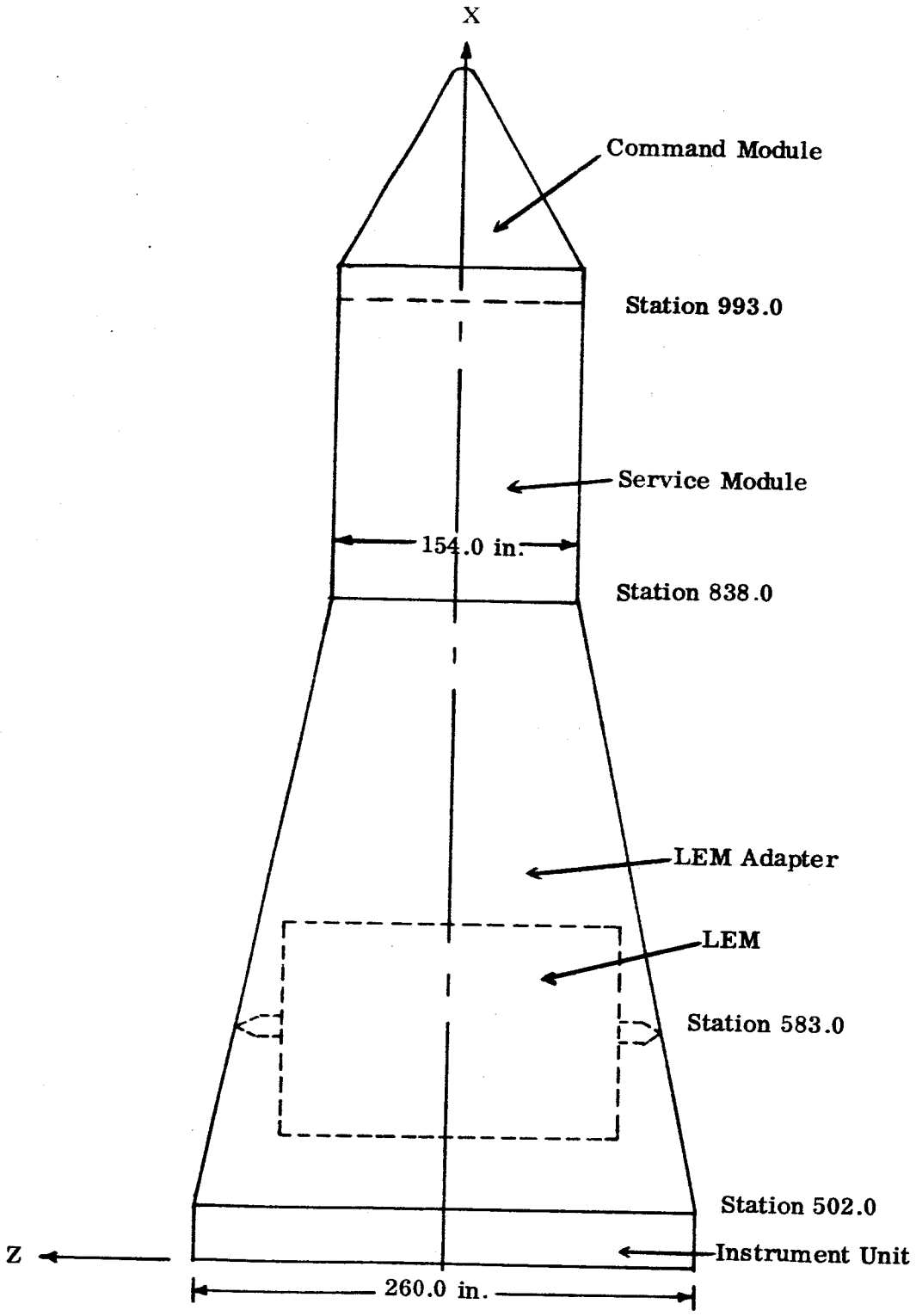

Figure 1. Apollo Vehicle

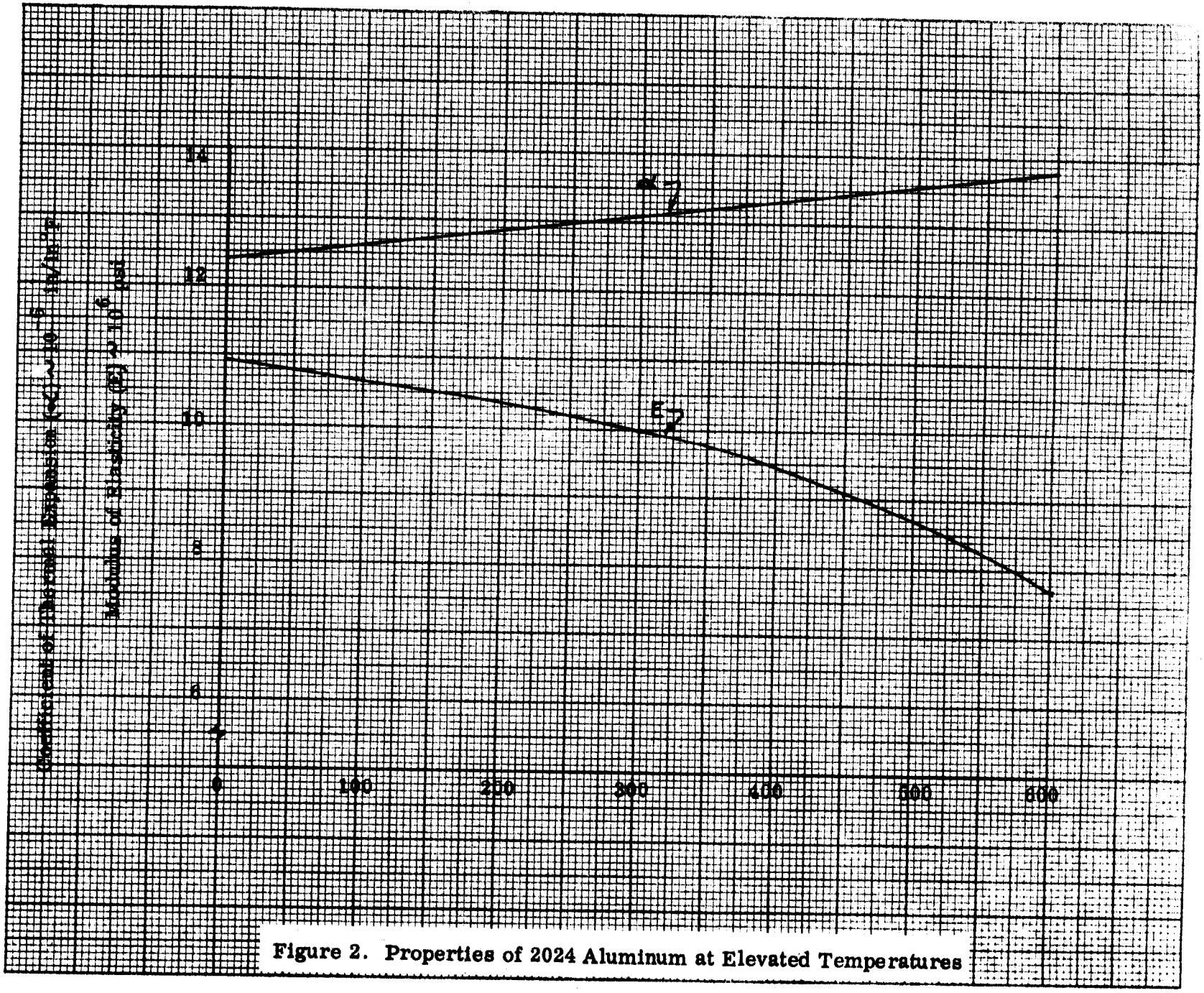

Figure 2. Properties of 2024 Aluminum at Elevated Temperatures

See Table 3 for Properties of Structural Elements

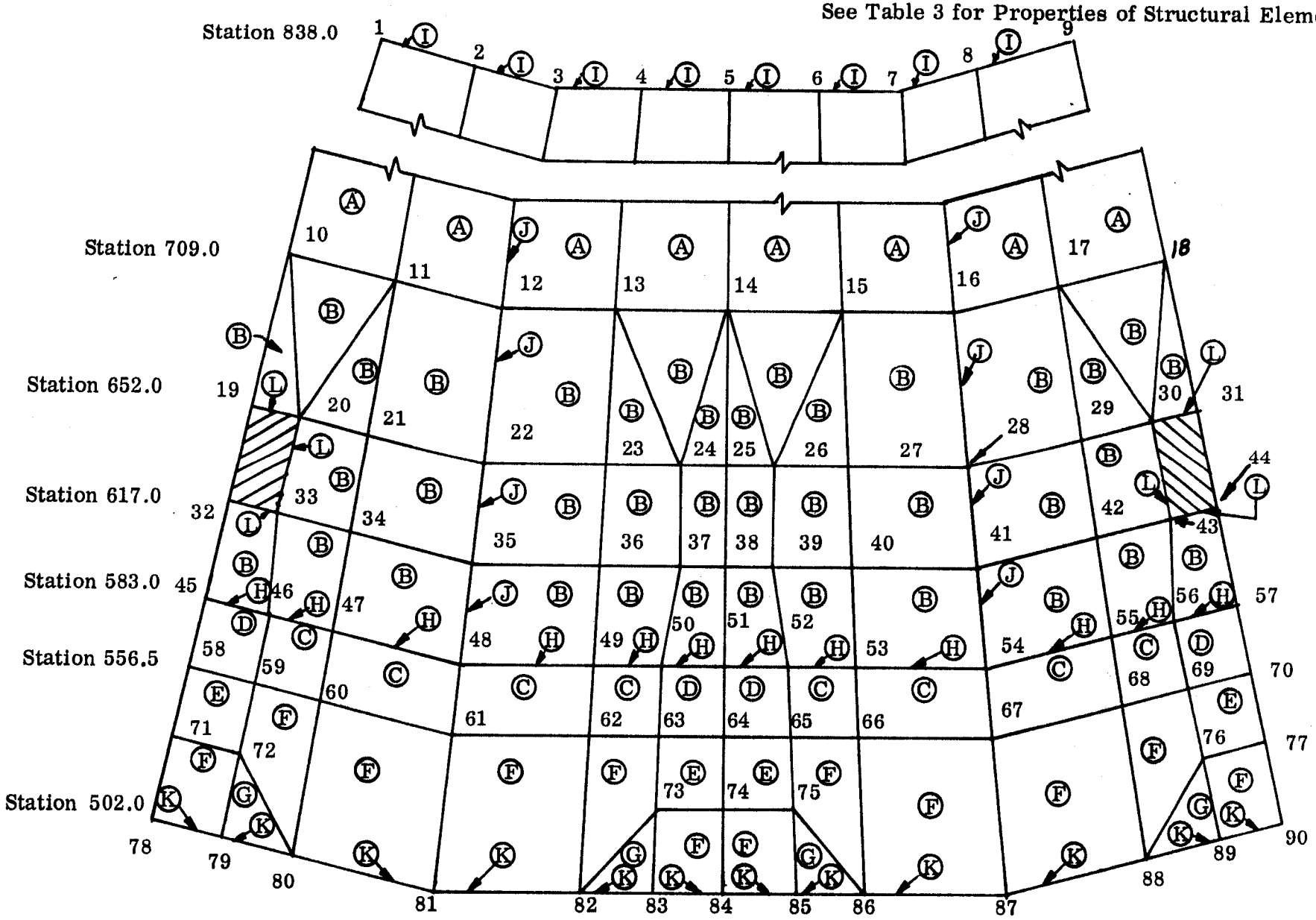

Figure 3. Idealization Geometry - 0° Air Load Orientation

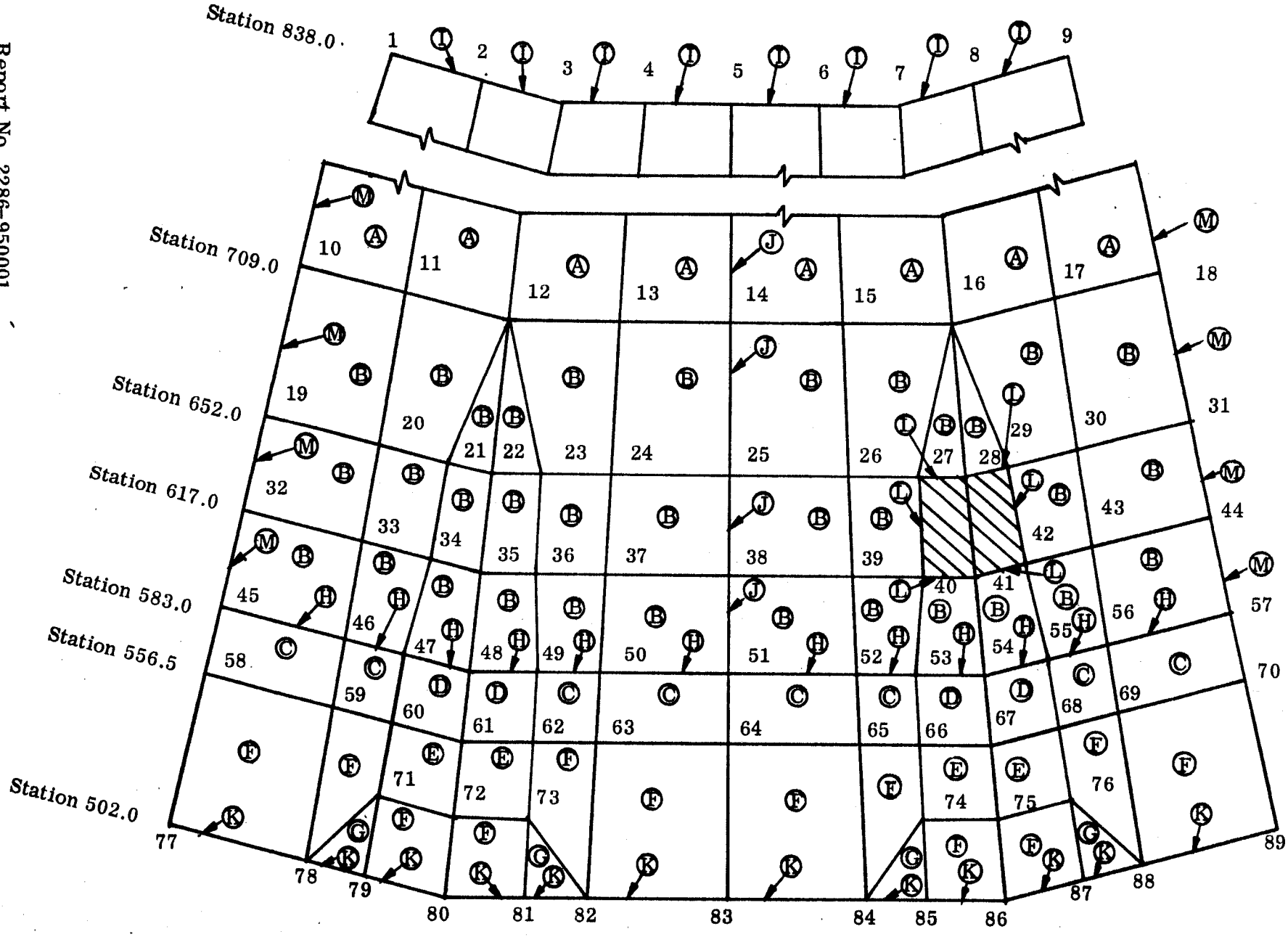

See Table 3 for Properties of Structural Elements

Figure 4. Idealization Geometry - 45° Air Load Orientation

TABLE 1

NODE POINT NUMBERS WITH RESPECTIVE COORDINATES*
0° AIR LOAD ORIENTATION

Node Pt.	X	Y	Z	Node Pt.	X	Y	Z
1	838.0	0	-77.0	46	583.0	20.199	-115.470
2	838.0	29.467	-71.138	47	583.0	44.859	-108.300
3	838.0	54.447	-54.447	48	583.0	82.889	-82.889
4	838.0	71.138	-29.467	49	583.0	108.300	-44.859
5	838.0	77.0	0	50	583.0	115.470	-20.199
6	838.0	71.138	29.467	51	583.0	117.223	0
7	838.0	54.447	54.447	52	583.0	115.470	20.199
8	838.0	29.467	71.138	53	583.0	108.300	44.859
9	838.0	0	77.0	54	583.0	82.889	82.889
10	709.0	0	-97.348	55	583.0	44.859	108.300
11	709.0	37.253	-89.938	56	583.0	20.199	115.470
12	709.0	68.835	-68.835	57	583.0	0	117.223
13	709.0	89.938	-37.253	58	556.5	0	-121.403
14	709.0	97.348	0	59	556.5	20.206	-119.710
15	709.0	89.938	37.253	60	556.5	46.459	-112.162
16	709.0	68.835	68.835	61	556.5	85.845	-85.845
17	709.0	37.253	89.938	62	556.5	112.162	-46.459
18	709.0	0	97.348	63	556.5	119.710	-20.206
19	652.0	0	-106.339	64	556.5	121.403	0
20	652.0	14.455	-105.352	65	556.5	119.710	20.206
21	652.0	40.694	-98.224	66	556.5	112.162	46.459
22	652.0	75.193	-75.193	67	556.5	85.845	85.845
23	652.0	98.244	-40.693	68	556.5	46.459	112.162
24	652.0	105.352	-14.455	69	556.5	20.206	119.710
25	652.0	106.339	0	70	556.5	0	121.403
26	652.0	105.352	14.455	71	532.0	0	-125.268
27	652.0	98.244	40.693	72	532.0	20.211	-123.627
28	652.0	75.193	75.193	73	532.0	123.627	-20.211
29	652.0	40.694	98.224	74	532.0	125.268	0
30	652.0	14.455	105.352	75	532.0	123.627	20.211
31	652.0	0	106.339	76	532.0	20.211	123.627
32	617.0	0	-111.860	77	532.0	0	125.268
33	617.0	14.459	-110.922	78	502.0	0	-130.000
34	617.0	42.807	-103.345	79	502.0	20.218	-128.418
35	617.0	79.097	-79.097	80	502.0	49.749	-120.104
36	617.0	103.345	-42.807	81	502.0	91.924	-91.924
37	617.0	110.922	-14.459	82	502.0	120.104	-49.749
38	617.0	111.860	0	83	502.0	128.418	-20.218
39	617.0	110.922	14.459	84	502.0	130.000	0
40	617.0	103.345	42.807	85	502.0	128.418	20.218
41	617.0	79.097	79.097	86	502.0	120.104	49.749
42	617.0	42.807	103.345	87	502.0	91.924	91.924
43	617.0	14.459	110.922	88	502.0	49.749	120.104
44	617.0	0	111.860	89	502.0	20.218	128.418
45	583.0	0	-117.223	90	502.0	0	130.000

Note: Node Point 91 is the c.g. of the LEM and hence, requires no coordinates. (*Dimensions are in inches.)

TABLE 2

NODE POINT NUMBERS WITH RESPECTIVE COORDINATES*
45° AIR LOAD ORIENTATION

Node Pt.	X	Y	Z	Node Pt.	X	Y	Z
1	838.0	0	-77.0	45	583.0	0	-117.223
2	838.0	29.467	-71.138	46	583.0	44.859	-108.300
3	838.0	54.447	-54.447	47	583.0	67.367	-95.932
4	838.0	71.138	-29.467	48	583.0	82.889	-82.889
5	838.0	77.0	0	49	583.0	95.932	-67.367
6	838.0	71.138	29.467	50	583.0	108.300	-44.859
7	838.0	54.447	54.447	51	583.0	117.223	0
8	838.0	29.467	71.138	52	583.0	108.300	44.859
9	838.0	0	77.0	53	583.0	95.932	67.367
10	709.0	0	-97.348	54	583.0	82.889	82.889
11	709.0	37.253	-89.938	55	583.0	67.367	95.932
12	709.0	68.835	-68.835	56	583.0	44.859	108.300
13	709.0	89.938	-37.253	57	583.0	0	117.223
14	709.0	97.348	0	58	556.5	0	-121.403
15	709.0	89.938	37.253	59	556.5	46.459	-112.162
16	709.0	68.835	68.835	60	556.5	70.360	-98.935
17	709.0	37.253	89.938	61	556.5	85.845	-85.845
18	709.0	0	97.348	62	556.5	98.935	-70.360
19	652.0	0	-106.339	63	556.5	112.162	-46.459
20	652.0	40.694	-98.224	64	556.5	121.403	0
21	652.0	64.274	-84.716	65	556.5	112.162	46.459
22	652.0	75.193	-75.193	66	556.5	98.935	70.360
23	652.0	84.716	-64.274	67	556.5	85.845	85.845
24	652.0	98.244	-40.693	68	556.5	70.360	98.935
25	652.0	106.339	0	69	556.5	46.459	112.162
26	652.0	98.244	40.693	70	556.5	0	121.403
27	652.0	84.716	64.274	71	532.0	73.126	-101.709
28	652.0	75.193	75.193	72	532.0	88.578	-88.578
29	652.0	64.274	84.716	73	532.0	101.709	-73.126
30	652.0	40.694	98.224	74	532.0	101.709	73.126
31	652.0	0	106.339	75	532.0	88.578	88.578
32	617.0	0	-111.860	76	532.0	73.126	101.709
33	617.0	42.807	-103.345	77	502.0	0	-130.0
34	617.0	68.209	-88.658	78	502.0	49.749	-120.104
35	617.0	79.097	-79.097	79	502.0	76.509	-105.101
36	617.0	88.658	-68.209	80	502.0	91.924	-91.924
37	617.0	103.345	-42.807	81	502.0	105.101	-76.509
38	617.0	111.860	0	82	502.0	120.104	-49.749
39	617.0	103.345	42.807	83	502.0	130.0	0
40	617.0	88.658	68.209	84	502.0	120.104	49.749
41	617.0	79.097	79.097	85	502.0	105.101	76.509
42	617.0	68.209	88.658	86	502.0	91.924	91.924
43	617.0	42.807	103.345	87	502.0	76.509	105.101
44	617.0	0	111.860	88	502.0	49.749	120.104
				89	502.0	0	130.0

Note: Node Point 90 is the c.g. of the LEM and hence, requires no coordinates. (*Dimensions are in inches.)

(Reference 8), however, the angular rotation of a plate element in its own plane is very small and may be assumed to be zero. This degree of freedom can be eliminated by the introduction of an oblique coordinate system in a manner described in Appendix A. Thus, only 5 degrees of freedom remain, in general, at each node point. This approach has been used in the analysis of the LEM Adapter.

The lower edge of the LEM Adapter (Station 502.0) is assumed simply supported, i.e., all linear displacements are restrained and only one rotatory degree of freedom is allowed as shown in the sketch below.

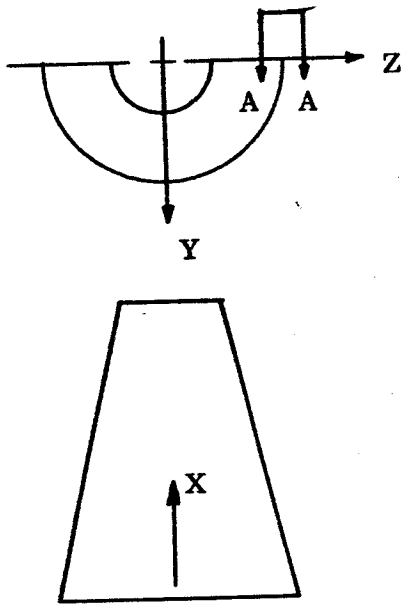

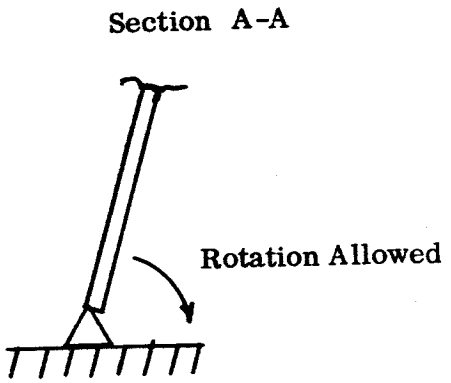

TABLE 3

GEOMETRIC PROPERTIES OF ELEMENTS

a) Plate Element Properties

Element*	Outer Thickness (Inches)	Inner Thickness (Inches)	Equivalent Bending Thickness (Inches)
Ⓐ	0.032	0.015	0.714
Ⓑ	0.029	0.015	0.706
Ⓒ	0.027	0.015	0.699
Ⓓ	0.051	0.041	0.940
Ⓔ	0.041	0.029	0.846
Ⓕ	0.027	0.015	0.699
Ⓖ	0.027	0.022	0.737

b) Flexural Element Properties

Element*	Area ($in.^2$)	I_{xx} ($in.^4$)	I_{yy} ($in.^4$)	J ($in.^4$)
Ⓗ	0.977	0.2534	1.532	0.00424
Ⓘ	1.91188	8.73254	1000.0	0.0383
Ⓙ	0.719	0.0285	0.6285	0.1990
Ⓚ	0.5279	0.2090	0.0710	0.00294
Ⓛ	0.439	0.287	0.16774	0.002744
Ⓜ	0.360	0.01425	0.31425	0.0995

*See Figures 3 and 4 for location

D. LOADING CONDITIONS

The LEM Adapter has been analyzed for the following three distinct design conditions:

1. Maximum q_α
2. End Boost Phase
3. Hardover Engine Burnout

The first condition contains only mechanical loads, as given in Reference 2. However, the second and third conditions involve both mechanical loads and temperature distributions over the Adapter as given in Reference 3.

Mechanical loads given in references 2 and 3 are presented in Figures 5 through 8. These loads were transformed into equivalent loads that are consistent with the form of input data as required by the Bell General Purpose Structural Analysis Computer Program. The manner in which these equivalent loads were determined for the analysis is discussed in detail in Section III and are tabulated in Tables 4 - 7. Applied forces at the support, Station 502, are omitted because they are reacted directly by the support and therefore do not effect the behavior of the LEM Adapter Structure.

The temperature distribution of the inner and outer skins, shown in Figure 9, was obtained from Reference 3. Not only does the temperature level cause a significant variation in the mechanical properties of the material as shown in Figure 2, but a significant thermal moment is introduced due to the difference in the inner and outer skins. The Bell General Purpose Structural Analysis Computer Program automatically accounts for the variation of temperature (see Appendix A), but the thermal moment loads for the LEM Structure must first be hand-computed, using an equation derived in Section III. For all design conditions, the LEM is assumed to be at the original ambient temperature, 70°F.

E. AIRLOAD ORIENTATION

From Reference (1), it is noted that the LEM Adapter may behave differently when subjected to the various possible orientations of the airload (wind load). To determine the significance of the orientation of the pressure load on the LEM Adapter stresses and deformations, two different conditions of load orientations were considered for analysis. These orientations are referred to the Z reference coordinate axis of the Apollo (see Figure 1) and are defined as follows:

1. 0° Airload Orientation
2. 45° Airload Orientation

It is noted from References (2) and (3), that since End Boost and Hardover Engine Conditions have no pressure load, only the Max q_α condition must be analyzed for both orientations.

TABLE 4

NODE POINT LOAD COMPONENTS DUE TO INTERFACE LOADINGS

Node Point	Condition: Max. $q\alpha$			End Boost			Hardover Engine		
	F_x [1] (lbs)	F_z [2] (lbs)	F_x [3] (lbs)	F_x [1] (lbs)	F_z [2] (lbs)	F_x [3] (lbs)	F_x [1] (lbs)	F_z [2] (lbs)	F_x [3] (lbs)
1	7602	343	-5815	1016	57	-10812	2222	220	-4125
2	14046	2002	-11630	1877	330	-21624	4105	1283	-8250
3	10751	3710	-11630	1437	612	-21624	3142	2377	-8250
4	5818	4847	-11630	778	799	-21624	1700	3105	-8250
5	0	5247	-11630	0	865	-21624	0	3361	-8250
6	-5818	4847	-11630	-778	799	-21624	-1700	3105	-8250
7	-10751	3710	-11630	-1437	612	-21624	-3142	2377	-8250
8	-14046	2002	-11630	-1877	330	-21624	-4105	1283	-8250
9	-7602	343	-5815	-1016	57	-10812	-2222	220	-4125

[1] Due to M_A, [2] Due to S_A, [3] Due to AF

TABLE 5 (a)

NORMAL NODE POINT LOADS, F, DUE TO PRESSURE LOADING

MAX. q_α CONDITION 0° AIR LOAD ORIENTATION

Node Pt.	F (lbs)	Node Pt.	F (lbs)	Node Pt.	F (lbs)	Node Pt.	F (lbs)
1	1161	21	1168	41	42	61	814
2	2068	22	1121	42	34	62	282
3	1487	23	519	43	20	63	33
4	909	24	192	44	7	64	-7
5	568	25	39	45	275	65	-19
6	468	26	81	46	638	66	-139
7	468	27	98	47	852	67	-209
8	468	28	134	48	751	68	-139
9	234	29	98	49	310	69	-19
10	1647	30	47	50	55	70	-8
11	3075	31	16	51	7	71	185
12	2168	32	272	52	-7	72	455
13	1290	33	712	53	-11	73	-137
14	686	34	995	54	-15	74	-127
15	569	35	865	55	-11	75	-200
16	564	36	385	56	-7	76	-200
17	569	37	91	57	-4	77	-68
18	278	38	23	58	245		
19	264	39	20	59	544		
20	1074	40	34	60	975		

TABLE 5 (b)
NORMAL NODE POINT LOADS, F, DUE TO PRESSURE LOADING
MAXIMUM q_α CONDITION, 45° AIR LOAD ORIENTATION

Node Pt.	F (lbs)	Node Pt.	F (lbs)	Node Pt.	F (lbs)	Node Pt.	F (lbs)
1	1161	21	722	41	14	61	282
2	1068	22	322	42	21	62	183
3	1487	23	436	43	34	63	-143
4	909	24	446	44	20	64	-498
5	568	25	228	45	622	65	-364
6	468	26	120	46	926	66	-81
7	468	27	75	47	481	67	-20
8	468	28	45	48	316	68	-81
9	234	29	75	49	259	69	-364
10	1694	30	120	50	177	70	-293
11	2961	31	68	51	47	71	185
12	2211	32	696	52	-14	72	160
13	1209	33	1060	53	-9	73	39
14	717	34	541	54	-8	74	-218
15	557	35	323	55	-9	75	-318
16	580	36	311	56	-14	76	-218
17	557	37	258	57	-9		
18	283	38	113	58	554		
19	883	39	34	59	758		
20	1433	40	21	60	365		

TABLE 6
NODE POINT LOADS DUE TO INERTIA LOADING
0° AIR LOAD ORIENTATION

Node Pt.	Condition					
	Max q∝		End Boost		Hardover Engine	
	F_X* (lbs)	F_Z (lbs)	F_X* (lbs)	F_Z (lbs)	F_X* (lbs)	F_Z (lbs)
1	39.739	1.23	339.984	6.827	44.383	5.469
2	79.478	2.46	679.968	13.654	88.766	10.938
3	79.478	2.46	679.968	13.654	88.766	10.938
4	79.478	2.46	679.968	13.654	88.766	10.938
5	79.478	2.46	679.968	13.654	88.766	10.938
6	79.478	2.46	679.968	13.654	88.766	10.938
7	79.478	2.46	679.968	13.654	88.766	10.938
8	79.478	2.46	679.968	13.654	88.766	10.938
9	39.739	1.23	339.984	6.827	44.383	5.469
10	51.118	2.05	124.246	2.694	64.026	7.889
11	102.236	4.10	248.492	5.388	128.052	15.778
12	102.236	4.10	248.492	5.388	128.052	15.778
13	102.236	4.10	248.492	5.388	128.052	15.778
14	102.236	4.10	248.492	5.388	128.052	15.778
15	102.236	4.10	248.492	5.388	128.052	15.778
16	102.236	4.10	248.492	5.388	128.052	15.778
17	102.236	4.10	248.492	5.388	128.052	15.778
18	51.118	2.05	124.246	2.694	64.026	7.889
19	9.533	0.48	24.404	0.598	11.005	1.356
20	27.351	1.36	70.013	1.716	31.572	3.890
21	45.169	2.23	115.626	2.835	52.139	6.424
22	54.702	2.70	140.026	3.434	63.144	7.780
23	45.169	2.23	115.626	2.835	52.139	6.424
24	27.351	1.36	70.013	1.716	31.572	3.890
25	19.066	0.96	48.808	1.196	22.010	2.712
26	27.351	1.36	70.013	1.716	31.572	3.890
27	45.169	2.23	115.626	2.835	52.139	6.424
28	54.702	2.70	140.026	3.434	63.144	7.780
29	45.169	2.23	115.626	2.835	52.139	6.424
30	27.351	1.36	70.013	1.716	31.572	3.890
31	9.533	0.48	24.404	0.598	11.005	1.356
32	7.237	0.37	17.096	0.376	7.908	0.965
33	21.961	1.12	51.897	1.142	23.998	2.928
34	36.685	1.88	86.657	1.908	40.088	4.891
35	43.922	2.25	103.752	2.284	47.996	5.856
36	36.685	1.88	86.657	1.908	40.088	4.891
37	21.961	1.12	51.897	1.142	23.998	2.928
38	14.474	0.74	34.192	0.752	15.816	1.930
39	21.961	1.12	51.897	1.142	23.998	2.928
40	36.685	1.88	86.657	1.908	40.088	4.891

*All F_x Values are Negative Quantities.

TABLE 6 (CONT)

Node Pt.	Condition					
	Max q_α		End Boost		Hardover Engine	
	F_X* (lbs)	F_Z (lbs)	F_X* (lbs)	F_Z (lbs)	F_X* (lbs)	F_Z (lbs)
41	43.922	2.25	103.752	2.284	47.996	5.856
42	36.685	1.88	86.657	1.908	40.088	4.891
43	21.961	1.12	51.897	1.142	23.998	2.928
44	7.237	0.37	17.096	0.376	7.908	0.965
45	14.639	0.86	39.382	0.790	11.483	1.079
46	33.244	1.95	89.434	1.794	26.078	2.451
47	51.849	3.04	139.486	2.798	40.673	3.823
48	66.488	3.87	178.868	3.588	52.156	4.902
49	51.849	3.04	139.486	2.798	40.673	3.823
50	33.244	1.95	89.434	1.794	26.078	2.451
51	29.278	1.72	78.764	1.580	22.966	2.158
52	33.244	1.95	89.433	1.794	26.078	2.451
53	51.849	3.04	139.486	2.798	40.673	3.823
54	66.488	3.87	178.868	3.588	52.156	4.902
55	51.849	3.04	139.486	2.798	40.673	3.823
56	33.244	1.95	89.433	1.794	26.078	2.451
57	14.639	0.86	39.382	0.790	11.483	1.079
58	7.156	0.40	18.341	0.401	11.586	0.828
59	16.815	0.93	43.097	0.942	27.224	1.945
60	41.452	2.34	166.297	2.272	65.946	4.710
61	52.501	2.97	134.631	2.879	83.532	5.966
62	41.452	2.34	166.297	2.272	65.946	4.710
63	16.815	0.93	43.097	0.942	27.224	1.945
64	14.312	0.80	36.681	0.802	23.172	1.656
65	16.815	0.93	43.097	0.942	27.224	1.945
66	41.452	2.34	166.297	2.272	65.946	4.710
67	52.501	2.97	134.631	2.879	83.532	5.966
68	41.452	2.34	166.297	2.272	65.946	4.710
69	16.815	0.93	43.097	0.942	27.224	1.945
70	7.156	0.40	18.341	0.401	11.586	0.828
71	7.786	0.47	19.985	0.410	11.999	0.857
72	18.871	1.12	48.437	0.993	29.082	2.077
73	18.871	1.12	48.437	0.993	29.082	2.077
74	15.572	0.94	39.970	0.820	23.998	1.714
75	18.871	1.12	48.437	0.993	29.082	2.077
76	18.871	1.12	48.437	0.993	29.082	2.077
77	7.786	0.47	19.985	0.410	11.999	0.857

* All F_X values are negative quantities.

TABLE 7 NODE POINT LOADS DUE TO INERTIA LOADING MAX q_d CONDITION

45° AIR LOAD ORIENTATION

Node Pt.	F_X* (lbs)	F_Z (lbs)	Node Pt.	F_X* (lbs)	F_Z (lbs)
1	39.739	1.23	39	36.685	1.88
2	79.478	2.46	40	21.961	1.12
3	79.478	2.46	41	14.474	0.74
4	79.478	2.46	42	21.961	1.12
5	79.478	2.46	43	36.685	1.88
6	79.478	2.46	44	21.961	1.12
7	79.478	2.46	45	33.244	1.95
8	79.478	2.46	46	51.849	3.04
9	39.739	1.23	47	33.244	1.95
10	51.118	2.05	48	29.278	1.73
11	102.236	4.10	49	33.244	1.95
12	102.236	4.10	50	51.849	3.04
13	102.236	4.10	51	66.488	3.89
14	102.236	4.10	52	51.849	3.04
15	102.236	4.10	53	33.244	1.95
16	102.236	4.10	54	29.278	1.73
17	102.236	4.10	55	33.244	1.95
18	51.118	2.05	56	51.849	3.04
19	27.351	1.35	57	33.244	1.95
20	45.169	2.23	58	27.250	1.49
21	27.351	1.35	59	41.452	2.34
22	19.066	0.96	60	16.815	0.93
23	23.351	1.35	61	14.312	0.80
24	45.169	2.23	62	16.815	0.93
25	54.702	2.70	63	41.452	2.34
26	45.169	2.23	64	52.501	2.97
27	27.351	1.35	65	41.452	2.34
28	19.066	0.96	66	16.815	0.93
29	27.351	1.35	67	14.312	0.80
30	45.169	2.23	68	16.815	0.93
31	27.351	1.35	69	41.452	2.34
32	21.961	1.12	70	27.250	1.49
33	36.685	1.88	71	18.871	1.12
34	21.961	1.12	72	15.572	0.94
35	14.474	0.74	73	18.871	1.12
36	21.961	1.12	74	18.871	1.12
37	36.685	1.88	75	15.572	0.94
38	43.922	2.25	76	18.871	1.12

* All F_X loads are negative quantities.

III. DETAIL STRUCTURAL AND LOAD IDEALIZATION

A. STRUCTURAL IDEALIZATION

As discussed in Section IIC, the structure of the LEM Adapter is represented by equivalent plane stress-flexural plate elements and axial-flexural beam members.

For the 0° airload orientation (Figure 3), 62 quadrilateral plates, 16 triangular plates and 46 axial-flexural members were used in the idealization.

For the 45° airload orientation (Figure 4), 66 quadrilateral plates, 8 triangular plates, and 50 axial-flexural members were used in the idealization.

Considering the LEM as a discrete structural element and making use of the stiffness properties discussed in Appendix B results in stiffness matrices for the two appropriate airload orientations as shown in Figures 10 and 11.

B. DERIVATION OF SANDWICH PLATE EQUIVALENCES

The procedure for converting a sandwich plate having unequal face thicknesses to an equivalent isotropic sandwich plate of thickness, t, is described as follows. Consideration is given only to situations in which flexural and extensional deformations are not coupled. Such a situation arises when a flexural element is superimposed on an element in plane stress.

By definition, sandwich and isotropic plates are equivalent when their stiffnesses are equal. Thus for the case of flexure

$$(EI)_{SANDWICH} = (EI)_{EQUIVALENT} \qquad \text{(III-1)}$$

and for extensional stiffness

$$(Et)_{SANDWICH} = (Et)_{EQUIVALENT} \qquad \text{(III-2)}$$

If it is assumed that Young's Modulus is the same for both plates, then (III-1) and (III-2) reduce to

$$I_{SANDWICH} = I_{EQUIVALENT} \qquad \text{(III-3)}$$

$$t_{SANDWICH} = t_{EQUIVALENT} \qquad \text{(III-4)}$$

Insertion of the expression for the moments of inertia, I, and thicknesses, t, into (III-3) and (III-4) results in

$$\frac{h^2 t_2 t_1}{t_1 + t_2} = \frac{t^3}{12} \qquad \text{(III-5)}$$

$$t_1 + t_2 = t \qquad \text{(III-6)}$$

where the symbols are defined in the accompanying sketches. From Equations (III-5) and (III-6), it is concluded that, for flexure, the equivalent plate thickness is

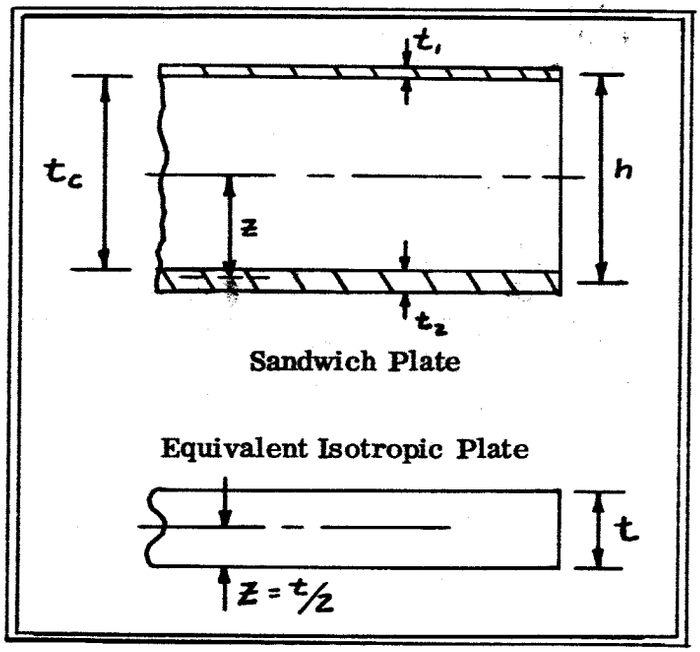

$$t = \left(\frac{12 h^2 t_2 t_1}{t_1 + t_2} \right)^{1/3} \qquad \text{(III-7)}$$

and for pure extension it is

$$t = t_1 + t_2 \qquad \text{(III-8)}$$

Results from analysis based on the use of the equivalent isotropic plate will yield equivalent stresses. The method by which the stresses in the sandwich are computed from the equivalent stresses is discussed below.

Conversion of flexural stresses is based on the fact that the curvatures of both sandwich and equivalent plates when loaded are equal (since they have the same stiffness). Hence, equating curvatures gives

$$\frac{d^2 w}{dx^2} = \frac{M}{EI} = \left(\frac{\sigma}{E z} \right)_{SAND} = \left(\frac{\sigma}{E z} \right)_{EQUIV} \qquad \text{(III-9)}$$

or, in general

$$\sigma_{sand} = Z_{sand} \left(\frac{\sigma}{Z}\right)_{equiv} \qquad \text{(III-10)}$$

where the symbols are defined in the sketches above.

Finally, from Equation III-10, the bending stress in the top face is determined as

$$\sigma_{top} = \frac{2ht_1}{t(t_1+t_2)} \sigma_{equiv} \qquad \text{(III-11)}$$

and in the bottom face as

$$\sigma_{bottom} = \frac{2ht_2}{t(t_1+t_2)} \sigma_{equiv} \qquad \text{(III-12)}$$

where σ_{equiv} is the computed outer fiber stress for the equivalent isotropic plate.

Membrane stresses in the sandwich faces are already equal to those computed for the equivalent isotropic plate.

C. DERIVATION OF THERMAL MOMENTS FOR SANDWICH PLATES

The thermal moment, M^{α}, for a plate is given by the expression

$$M^{\alpha} = \int \left(\frac{E\alpha T}{1-\nu}\right) \xi \, d\xi \qquad \text{(III-13)}$$

where E, α and ν are the properties at the average temperature of the plate, and ξ is the distance from the neutral axis to the top and bottom faces. Evaluating Equation (III-13) for the sandwich plate results in the following expression for the thermal moment.

$$M^{\alpha} = \frac{E\alpha h}{(1-\nu)} \left(\frac{t_1 t_2}{t_1+t_2}\right) (T_1 - T_2) \qquad \text{(III-14)}$$

The symbols in Equation (III-14) are defined in the sketch below:

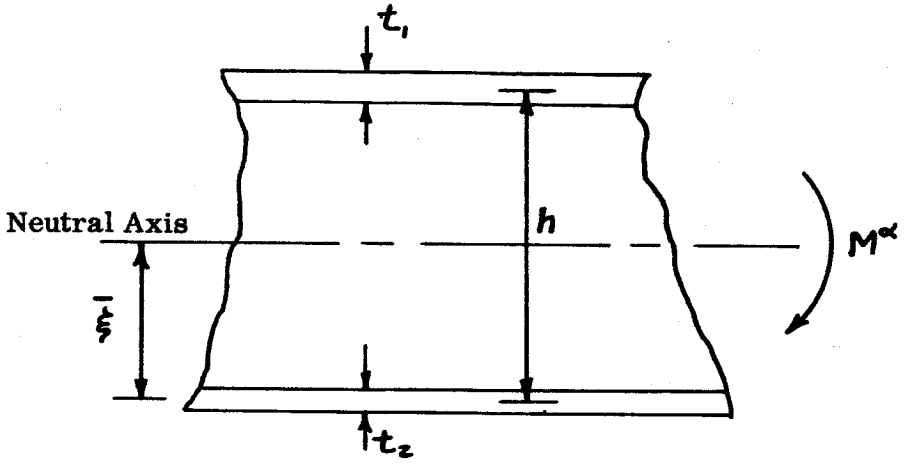

The distance $\bar{\xi}$, shown in the above sketch is defined as follows:

$$\bar{\xi} = \frac{t_1 h}{t_1 + t_2} \qquad \text{(III-15)}$$

D. LOAD IDEALIZATION

The mechanical loads for any design condition as given by References (2) and (3) have to be modified to be compatible with the input required by the Bell General Purpose Structural Analysis Computer Program. The modified loads are equivalent applied loads acting at the node points of the idealized structure as described in Appendix A.

The thermal loadings associated with temperature change, fall into two groups. The first of these is the inplane thermal loads which are generated automatically by the computer program from temperatures designated in the program input. The second group, which involves the thermal moment caused by temperature differences in the skin structure, is computed from Equation III-13. The thermal loadings computed act at the node points of the idealized structure (See Appendix A) and, therefore, need no further modifications.

A description of the method employed to determine the equivalent applied loads for the various mechanical loading systems is as follows:

1. Loads Due to Interface Loads

The interface loads of the Service Module and the LEM Adapter were assumed to be distributed circumferentially in accordance with strength of material concepts and therefore, were determined in the following manner.

a. Loads From the Bending Moment

From the engineering theory of bending

$$\sigma = \frac{Mc}{I} \tag{III-16}$$

The load intensity, ω, at any point on the circumference of the Adapter at the interface edge (Station 838.0) can be computed from

$$\omega = \sigma t = \frac{Mc}{I} t \tag{III-17}$$

where t, the effective thickness is given by

$$t = t_{OUTER} + t_{INNER} \tag{III-18}$$

Referring to the sketch shown below

$$I = I_{yy} = \pi r^3 t \tag{III-19}$$

and

$$c = Z = r \cos \phi \tag{III-20}$$

Substitution of Equations (III-18), (19) and (20) into Equation (III-17) yields

$$\omega = \frac{M \cos \phi}{\pi r^2} \tag{III-21}$$

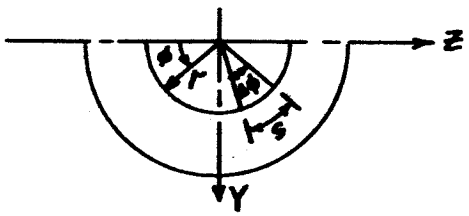

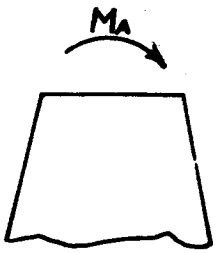

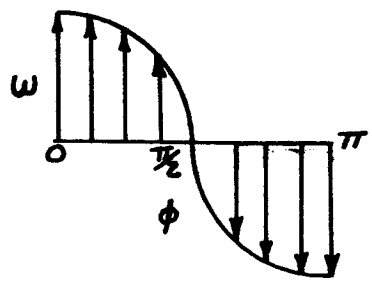

The equivalent applied load at any node on the edge circumference can be approximated from the assumed trapezoidal distribution as shown in the sketch below

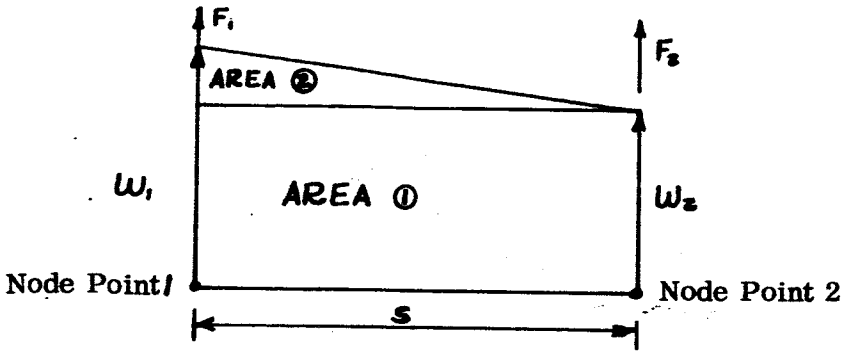

Thus, the equivalent applied loads are

$$F_1 = \frac{1}{2}\,\text{AREA}\,① + \frac{2}{3}\,\text{AREA}\,② = \frac{s}{6}\left[2\omega_1 + \omega_2\right]$$

and

$$F_2 = \frac{1}{2}\,\text{AREA}\,① + \frac{1}{3}\,\text{AREA}\,② = \frac{s}{6}\left[2\omega_2 + \omega_1\right] \qquad \text{(III-22)}$$

where from the previous sketches

$$s = r(\Delta\phi) \qquad \text{(III-23)}$$

and ω_1 , ω_2 are the load intensities at the respective nodes as computed from Equation (III-21).

b. Loads From the Shear Force (S_A)

The shear force (S_A) creates a shear flow, q, which is distributed circumferentially and given by the equation

$$q = q_{MAX}\ \sin\phi \qquad \text{(III-24)}$$

where the symbols are defined in the sketch below

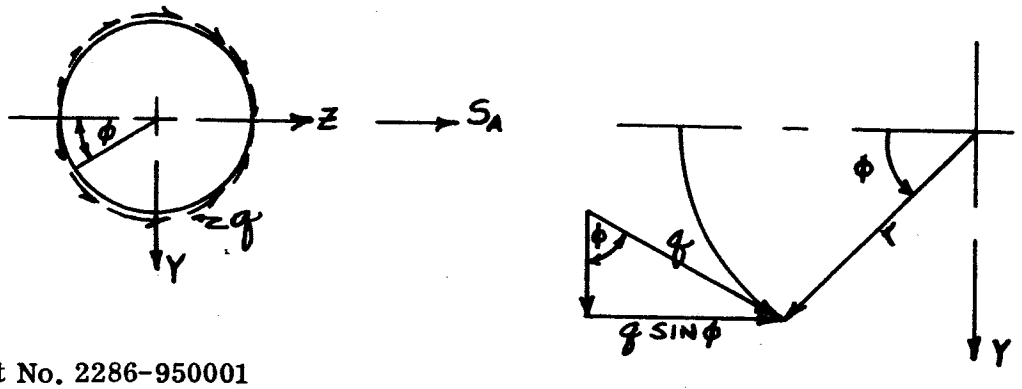

The expression for q_{MAX} is derived in the following manner.

First, we note that the shear force, S_A, is given by the expression

$$S_A = 2\int_0^{\pi} (q_{MAX} \sin\phi)(r \sin\phi)\, d\phi \qquad \text{(III-25)}$$

Integrating and solving the above expression for q_{MAX}, one obtained $q_{MAX} = \frac{S_A}{\pi r}$ and the expression for the shear flow becomes

$$q = \frac{S_A}{\pi r} \sin\phi \qquad \text{(III-26)}$$

Since the load distribution is assumed trapezoidal, the equivalent applied loads at the node points are determined in the same manner described previously (see Equation (III-22).

c. Loads From the Axial Force (AF)

The axial load (AF) is assumed to be distributed uniformly across the interface edge. Thus, the load intensity, ω, is found from

$$\omega = \frac{(AF)}{2\pi r} \qquad \text{(III-27)}$$

Being distributed uniformly between any two node points the equivalent load at both node points is

$$F_1 = F_2 = \frac{(AF)}{2\pi r}\left(\frac{1}{2} s\right) = \frac{(AF)\, s}{4\pi r} \qquad \text{(III-28)}$$

where again s is defined by Equation (III-23).

2. Inertia Loads

From Figures 6, 7, and 8 (References (2) and (3)), it is noted that the lateral and axial inertia loads are given as distributed loads, but are along the entire length of the structure. Since this load is of the same trapezoidal shape as discussed previously, the equivalent applied load acting at each station can be computed by Equation (III-22). Assuming this load now to be acting uniformily about the circumference of the respective station, the equivalent applied load at each node point is determined in the same manner as the axial load determination stated by Equation (III-28).

3. Pressure Loads

The method used to obtain equivalent node point loads for the pressure distribution given in Figure 5 (Reference (2)) is as follows. First, pressures were replotted at each station of the idalized structure in the circumferential direction. The result is a pressure value at all node points of the idealized structure. Knowing the surface area of any plate enclosed by three or four node points (triangular and quadrilateral plates respectively), the total load acting normal to the surface is computed by

$$F_{TOTAL} = (\text{SURFACE AREA}) \times (\text{AVERAGE PRESSURE}) \qquad \text{(III-29)}$$

The total load is then divided equally amongst the node points that contain the plate to obtain the equivalent applied load at each node point.

4. LEM Loads

The LEM loads were obtained from Reference (2) and (3) and are inputed directly into the analysis. These loads act at the center of gravity of the LEM (see Appendix B), and their particular magnitudes for each of the analysis condition examined in this report are contained in the figures of Section IV.

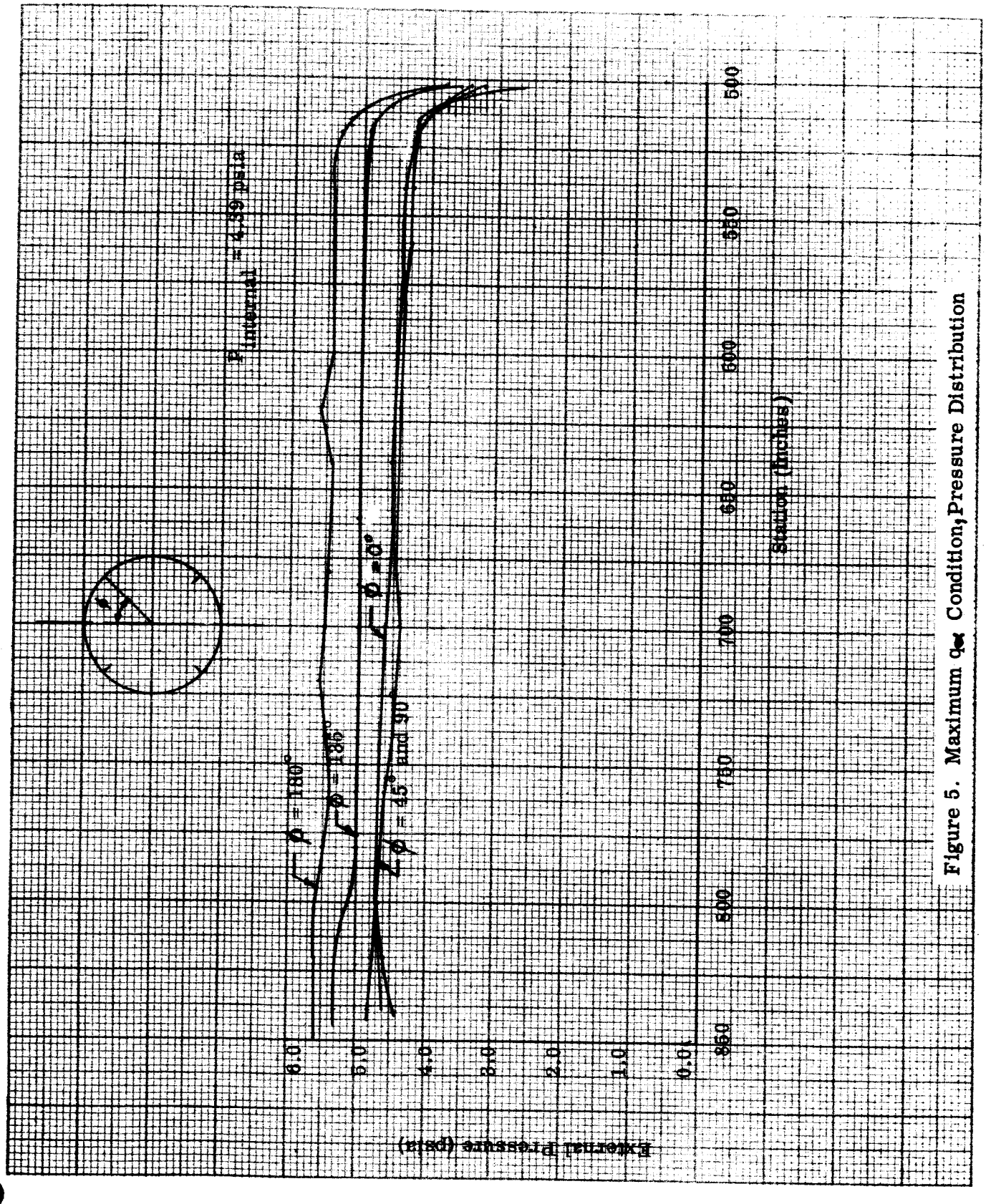

Figure 5. Maximum qα Condition, Pressure Distribution

Figure 6. Maximum g_x Condition, Axial and Lateral Inertia

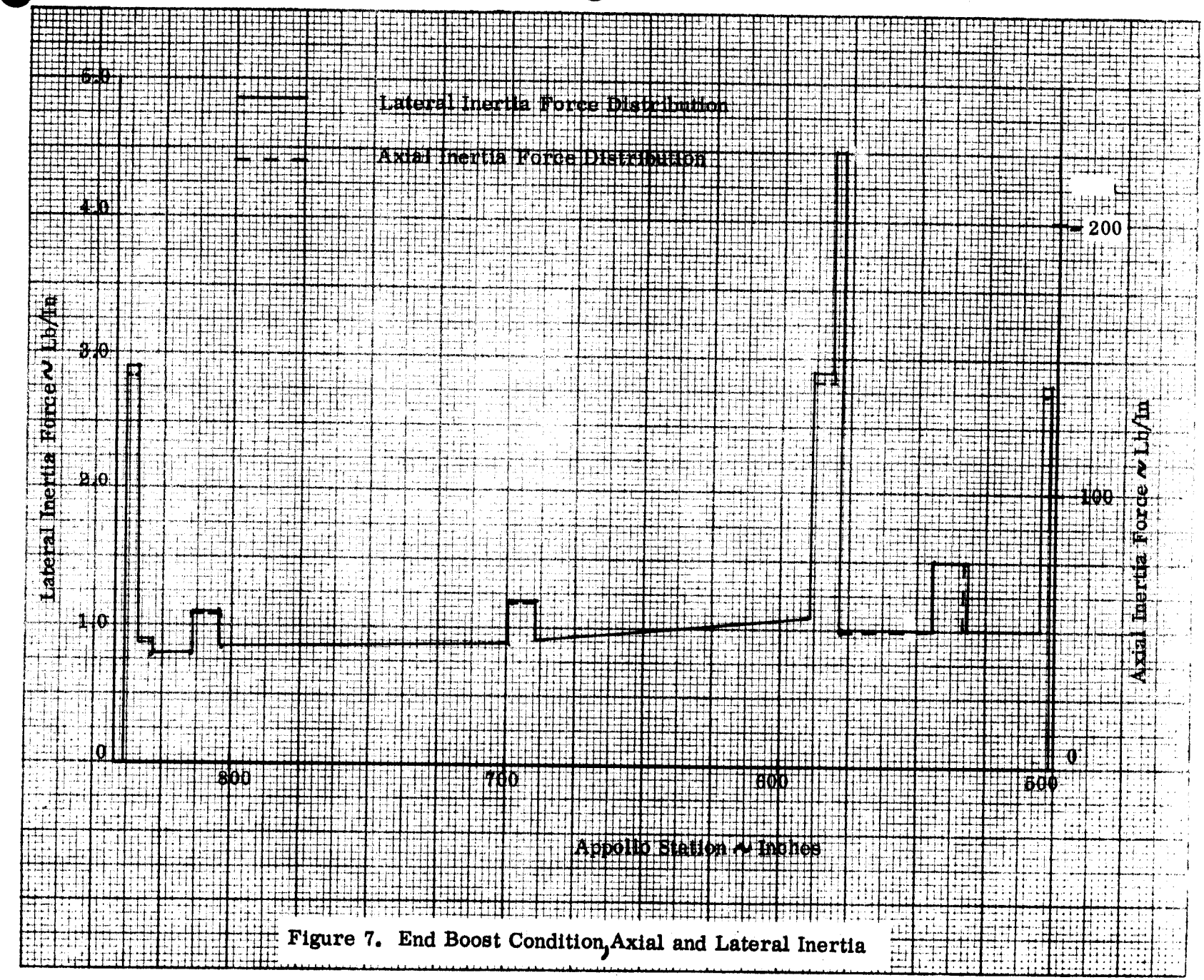

Figure 7. End Boost Condition, Axial and Lateral Inertia

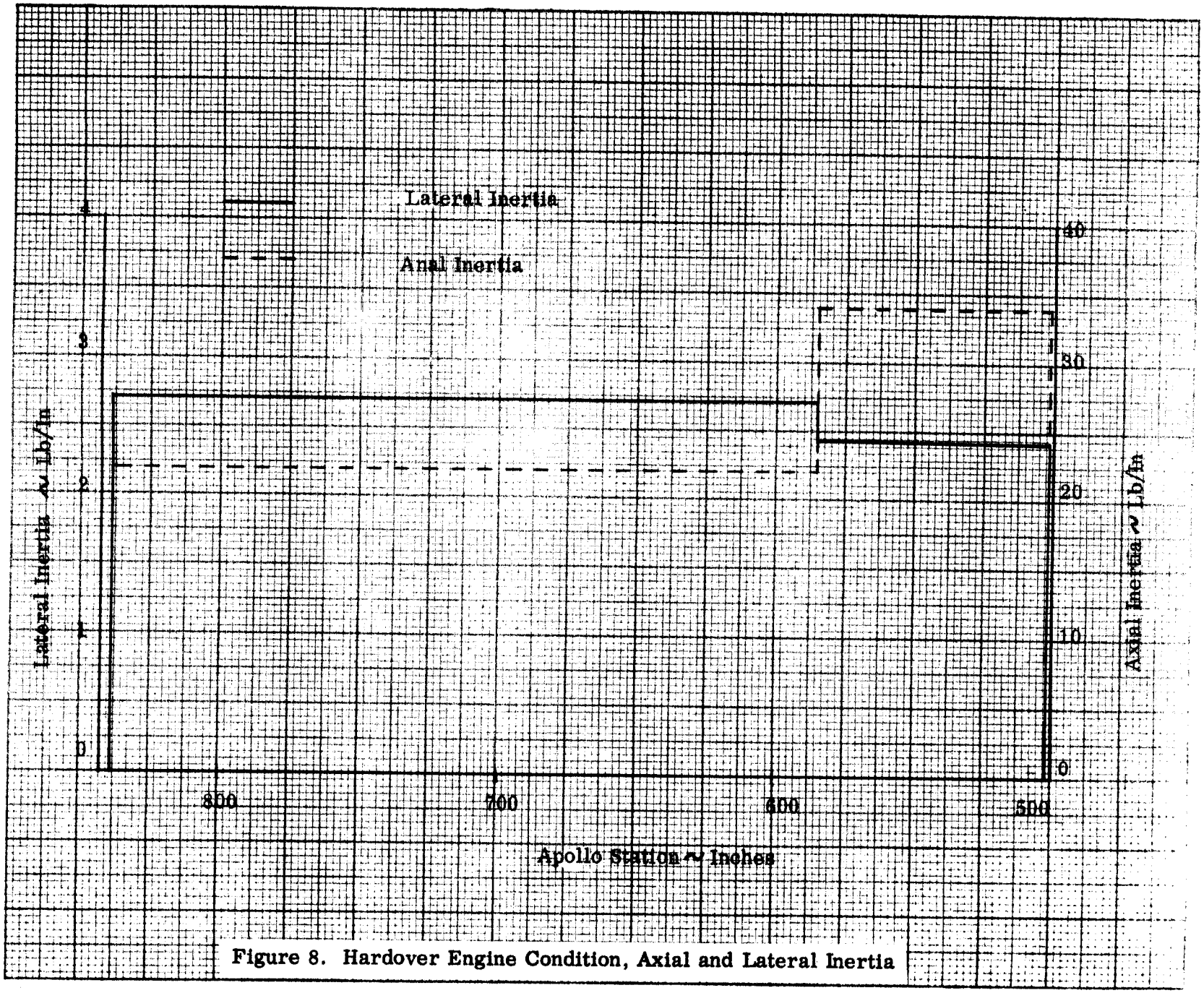

Figure 8. Hardover Engine Condition, Axial and Lateral Inertia

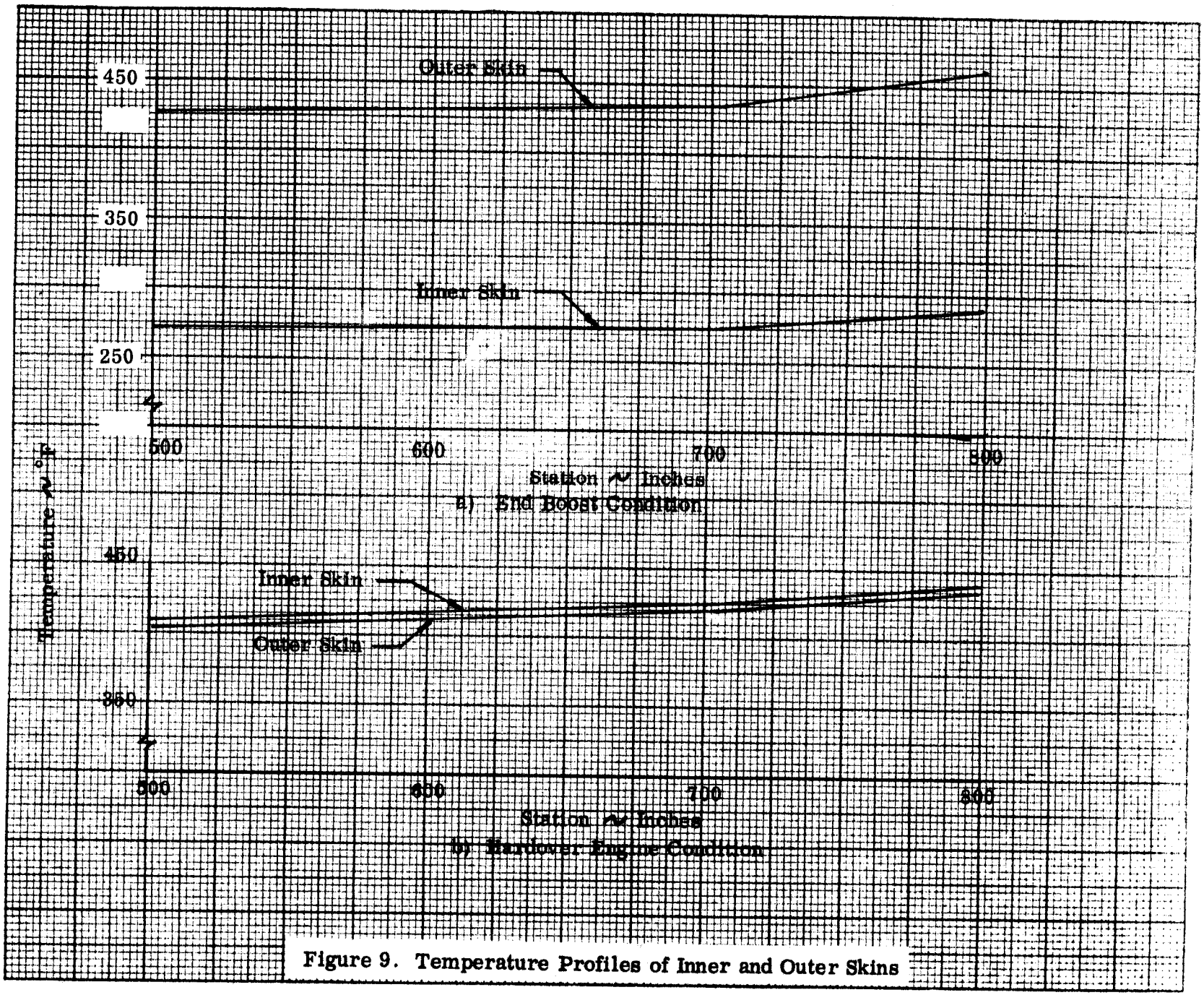

Figure 9. Temperature Profiles of Inner and Outer Skins

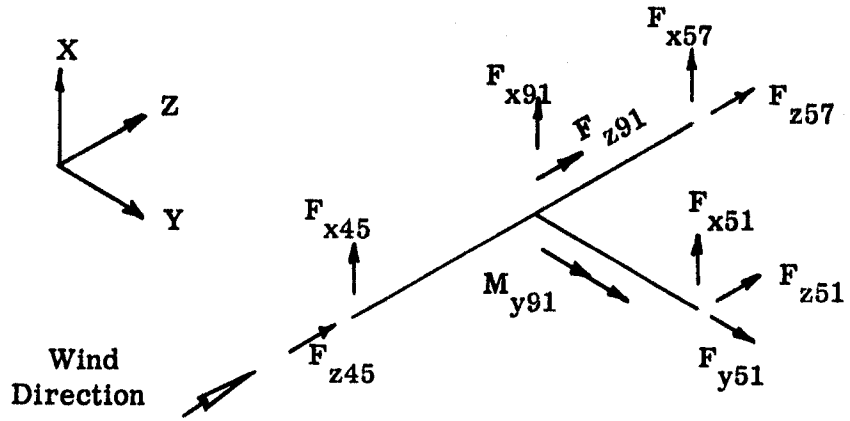

	u_{45}	u_{51}	u_{57}	u_{91}	v_{51}	θ_{y91}	w_{45}	w_{51}	w_{57}	w_{91}
F_{x45}	22759									
F_{x51}	3035	38823								
F_{x57}	2492	5312	11922			(Symmetric)				
F_{x91}	-28287	-47170	-19727	95184						
F_{y51}	-1104	-3943	3106	1942	131937					
M_{y91}	2330627	-263936	-1130684	-936006	-477701	405336400				
F_{z45}	3609	-1194	-996	-1418	5105	347139	60002			
F_{z51}	-1002	859	2209	-2066	727	-449816	-12004	41372		
F_{z57}	788	-1055	5721	-5454	-7984	-698550	-9804	-13646	49086	
F_{z91}	-3396	1391	-6934	8938	2152	801227	-38194	-15722	-25635	79551

Figure 10. LEM Stiffness Matrix – 0° Air Load Orientation

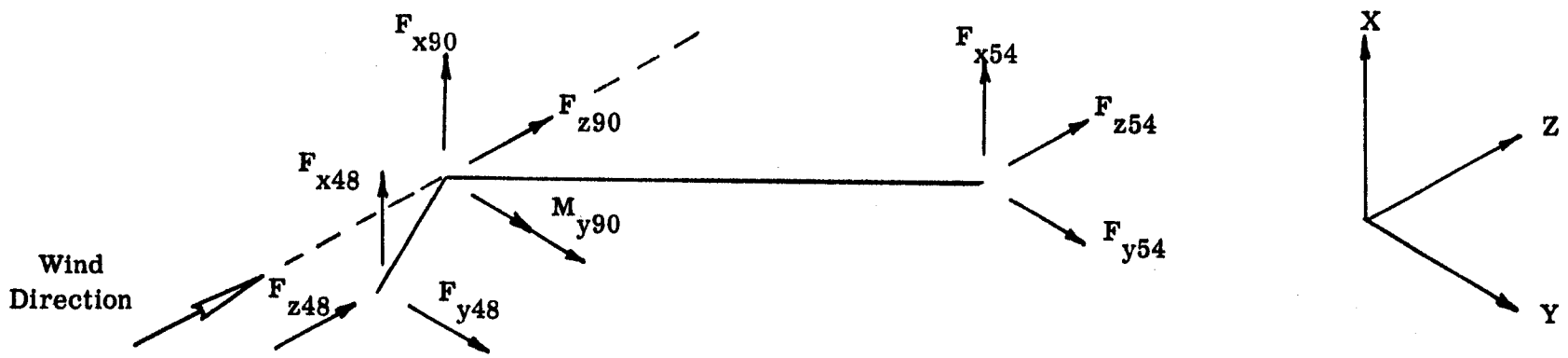

	u_{48}	u_{54}	u_{90}	v_{48}	v_{54}	Θ_{y90}	w_{48}	w_{54}	w_{90}
F_{x48}	21637								
F_{x54}	4298	17358							
F_{x90}	-25936	-21656	47592			(Symmetric)			
F_{y48}	-163	370	-207	47073					
F_{y54}	1688	218	-1906	2266	46103				
M_{y90}	1414138	-1083210	-330928	11572	66620	206178000			
F_{z48}	1168	-645	-524	-17554	-5472	33191	37431		
F_{z54}	-127	2764	-2636	6226	16445	-328995	-13846	32585	
F_{z90}	-1041	-2119	3160	11329	-10972	295804	-23585	-18739	42324

Figure 11. LEM Stiffness Matrix – 45° Air Load Orientation

Note: All LEM Reactions are in lbs.

⊙ F_x Reaction Up

⊗ F_x Reaction Down

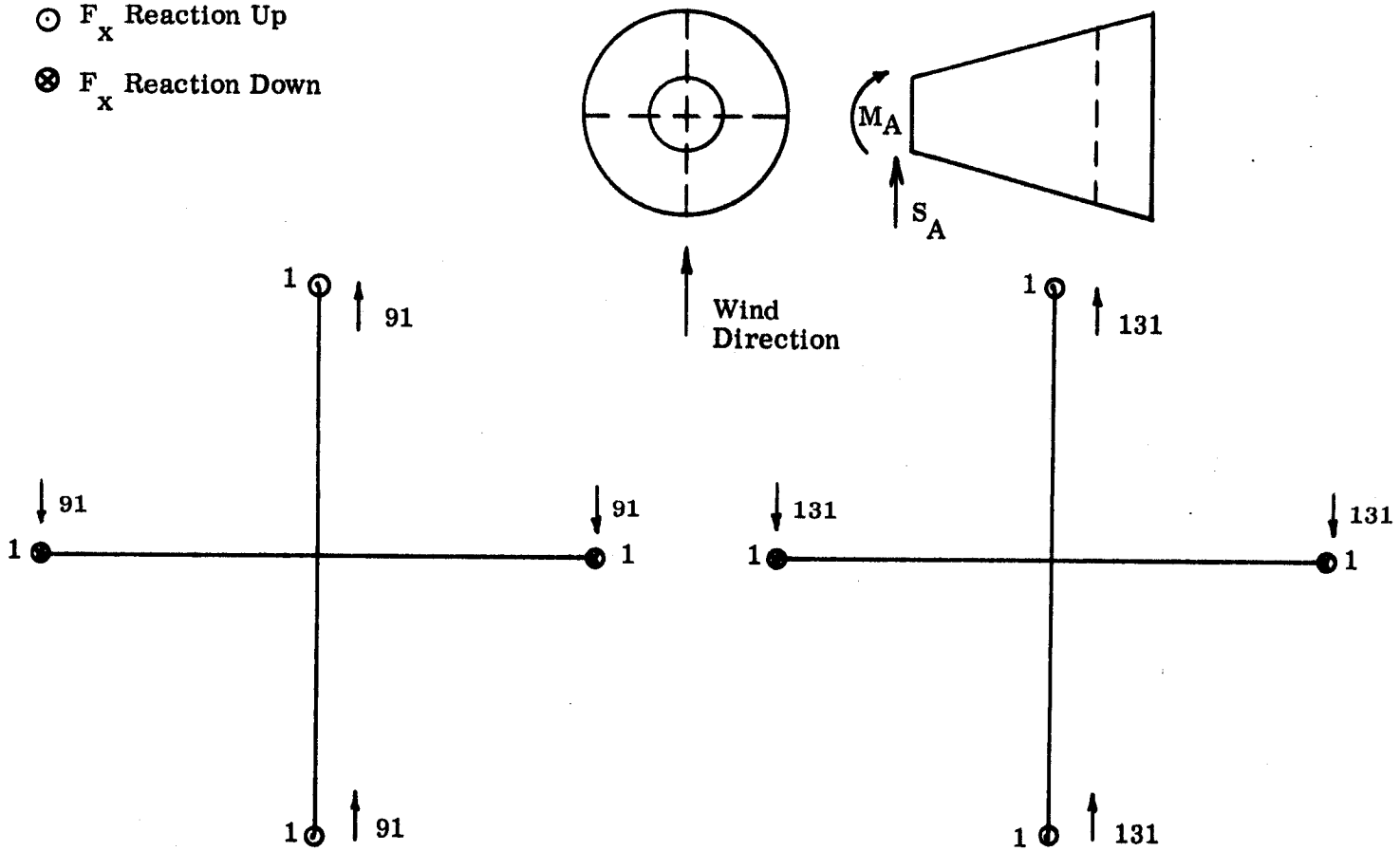

a) Bending Moment, $M_A = 9.609(10^6)$ lb-in.

b) Shear Load, $S_A = 43065$ lb

Figure 12. LEM Reactions, Maximum q_α Condition
0° Airload Orientation

Note: All LEM Reactions are in lbs.

⊙ F_x Reaction Up

⊗ F_x Reaction Down

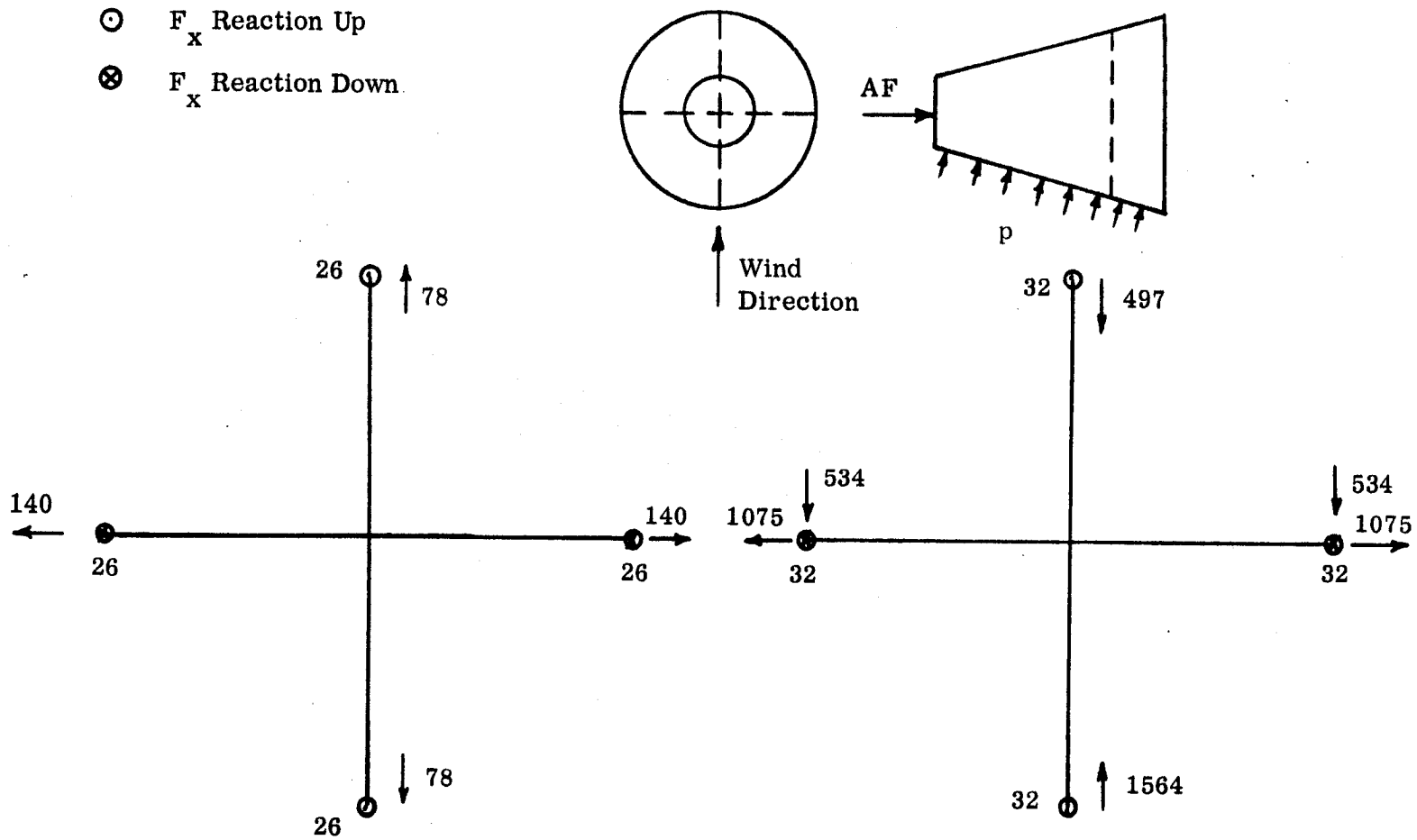

a) Axial Force,
AF = 186076 lb

b) Pressure Load, p

Figure 13. LEM Reactions Max q_{α} Condition
0° Airload Orientation

Note: All LEM Reactions are in lbs.

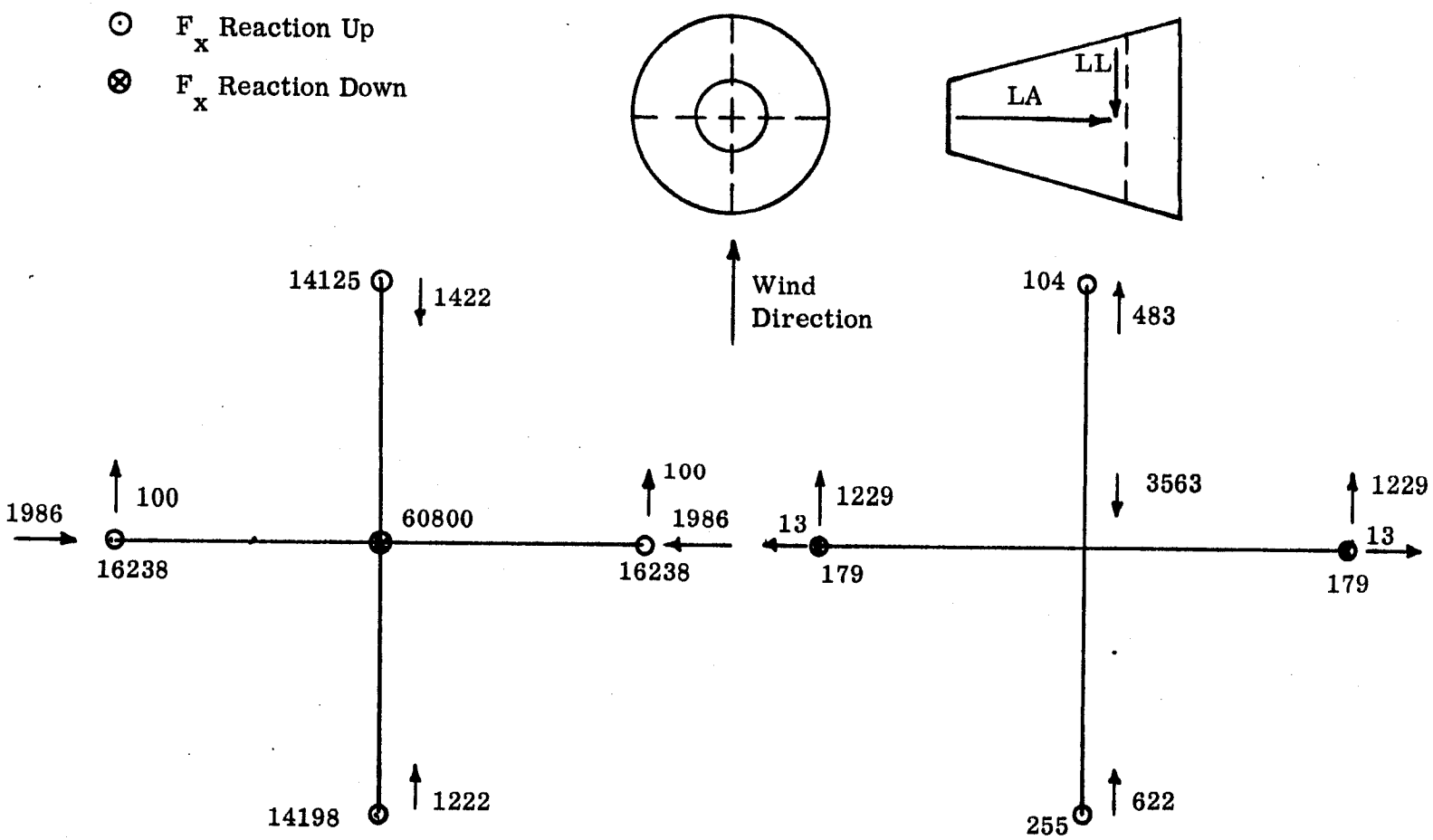

a) LEM Axial Load, LA = 60800 lb

b) LEM Laterial Load, LL = 3563 lb

Figure 14. LEM Reactions, Max q_α Condition
0° Airload Orientation

Note: All LEM Reactions are in lbs.

⊙ F_x Reaction Up

⊗ F_x Reaction Down

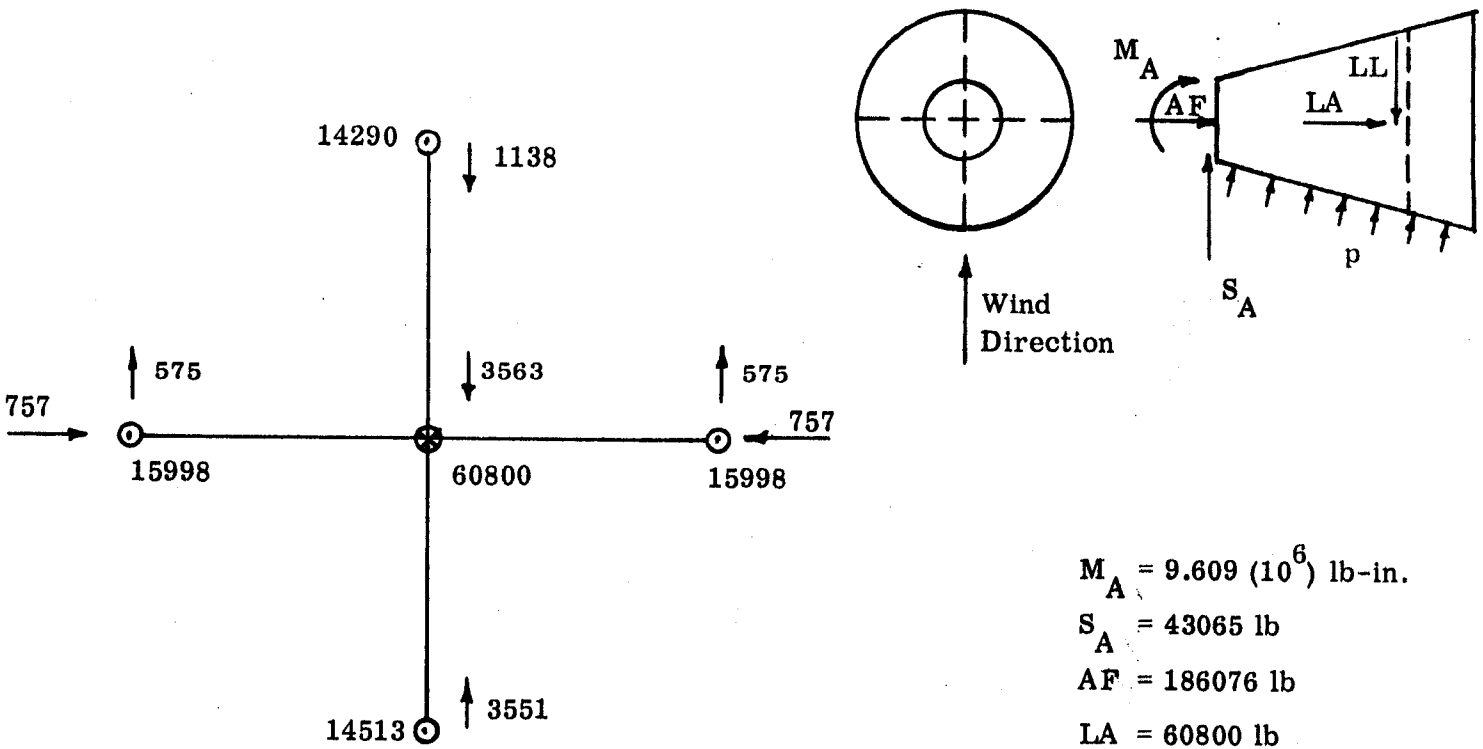

M_A = 9.609 (10^6) lb-in.

S_A = 43065 lb

AF = 186076 lb

LA = 60800 lb

LL = 3563 lb

Figure 15. LEM Reactions, Max q_{α} Condition, Due to All Loads
0° Airload Orientation

Note: All LEM Reactions are in lbs.

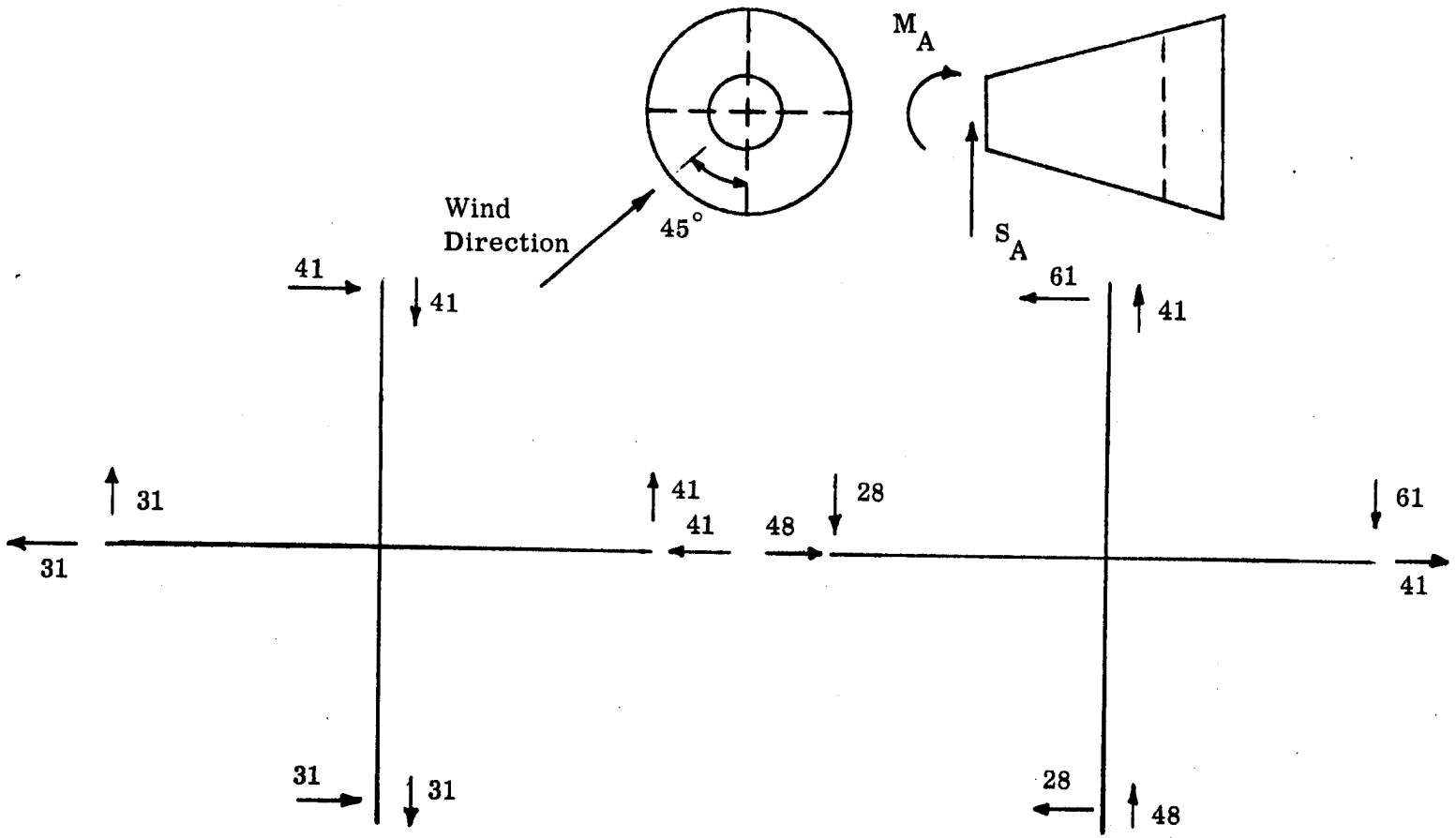

a) Bending Moment, M_A = 9.609 (10^6) lb-in.

b) Shear Load, S_A = 43065 lb

Figure 16. LEM Reactions, Max q_α Condition
45° Airload Orientation

Note: All LEM Reactions are in lbs.

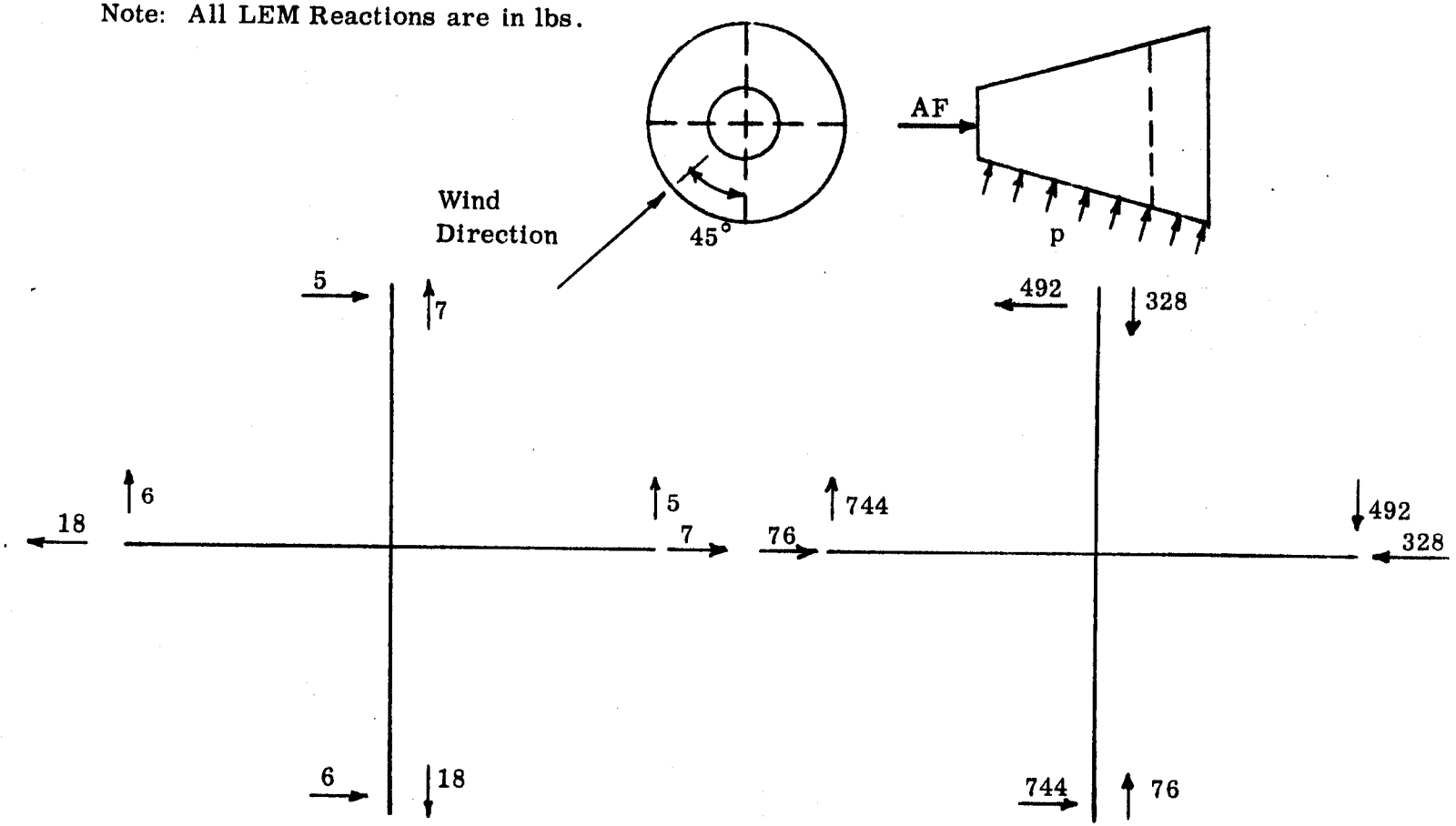

a) Axial Force,
AF = 186,076 lb

b) Pressure Load, p

Figure 17. LEM Reactions, Maximum q_{α} Condition
45° Airload Orientation

Note: All LEM Reactions are in lbs.

⊙ F_x Reaction Up

⊗ F_x Reaction Down

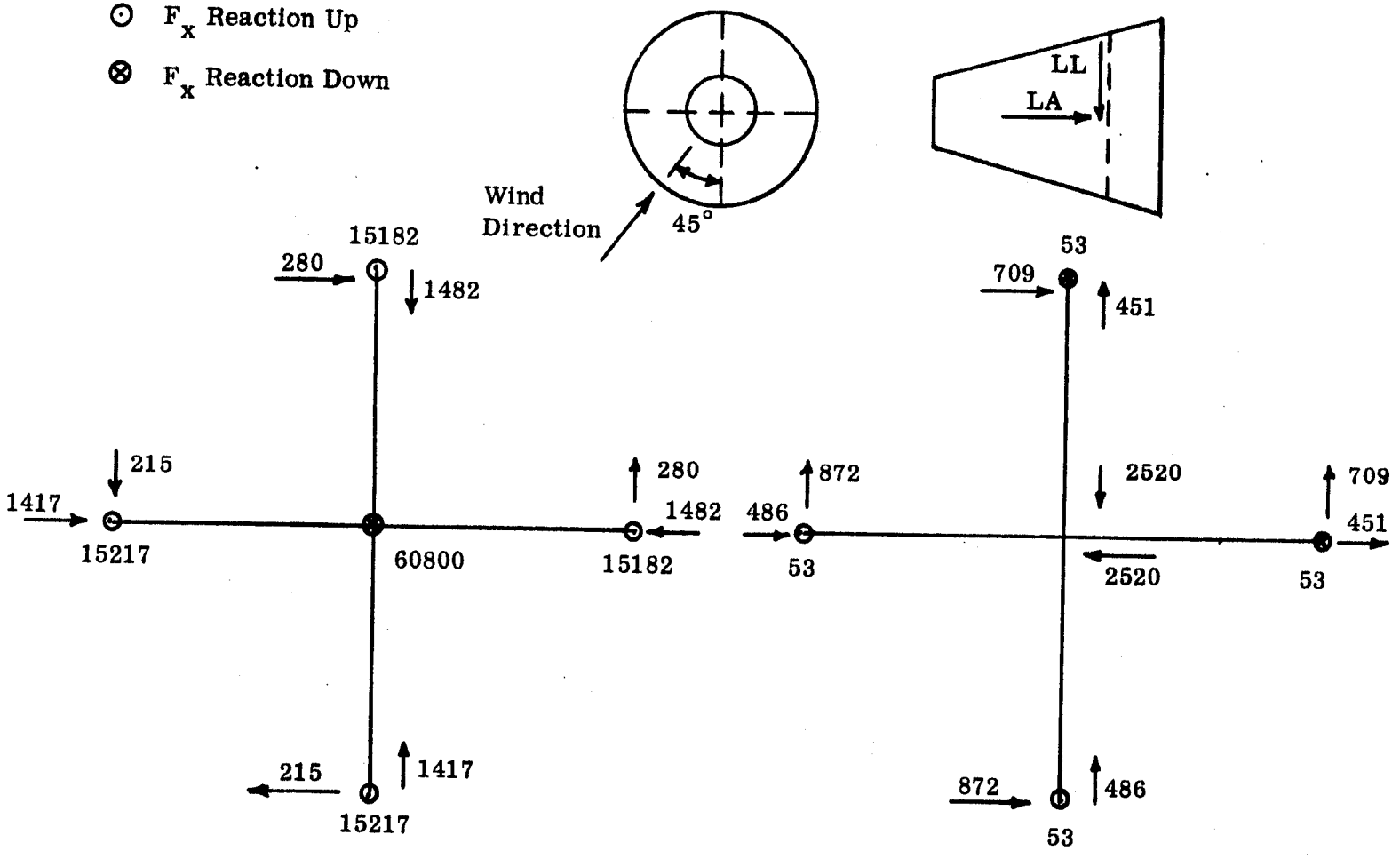

a) LEM Axial Load, LA = 60,800 lb

b) LEM Lateral Load, LL = 3563 lb

Figure 18. LEM Reactions, Maximum q_α Condition 45° Airload Orientation

Note: All LEM Reactions are in lbs.

⊙ F_x Reaction Up

⊗ F_x Reaction Down

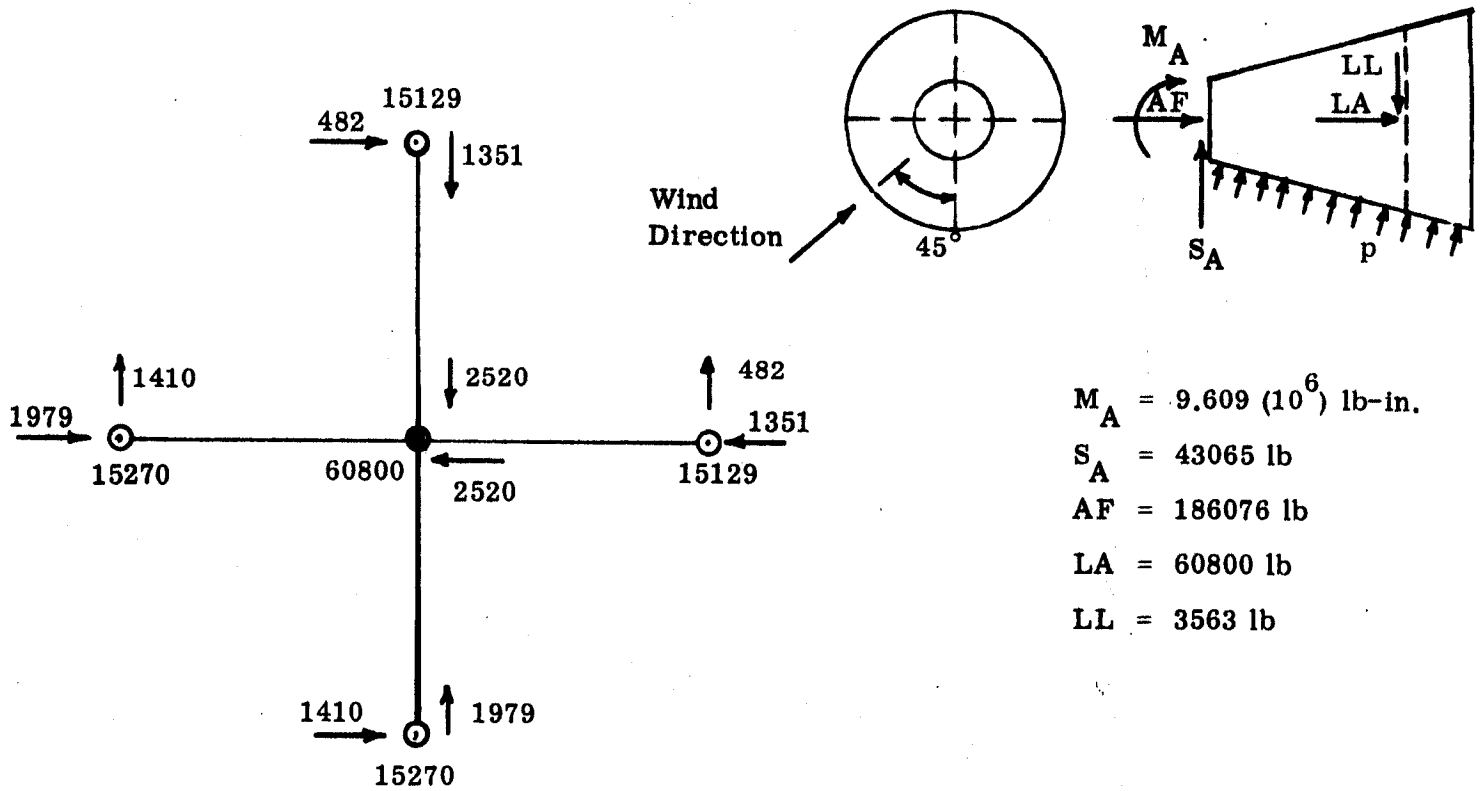

M_A = 9.609 (10^6) lb-in.

S_A = 43065 lb

AF = 186076 lb

LA = 60800 lb

LL = 3563 lb

Figure 19. LEM Reactions, Maximum q_α Condition, Due to All Loads
45° Airload Orientation

Note: All LEM Reactions are in lbs.

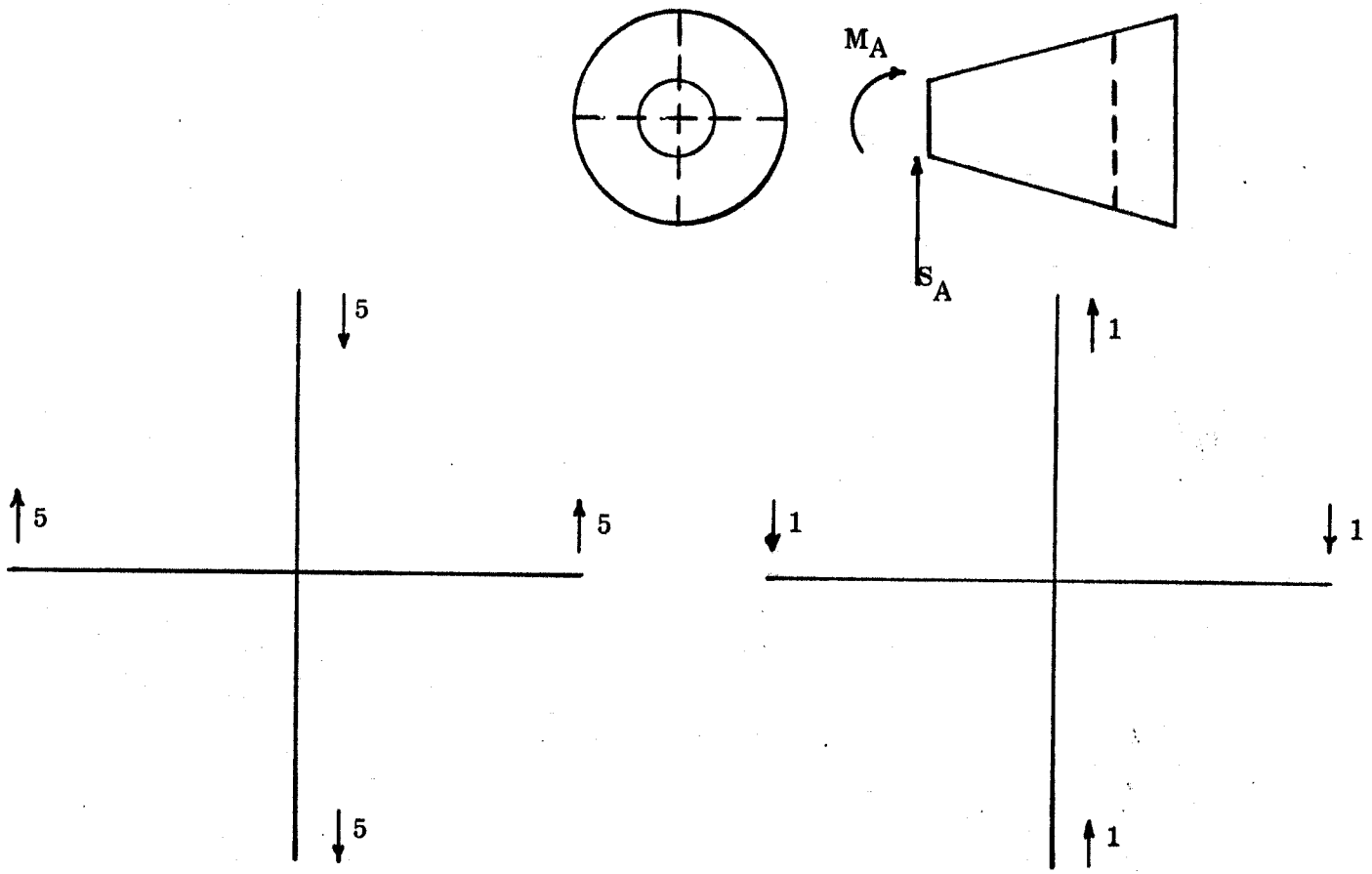

a) Bending Moment, $M_A = 1.284\ (10^6)$ lb-in.

b) Shear Load, $S_A = 7100$ lb

Figure 20. LEM Reactions, End Boost Condition

Note: All LEM Reactions are in lbs.

⊙ F_X Reaction Up

⊗ F_X Reaction Down

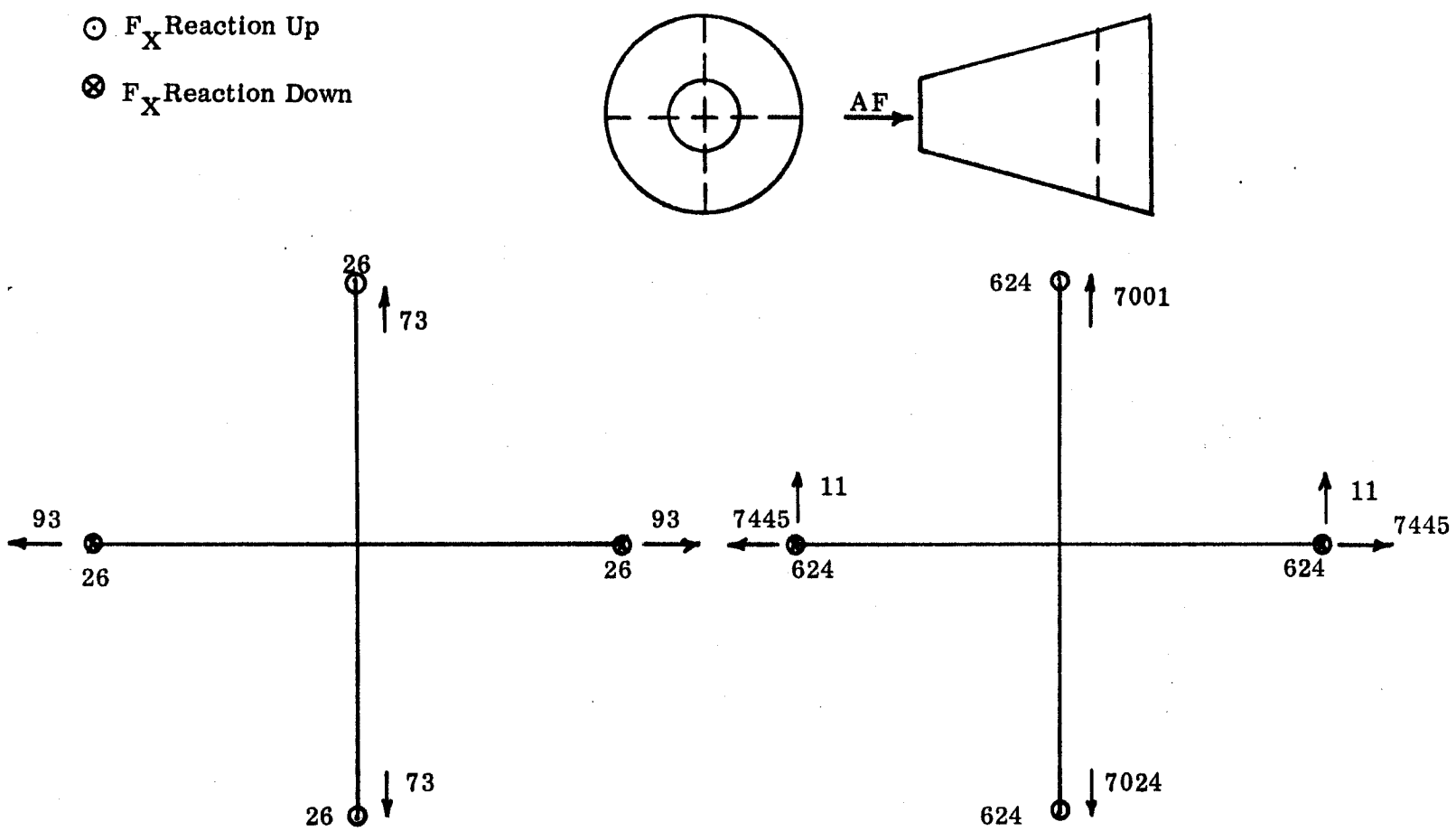

a) Axial Force, AF = 346000 lb

b) Temperature

Figure 21. LEM Reactions, End Boost Condition

Note: All LEM Reactions are in lbs.

⊙ F_X Reaction Up

⊗ F_X Reaction Down

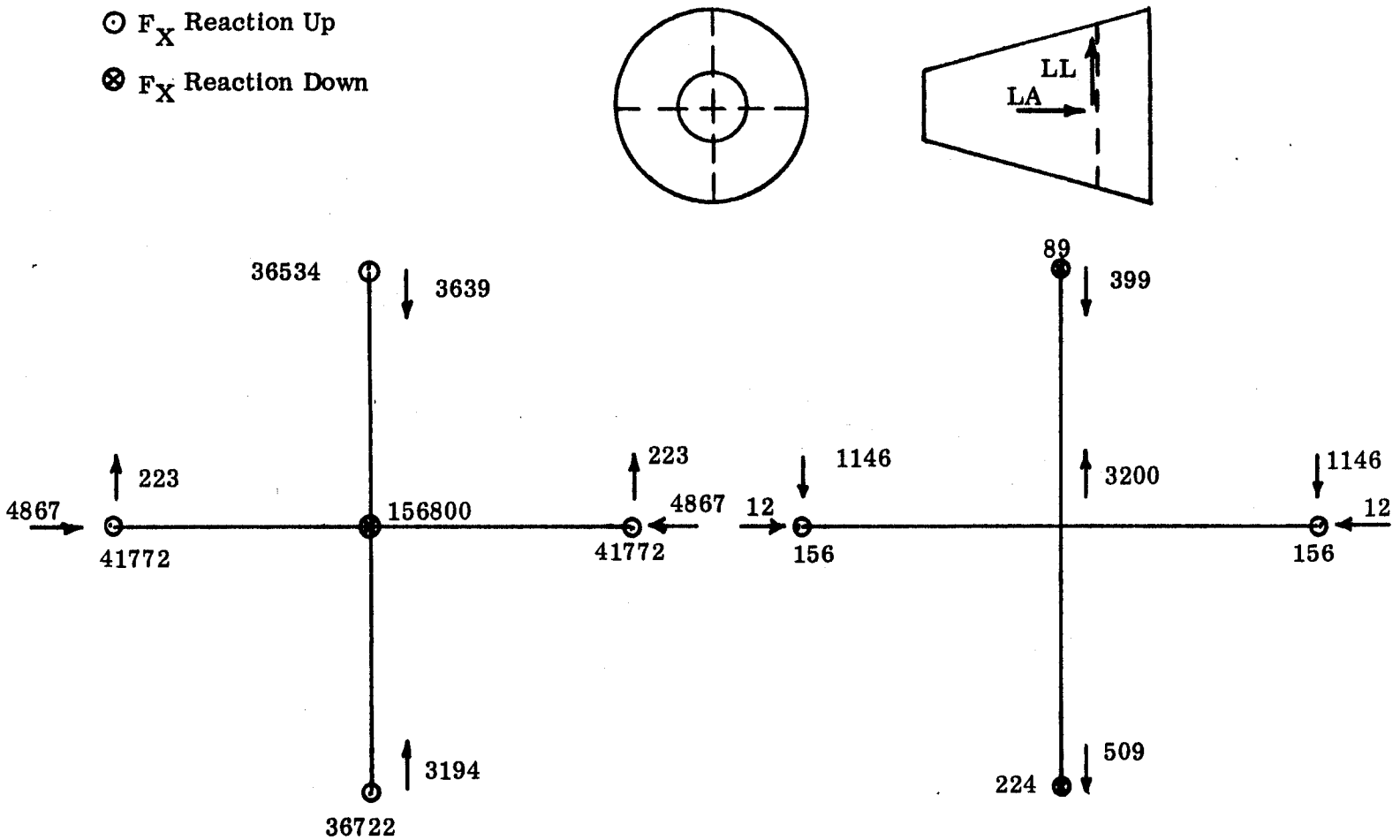

a) LEM Axial Load, LA = 156800 lb

b) LEM Lateral Load, LL = 3200 lb

Figure 22. LEM Reactions, End Boost Condition

Note: All LEM Reactions are in lbs.

⊙ F_X Reaction Up

⊗ F_X Reaction Down

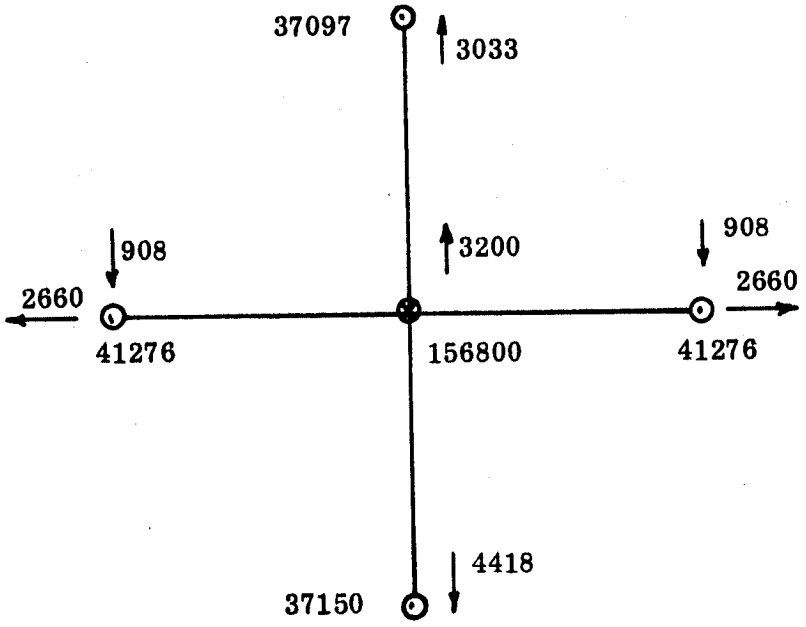

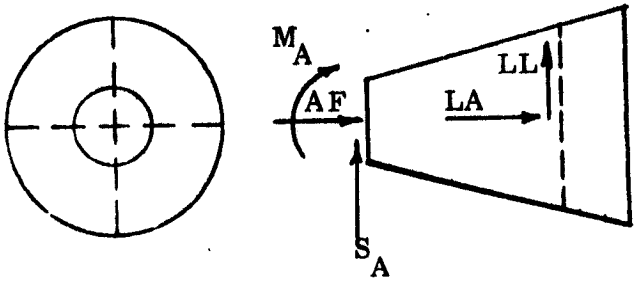

M_A = 1.284 (10^6) lb- in

S_A = 7100 lb

AF = 346000 lb

LA = 156800 lb

LL = 3200 lb

Figure 23. LEM Reactions, End Boost Condition, Due to All Loads

Note: All LEM Reactions are in lbs.

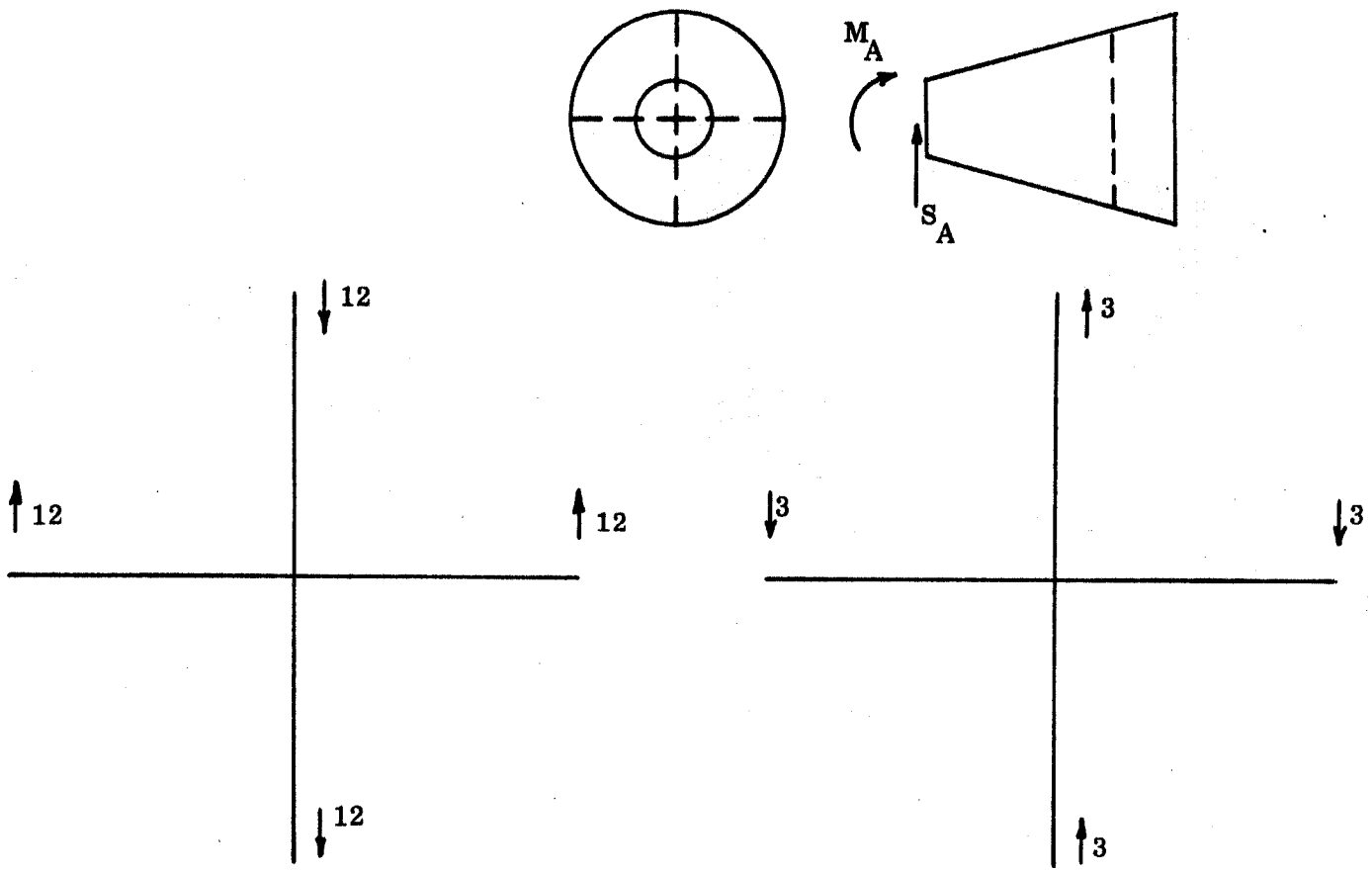

a) Bending Moment, $M_A = 2.808\ (10^6)$ lb-in.

b) Shear Load, $S_A = 27590$ lb

Figure 24. LEM Reactions, Hardover Engine Condition

Note: All LEM Reactions are in lbs.

⊙ F_x Reaction Up

⊗ F_x Reaction Down

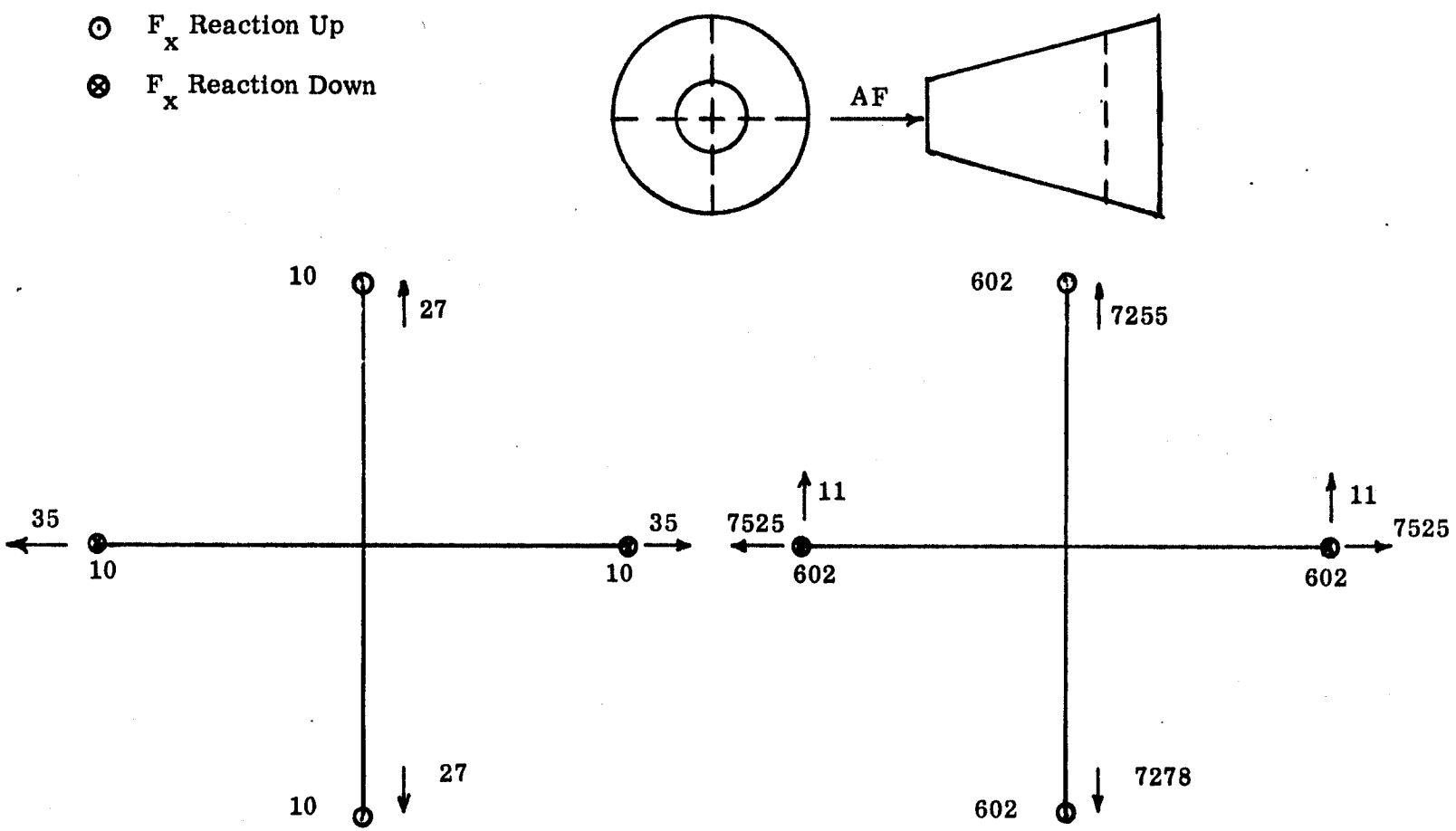

a) Axial Force, AF = 132000 lb

b) Temperature

Figure 25. LEM Reactions, Hardover Engine Condition

Note: All LEM Reactions are in lbs.

⊙ F_x Reaction Up

⊗ F_x Reaction Down

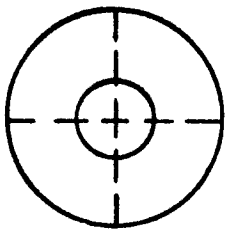

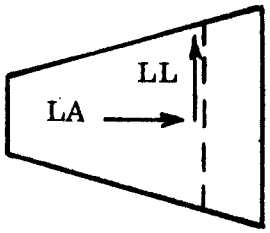

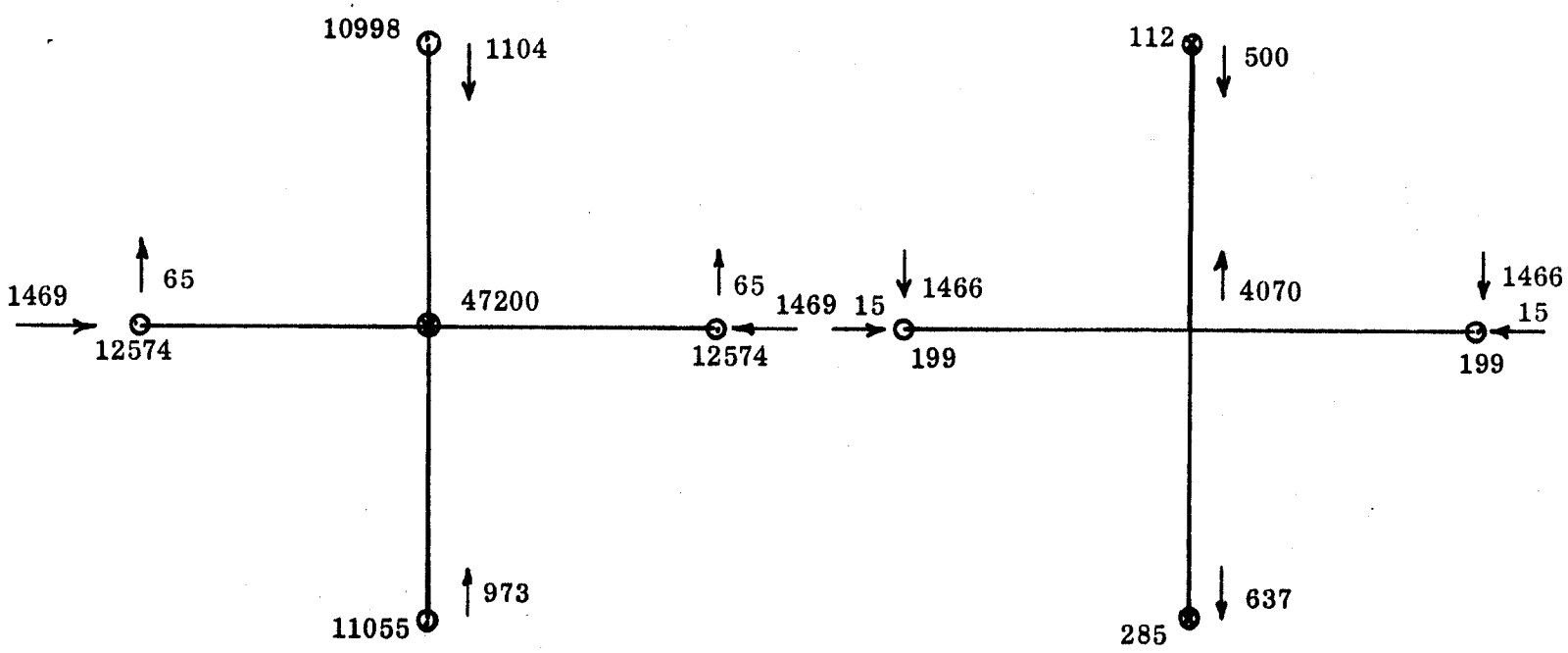

a) LEM Axial Load, LA = 47200 lb

b) LEM Lateral Load, LL = 4070 lb

Figure 26. LEM Reactions, Hardover Engine Condition

Note: All LEM Reactions are in lbs.

⊙ F_x Reaction Up

⊗ F_x Reaction Down

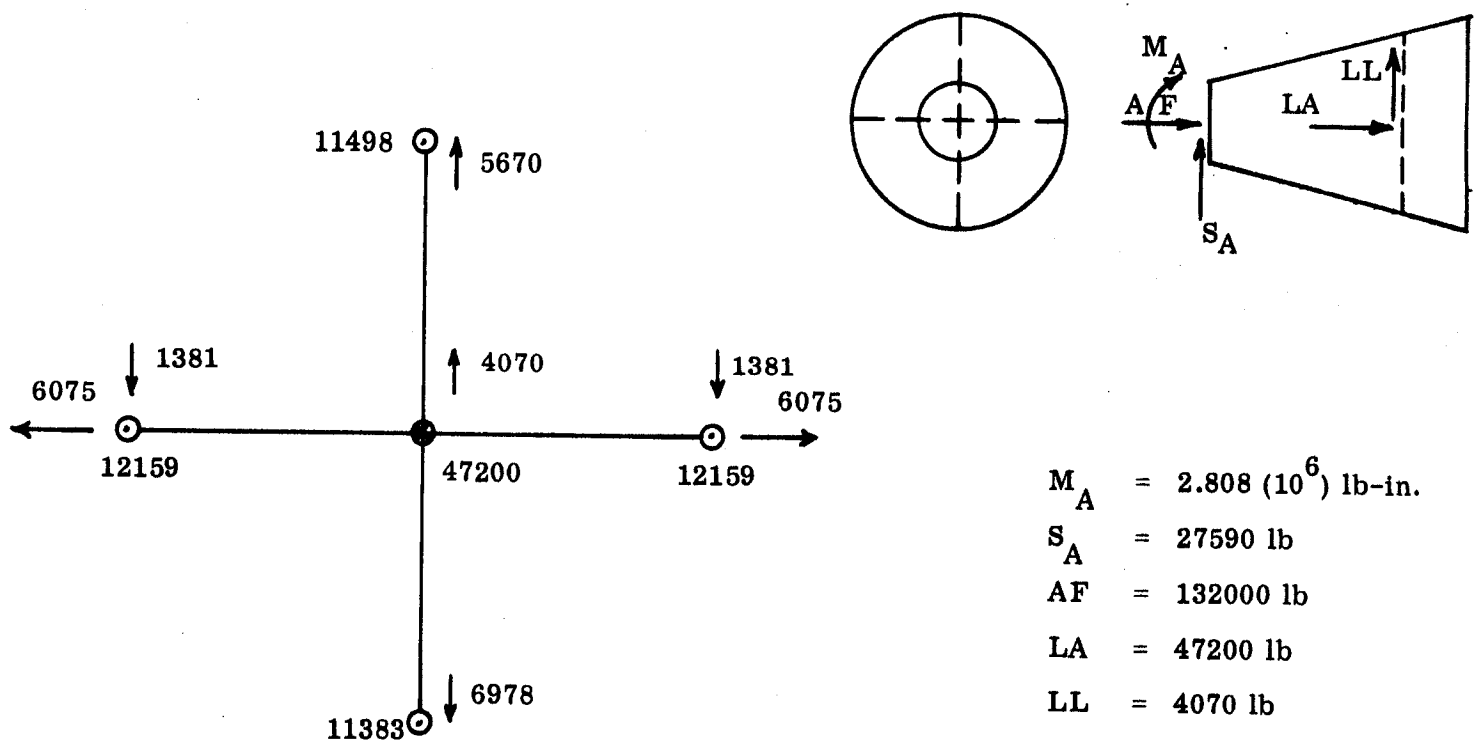

M_A = 2.808 (10^6) lb-in.

S_A = 27590 lb

AF = 132000 lb

LA = 47200 lb

LL = 4070 lb

Figure 27. LEM Reactions, Hardover Engine Condition, Due to All Loads

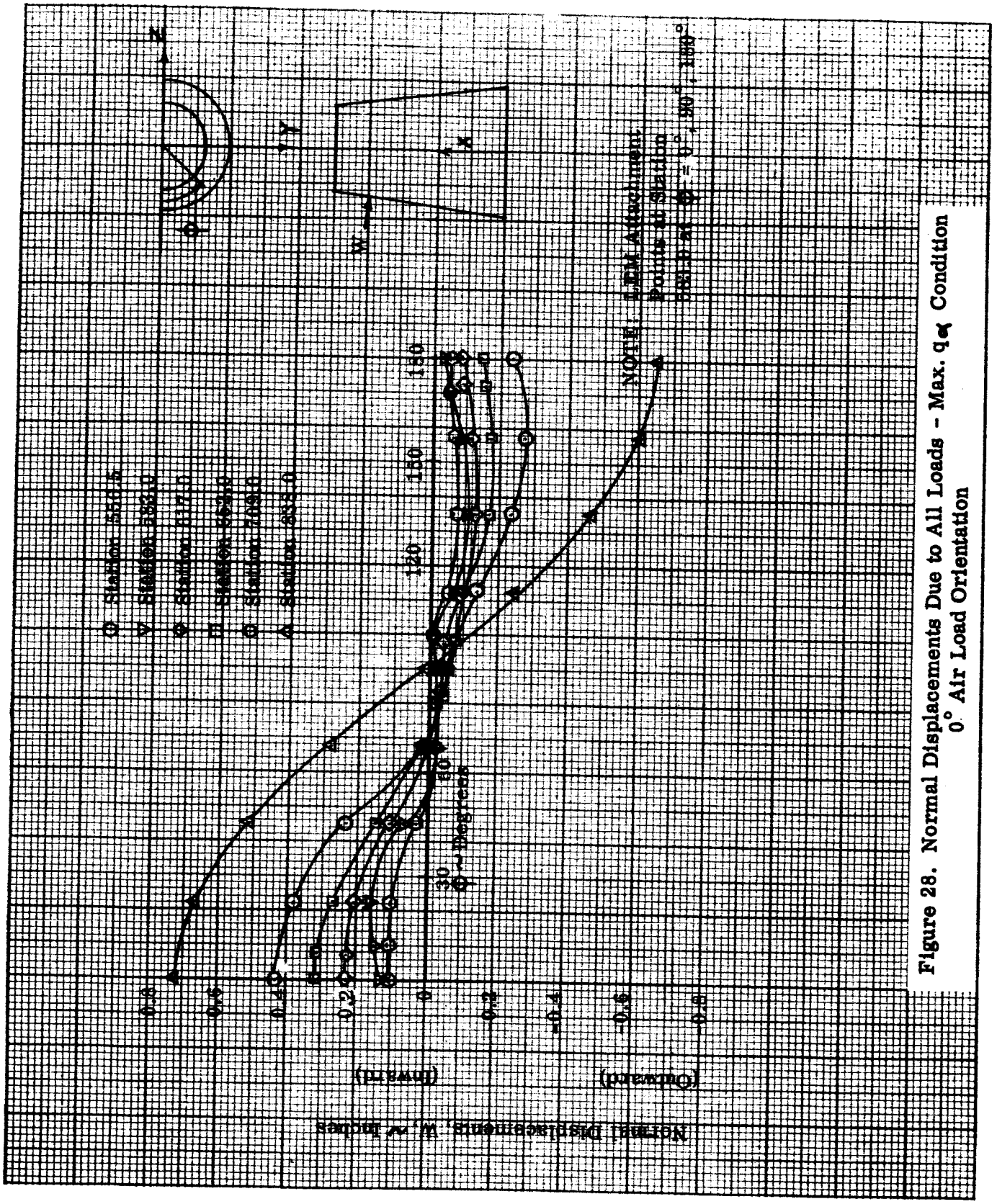

Figure 28. Normal Displacements Due to All Loads - Max. q_α Condition
0° Air Load Orientation

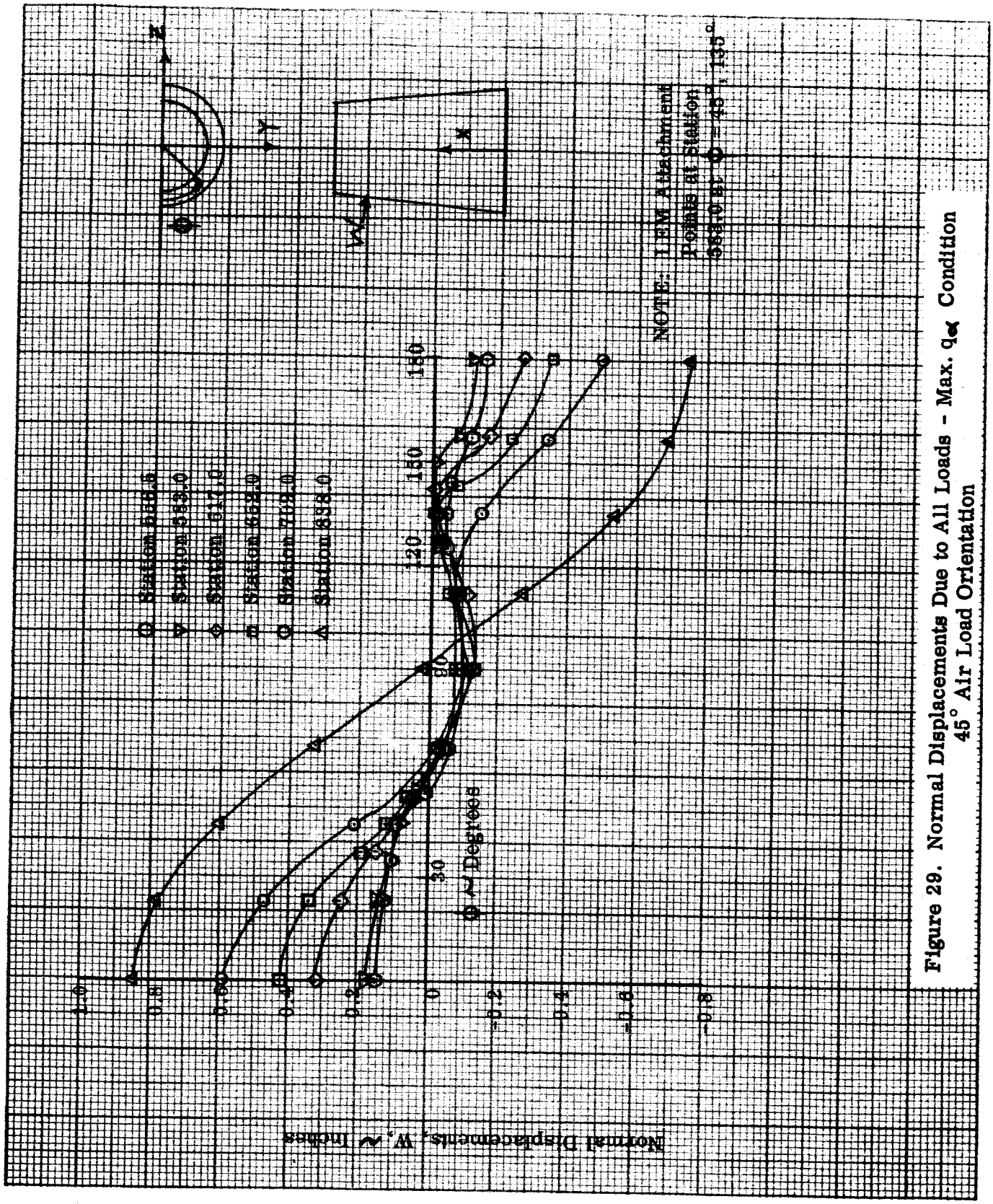

Figure 29. Normal Displacements Due to All Loads - Max. q_α Condition
45° Air Load Orientation

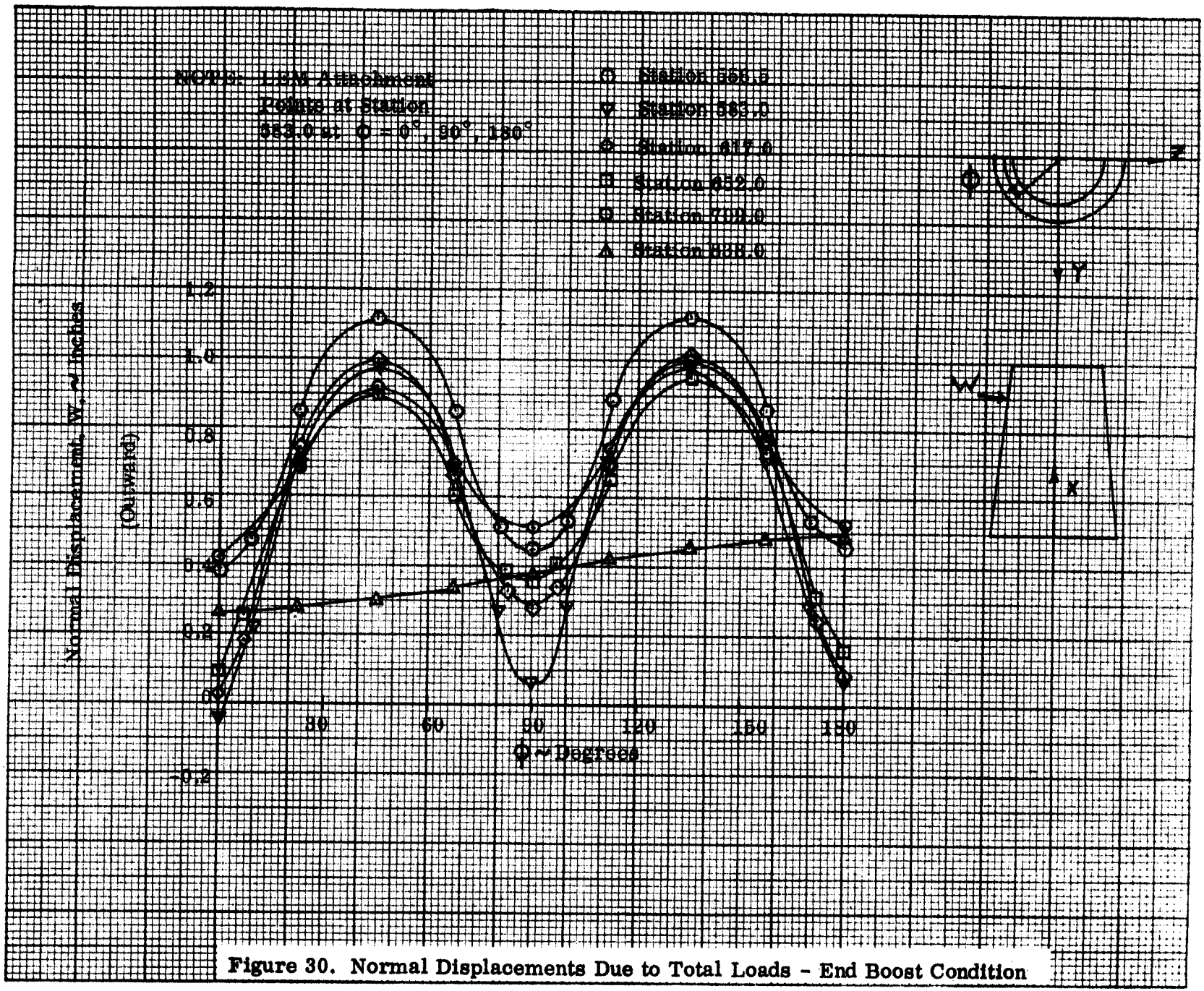

Figure 30. Normal Displacements Due to Total Loads - End Boost Condition

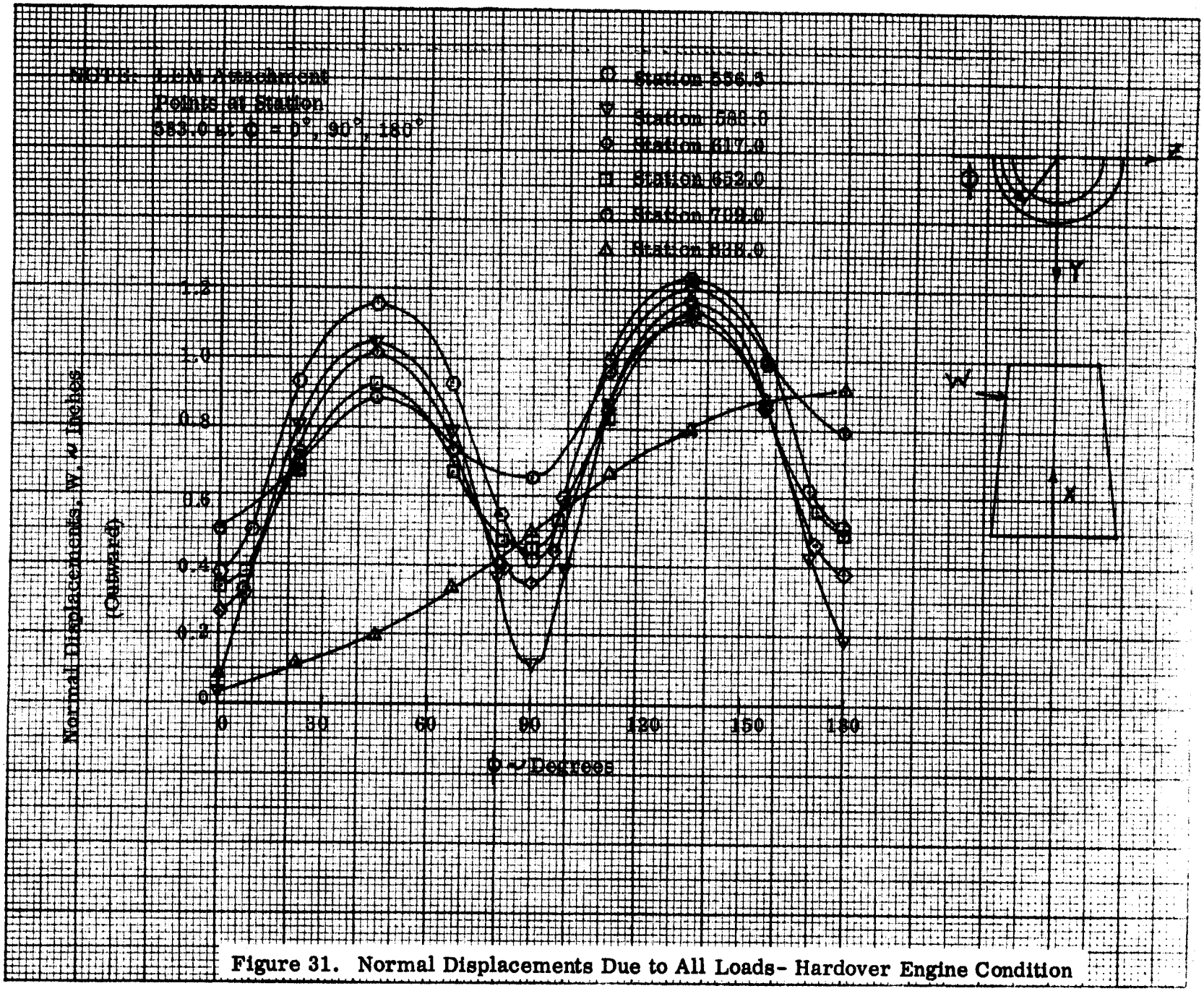

Figure 31. Normal Displacements Due to All Loads- Hardover Engine Condition

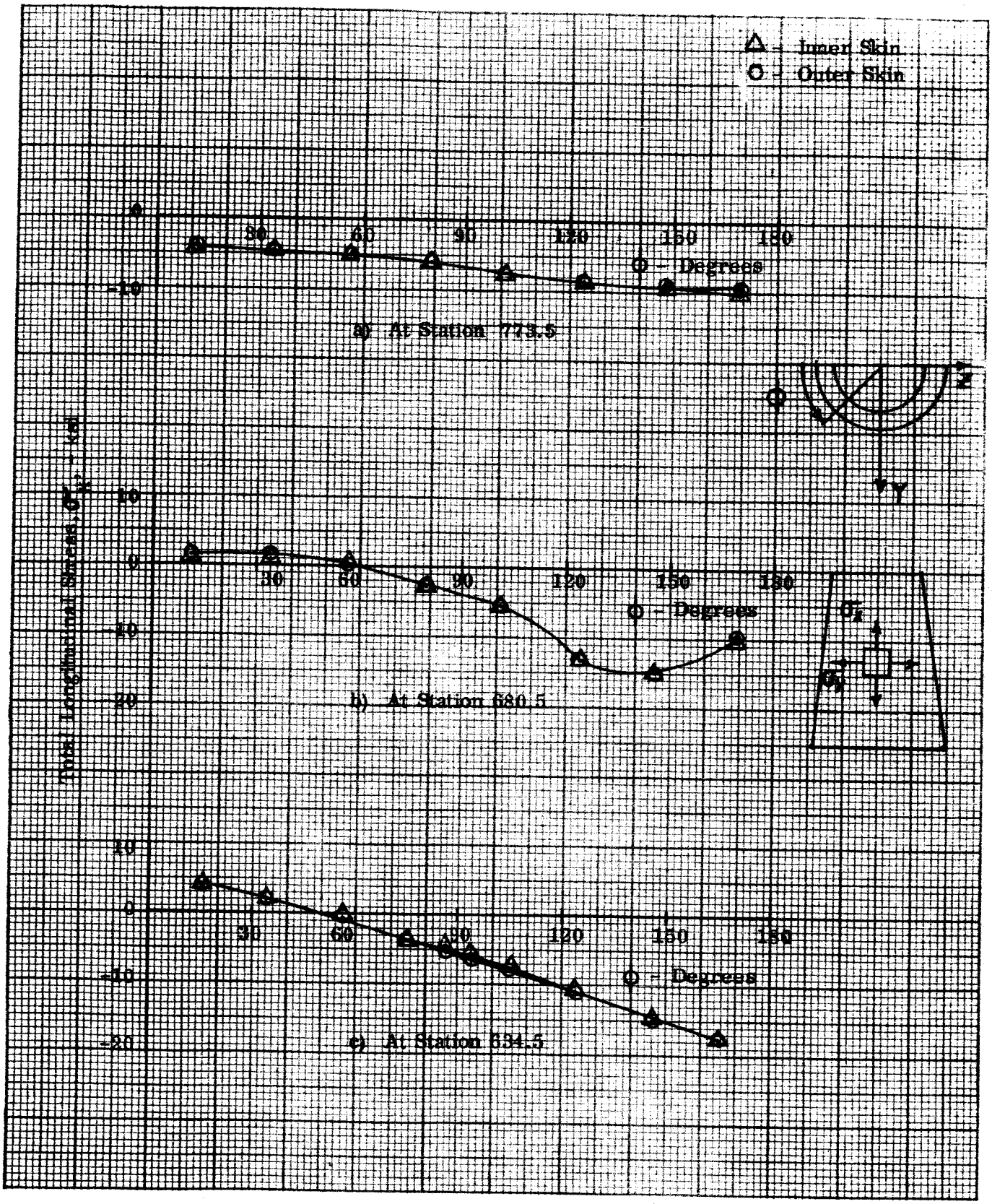

Figure 32. Total Longitudinal Stresses Due to all Loads, Max. q_α Condition
0° Air Load Orientation

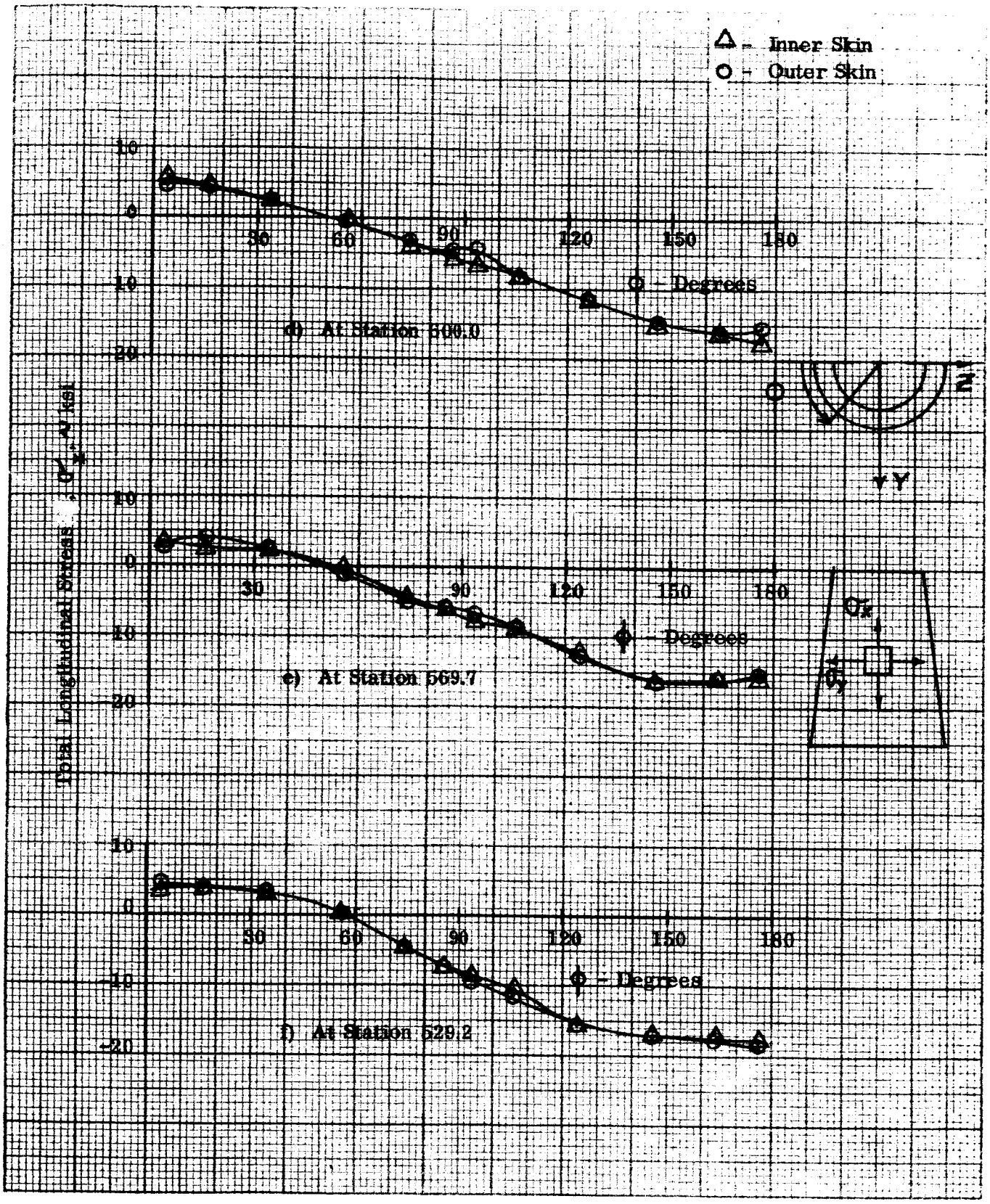

Figure 32. Total Longitudinal Stresses Due to all Loads, Max. q_{α} Condition
0° Air Load Orientation (Cont)

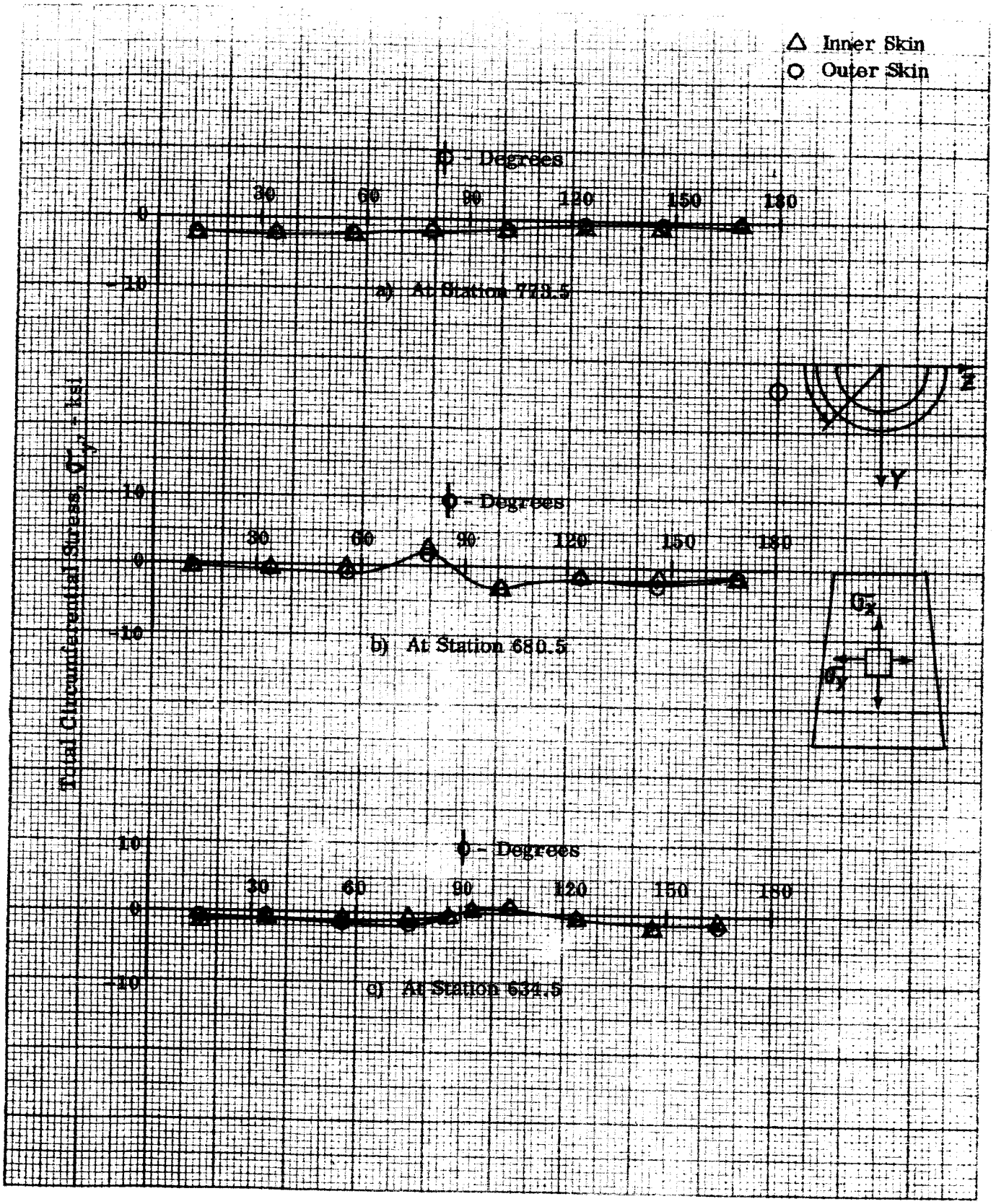

Figure 33. Total Circumferential Stresses Due to all Loads, Max. $q\alpha$ Condition
0° Air Load Orientation

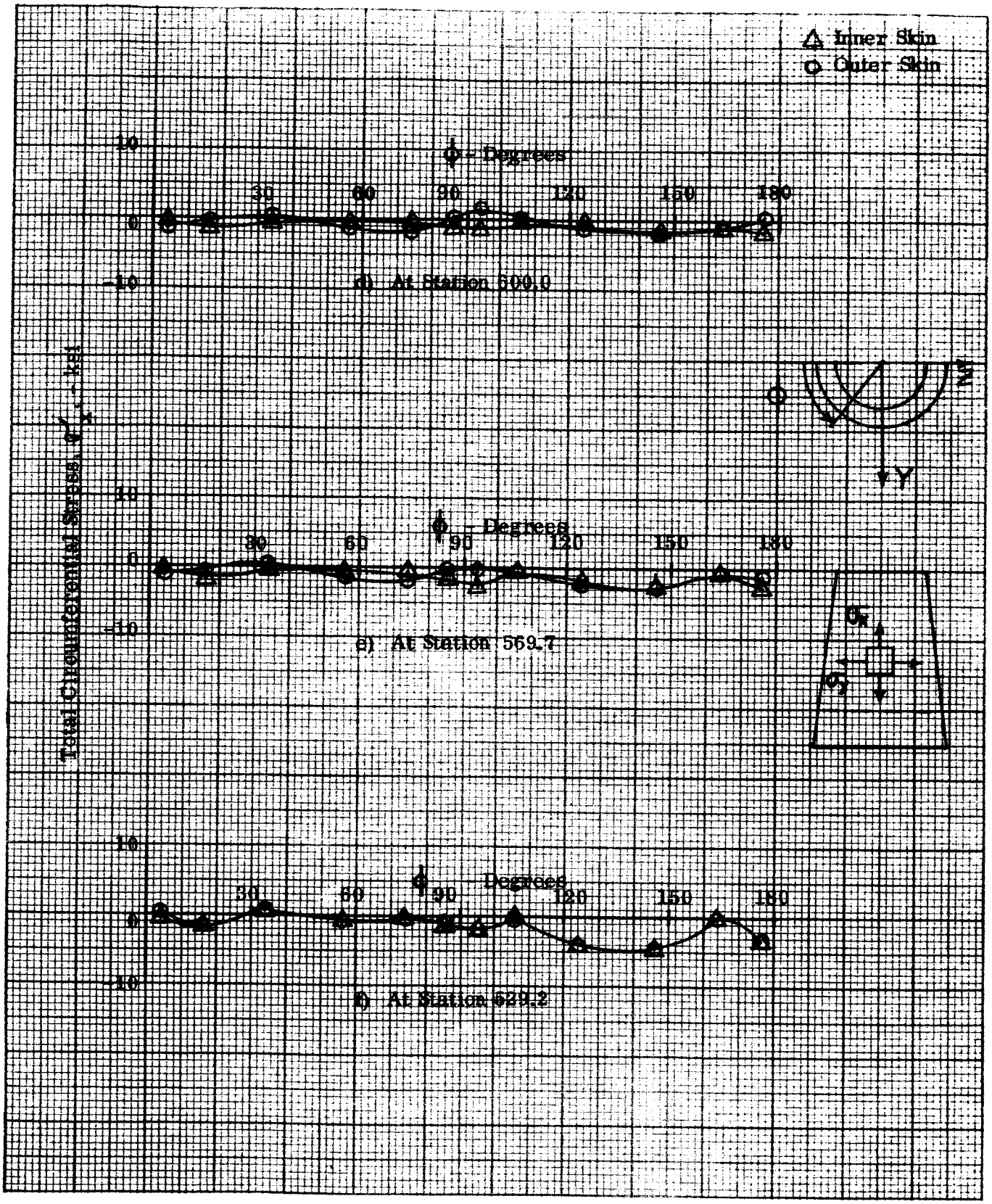

Figure 33. Total Circumferential Stresses Due to all Loads, Max. $q\alpha$ Condition 0° Air Load Orientation (Cont)

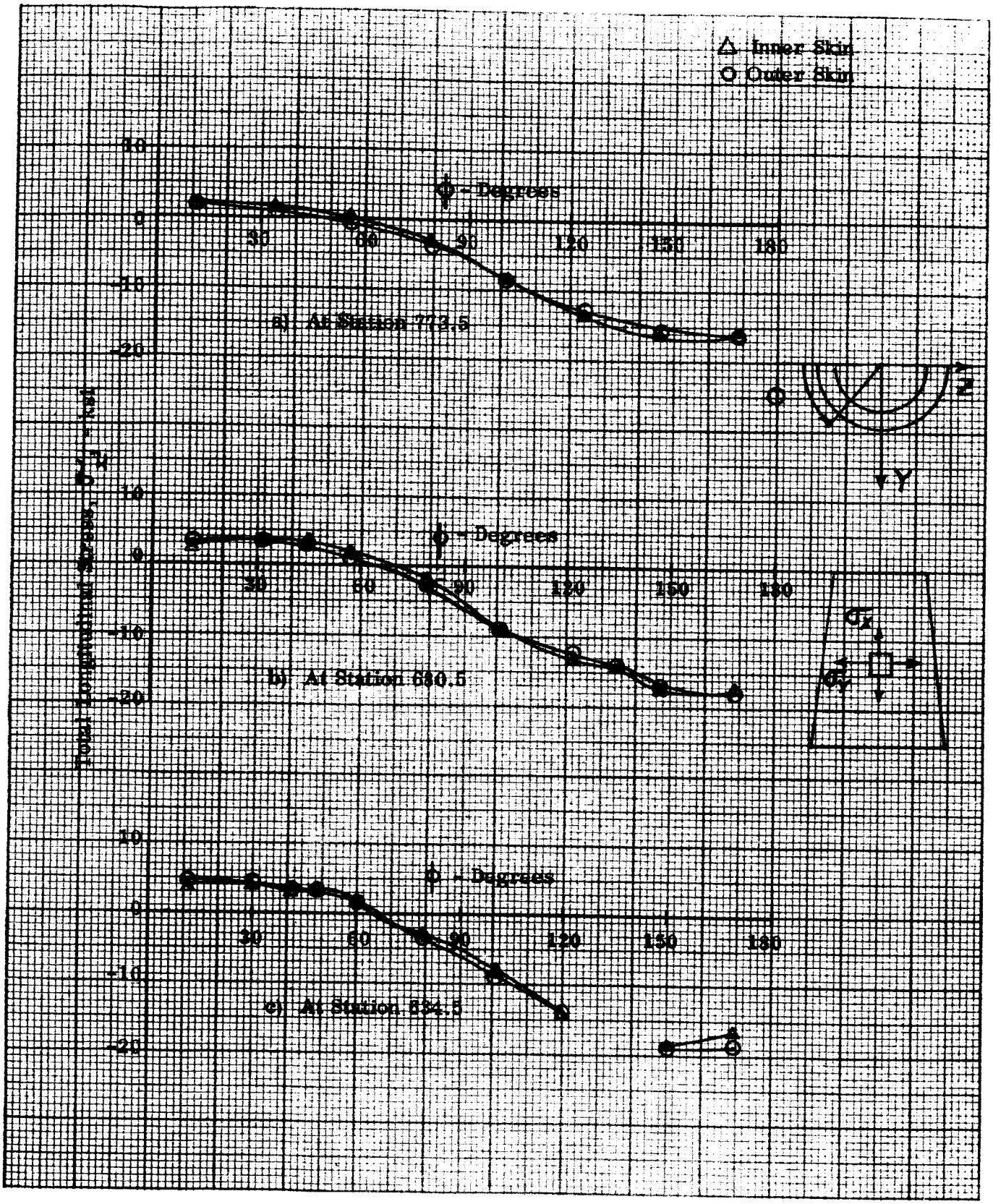

Figure 34. Total Longitudinal Stresses Due to all Loads, Max. qα Condition
45° Air Load Orientation

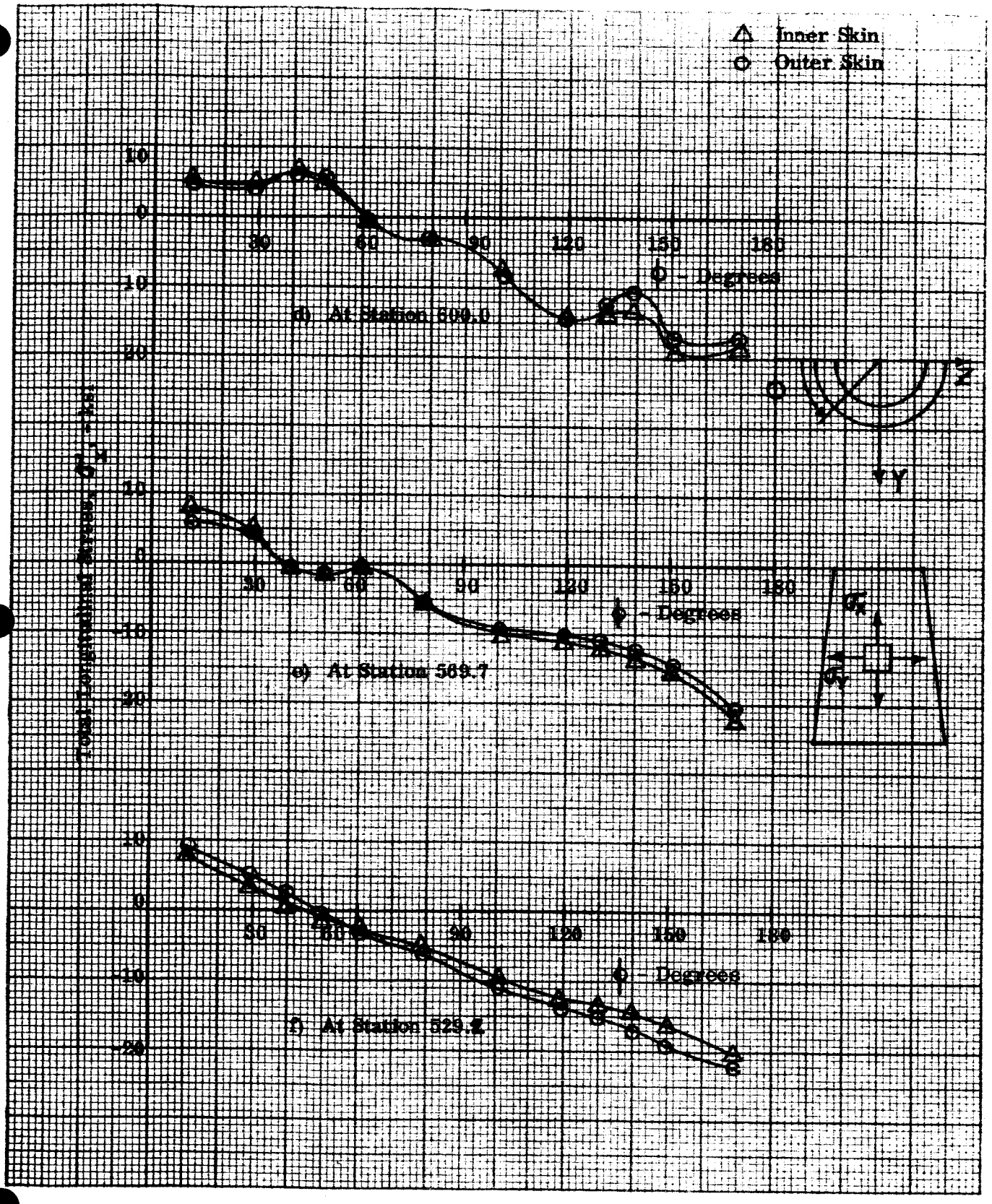

Figure 34. Total Longitudinal Stress Due to all Loads, Max. $q\alpha$ Condition
45° Air Load Orientation (Cont)

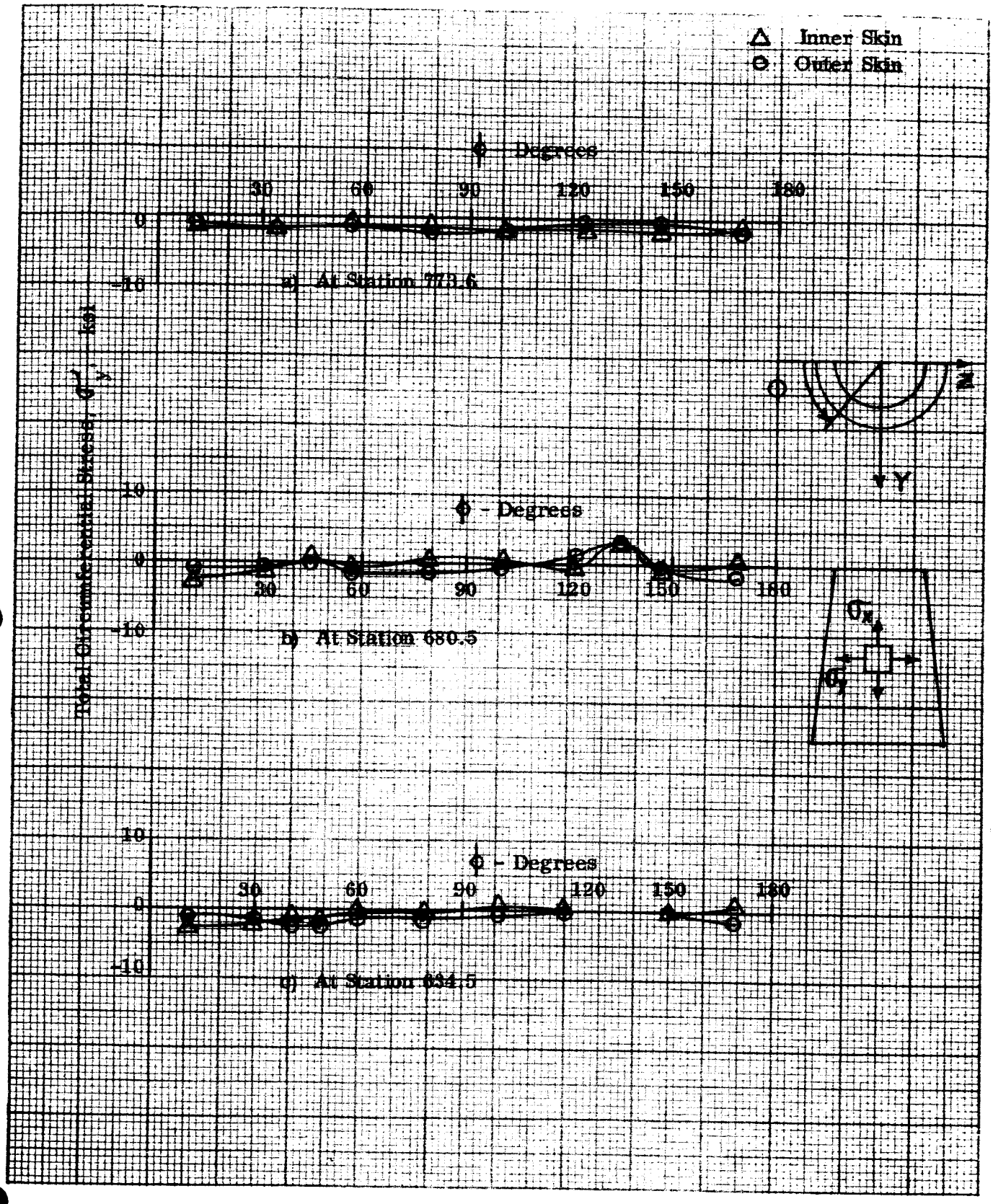

Figure 35. Total Circumferential Stresses Due to all Loads, Max. qα Condition
45° Air Load Orientation

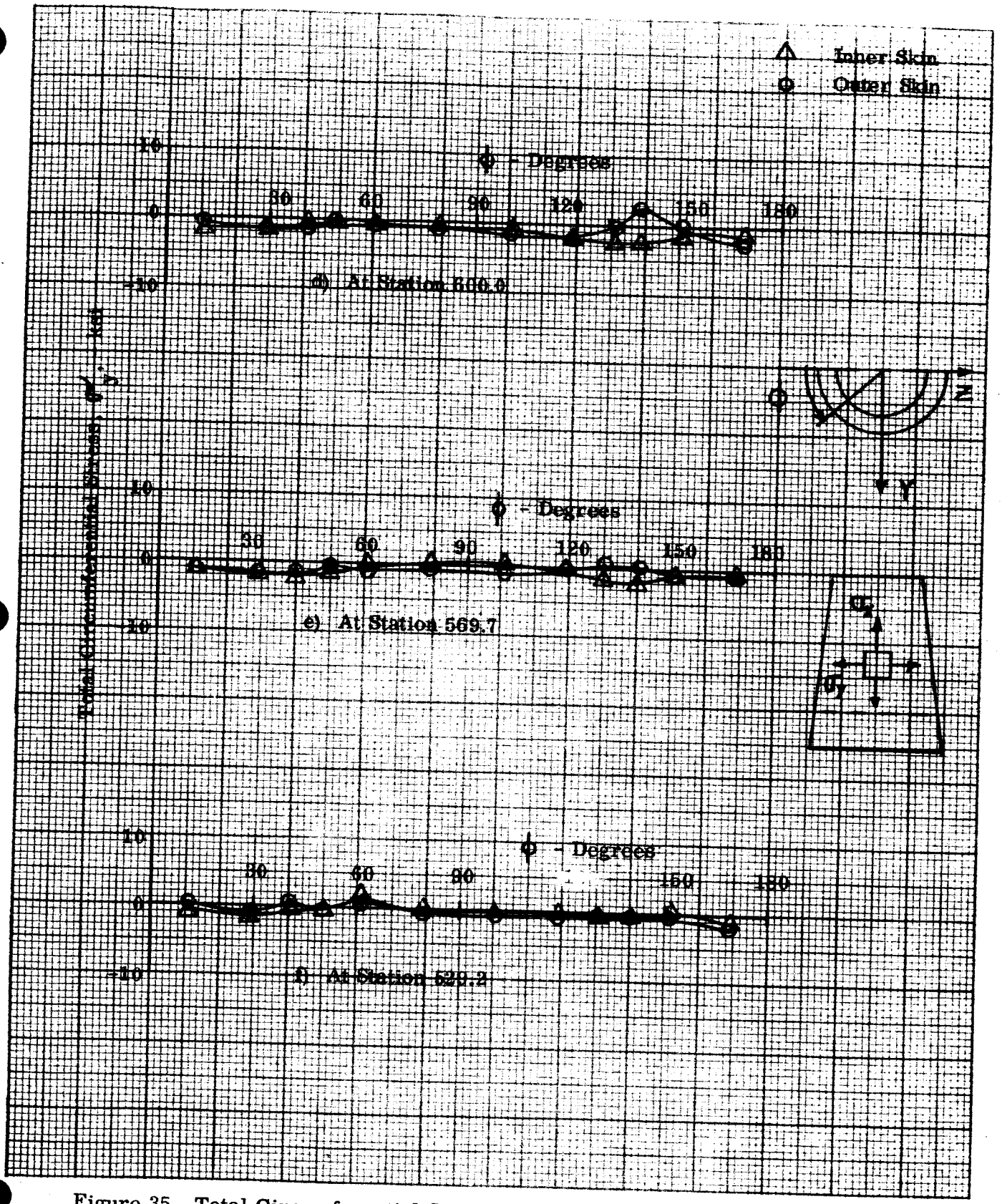

Figure 35. Total Circumferential Stresses Due to all Loads, Max. q∝ Condition 45° Air Load Orientation (Cont)

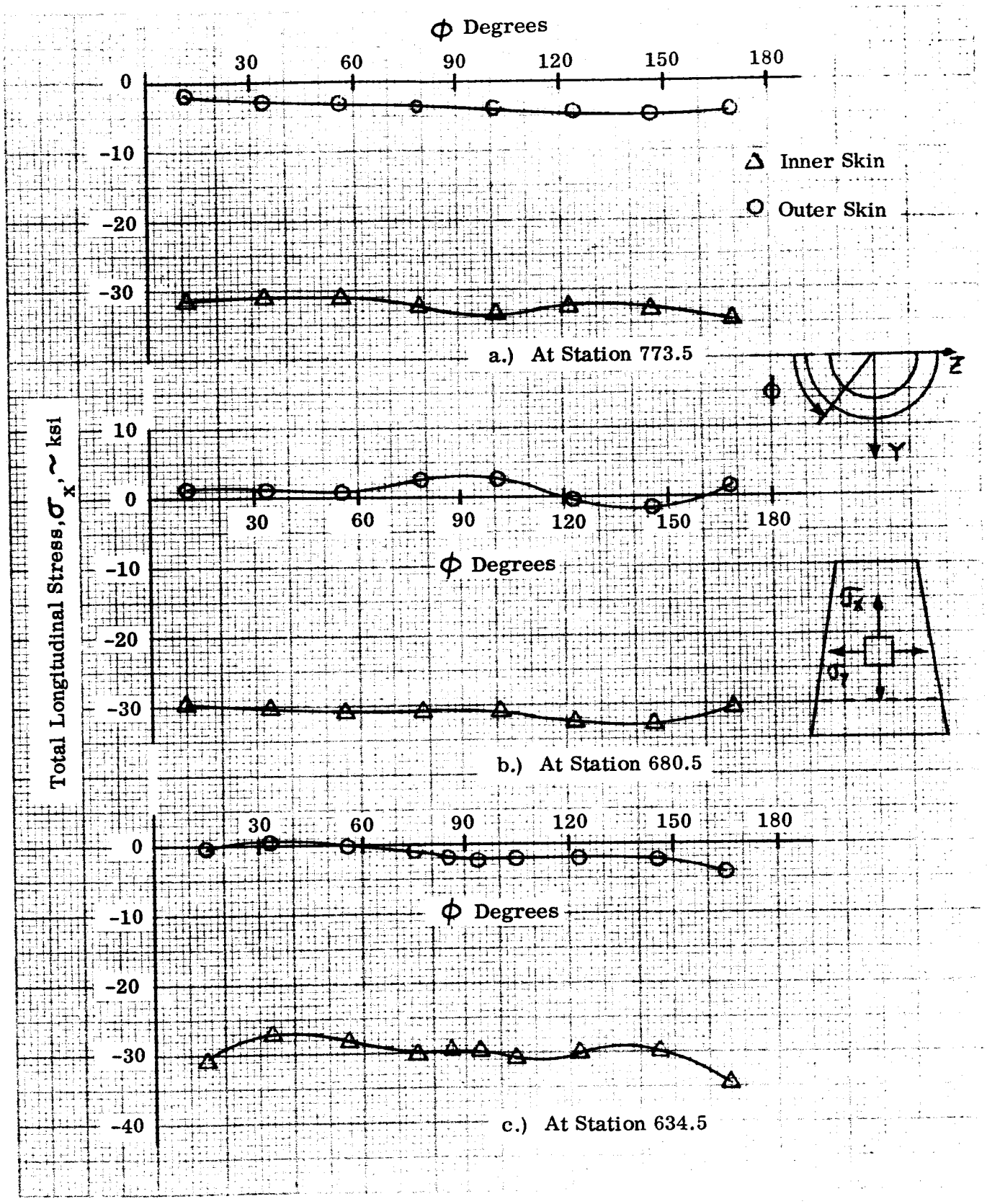

Figure 36. Total Longitudinal Stresses Due to all Loads, End Boost Condition

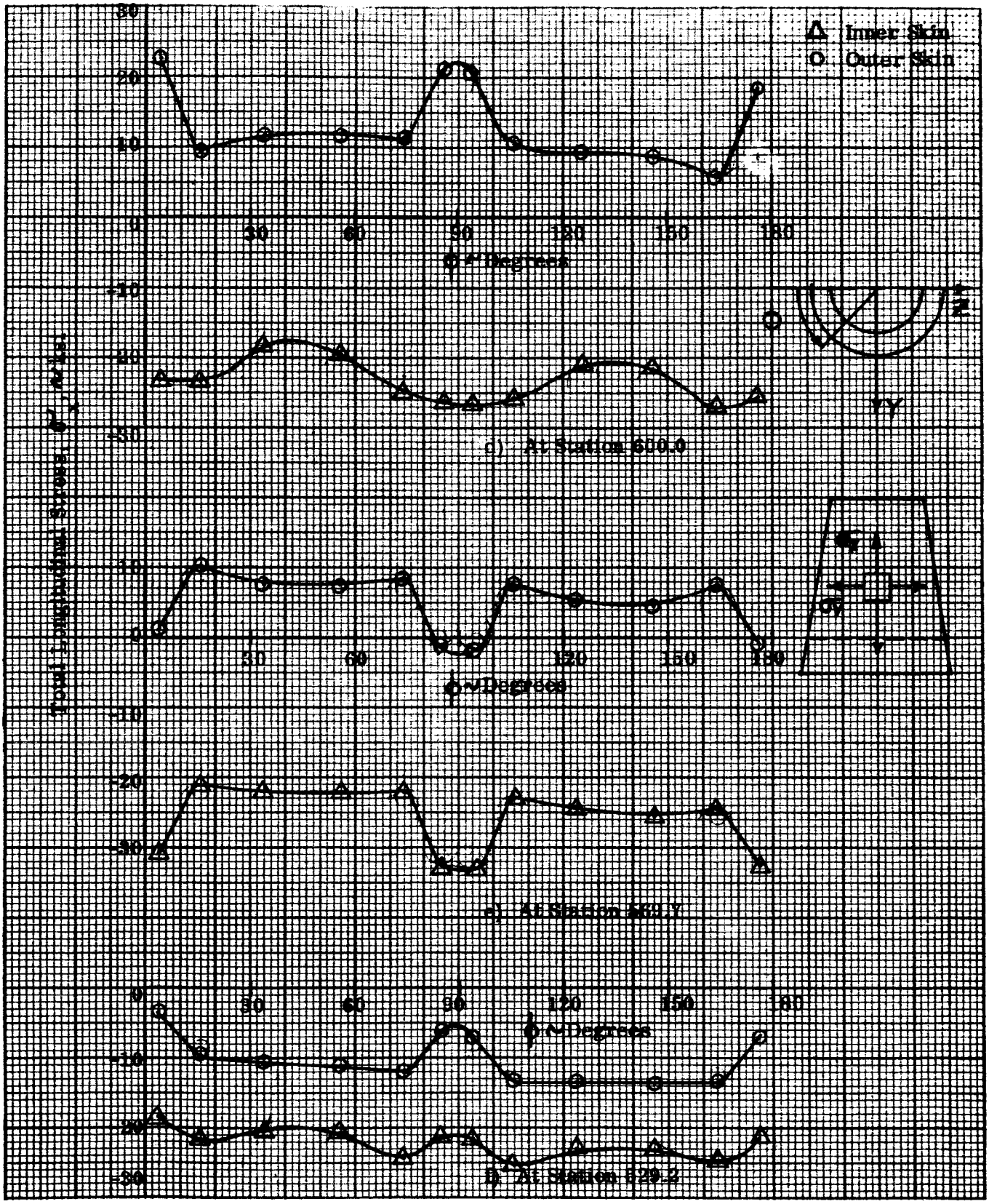

Figure 36. Total Longitudinal Stresses Due to All Loads, End Boost Condition (Cont)

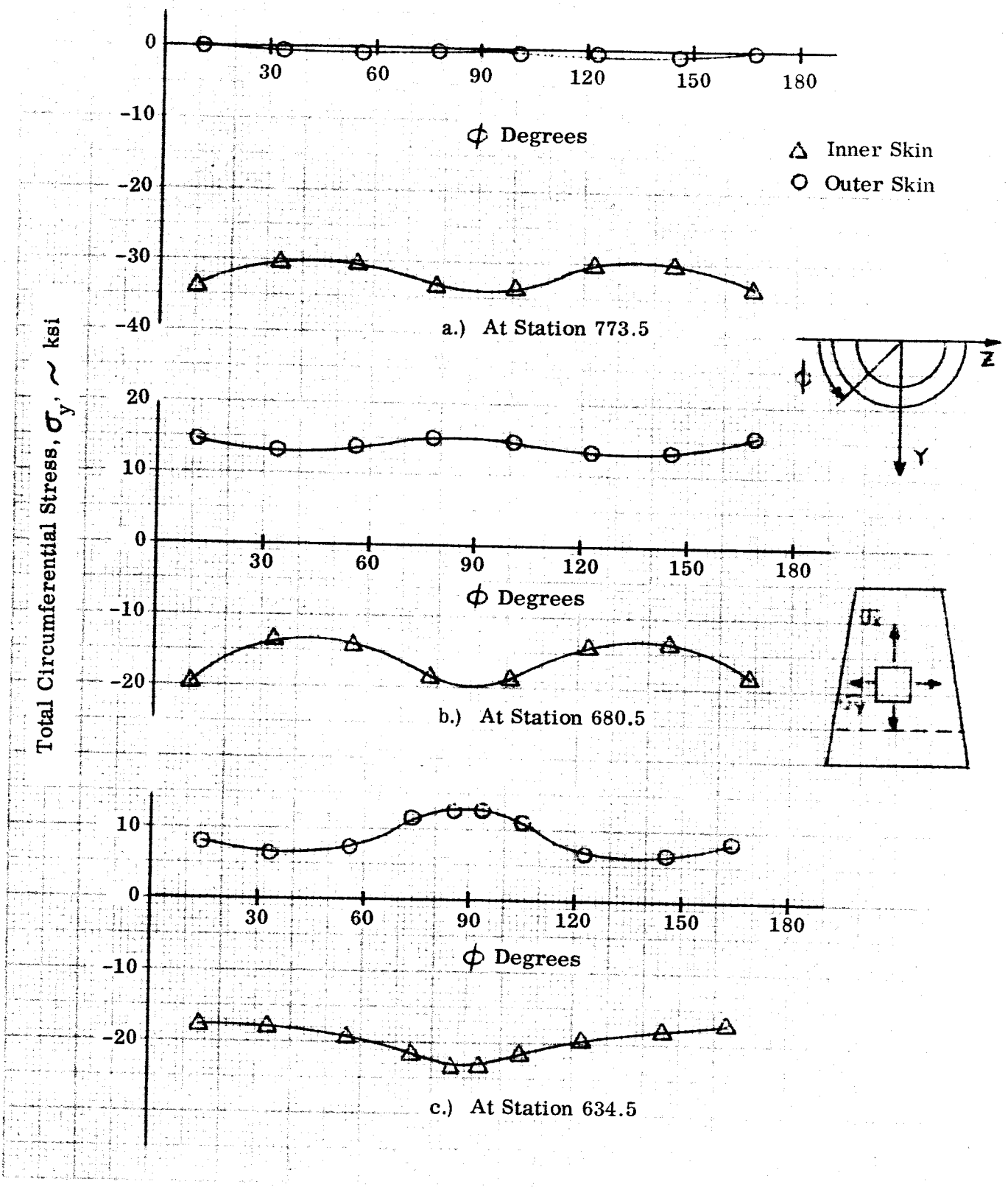

Figure 37. Total Circumferential Stresses Due to all Loads, End Boost Condition

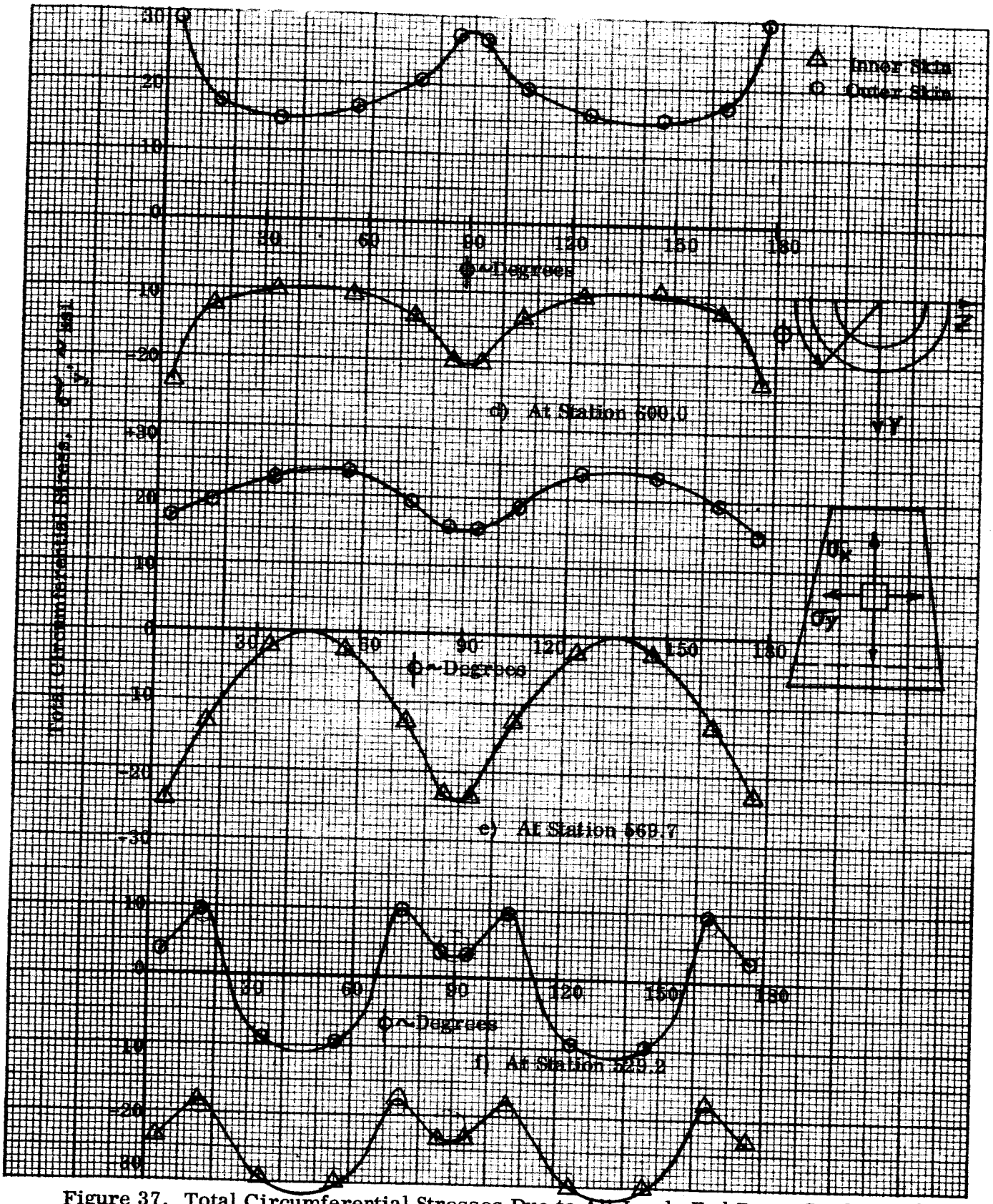

Figure 37. Total Circumferential Stresses Due to All Loads, End Boost Condition (Cont)

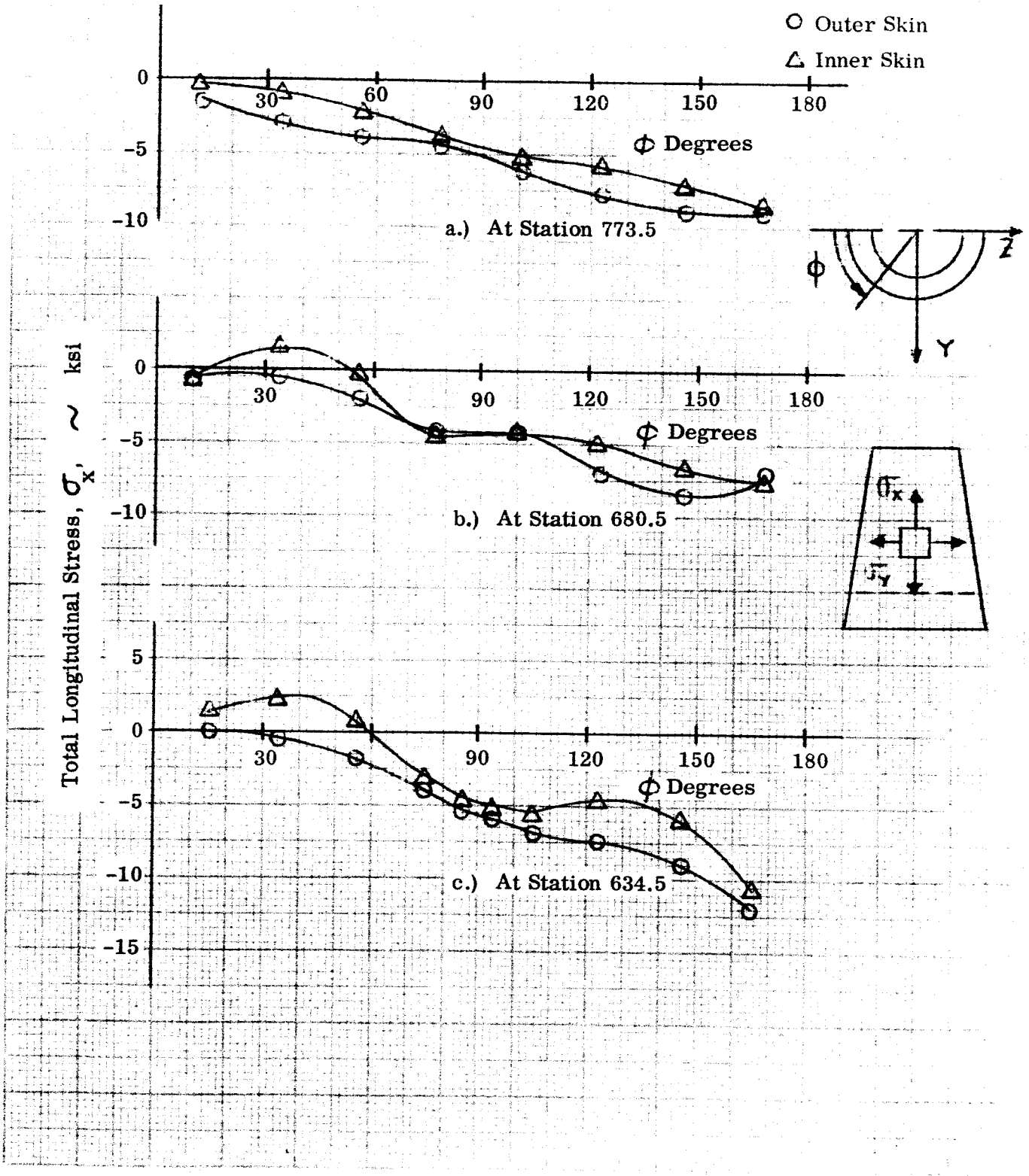

Figure 38. Total Longtudinal Stresses Due to all Loads, Hardover Engine Condition

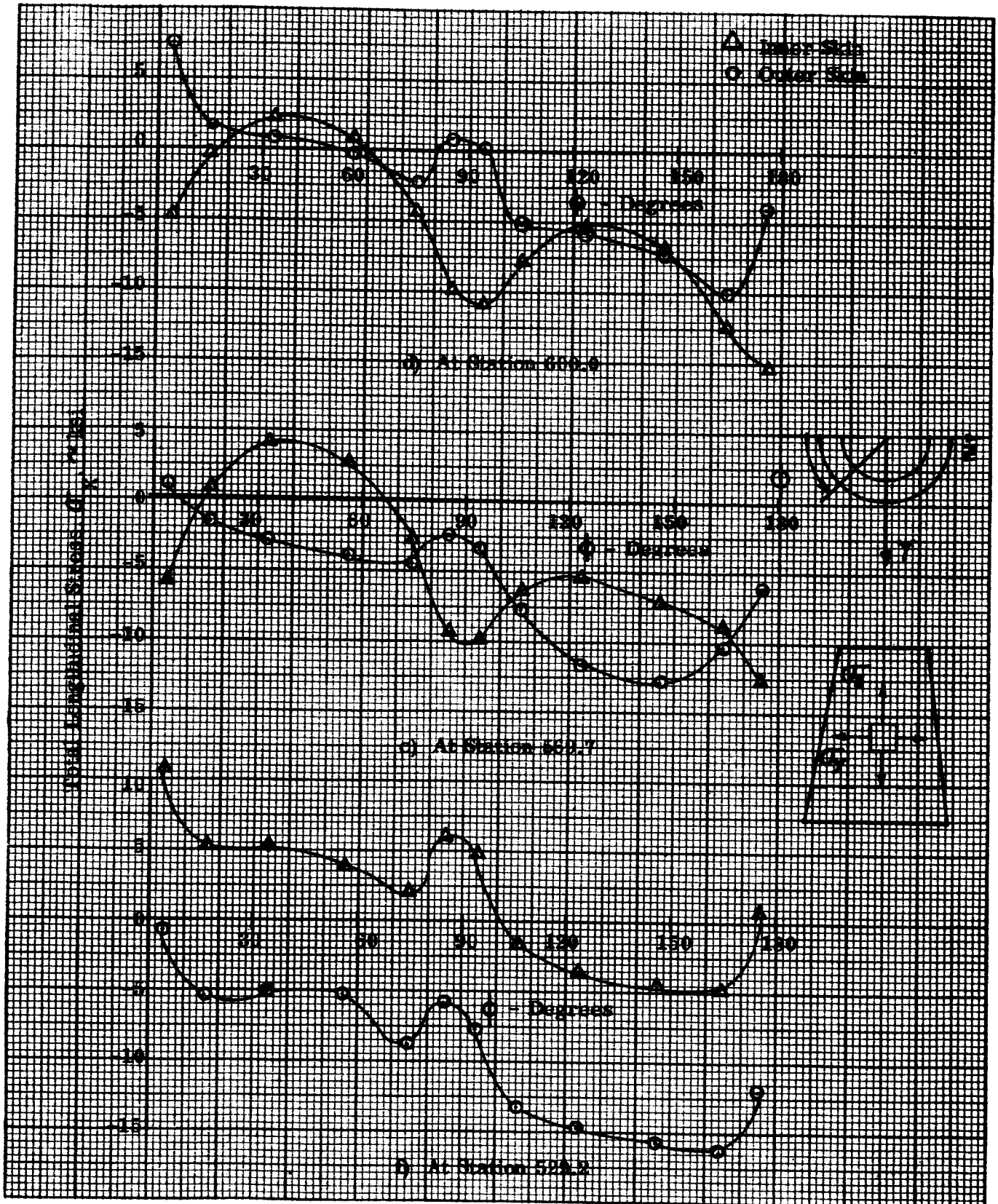

Figure 38. Total Longitudinal Stresses Due to all Loads, Hardover Engine Condition (Cont)

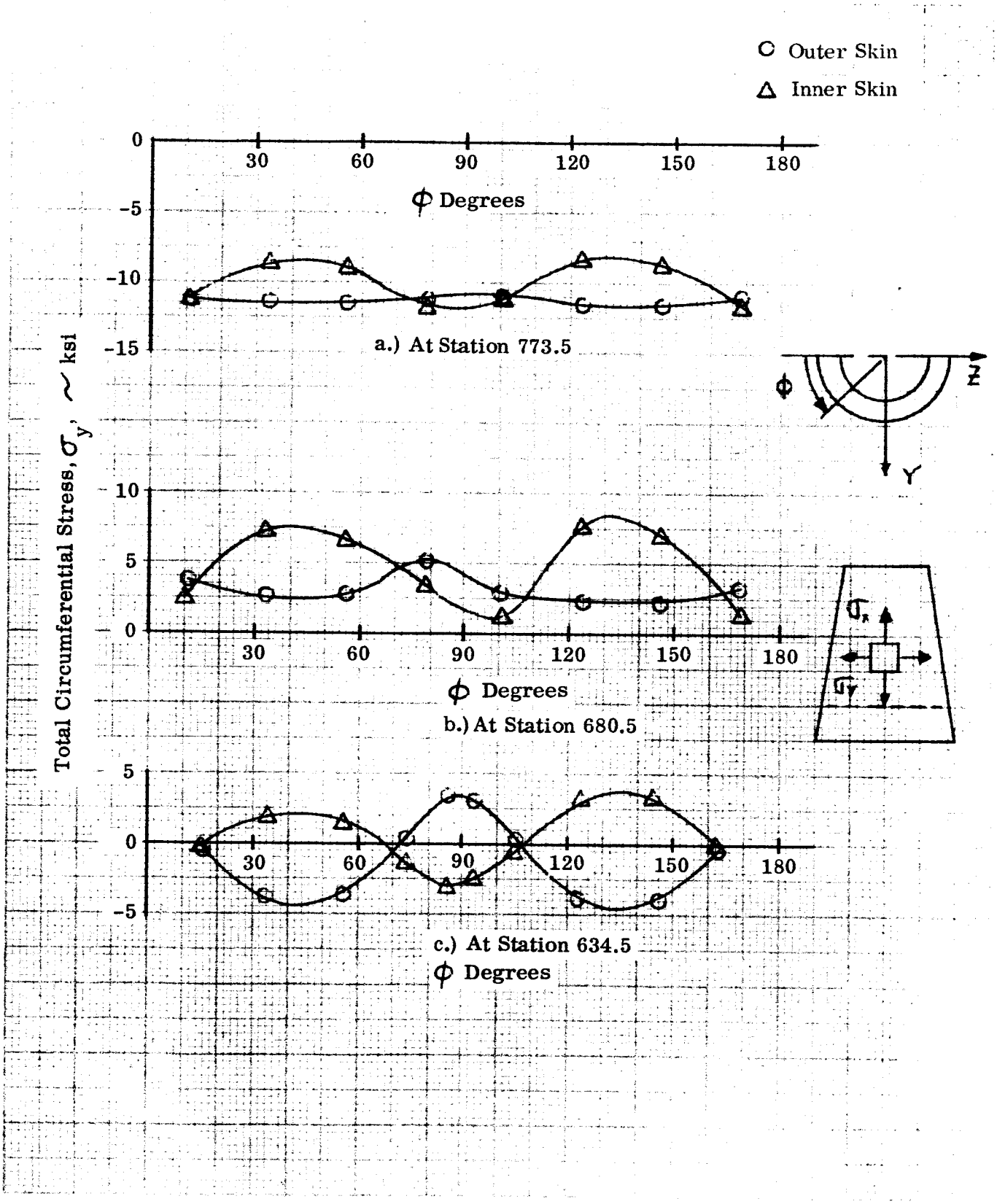

Figure 39. Total Circumferential Stresses Due to all Loads, Hardover Engine Condition

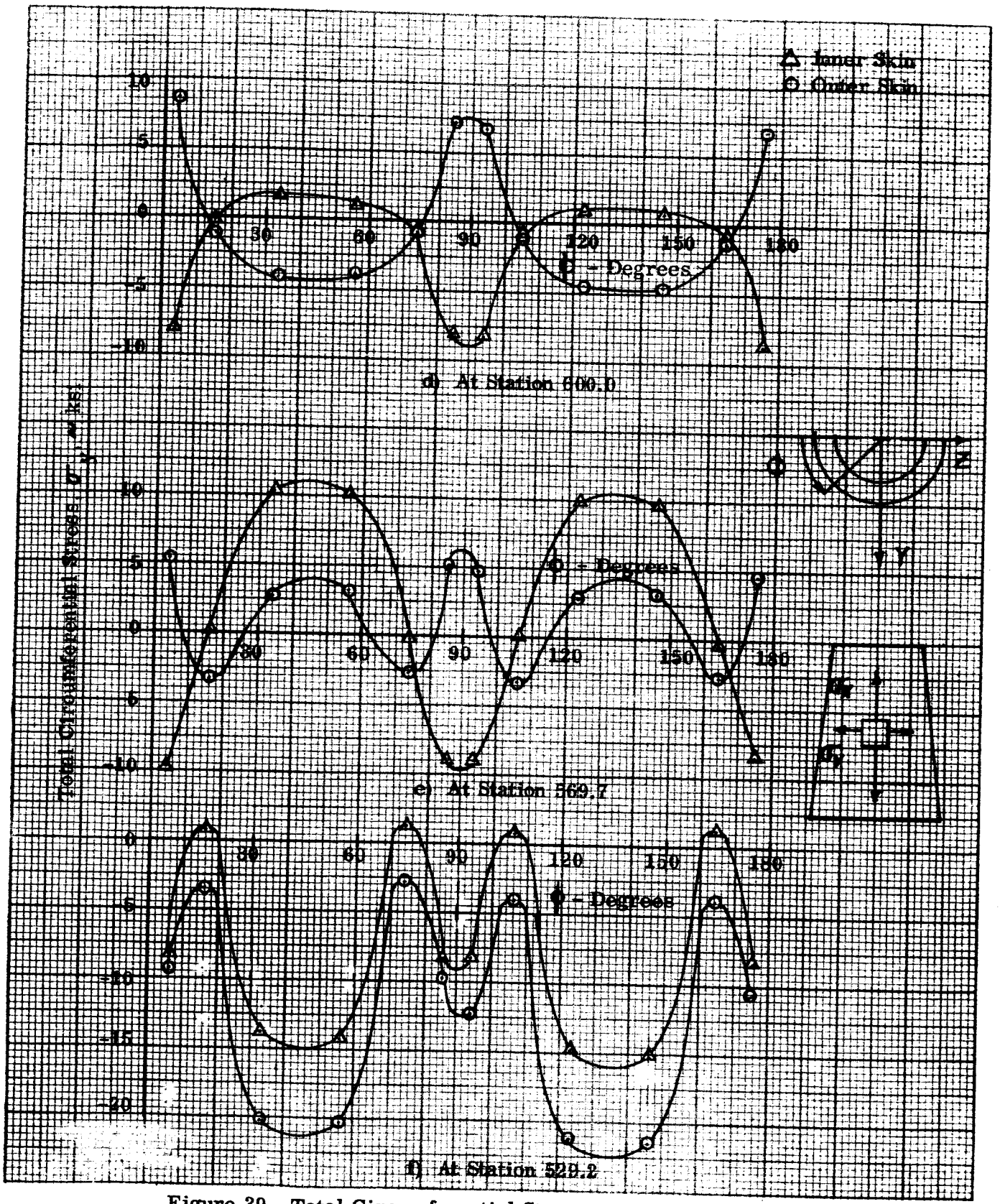

Figure 39. Total Circumferential Stresses Due to all Loads, Hardover Engine Condition (Cont)

IV. SUMMARY OF RESULTS

A. LEM SUPPORT INTERACTION LOADS

One of the main objectives of the analysis was the determination of the LEM interaction loads for any applied loading system. The LEM interaction loads are presented for all conditions treated in accordance with the following breakdown.

Case 1. SM-LEM Adapter Interface Loads
- (a) Bending Moment, M_A
- (b) Shear Load, S_A
- (c) Axial Force, AF

Case 2. Pressure Loads or Thermal Loads

Case 3. Inertial Loads

Case 4. LEM Loads
- (a) Lateral
- (b) Axial

Case 5. Sum of 4 above for Total Loads

LEM interaction loads obtained for the individual loading systems mentioned above are thus presented in Figures 12 through 27.

The LEM interaction loads due to inertia loads for the three conditions analyzed have been omitted because the numerical results obtained for this type of loading were negligible.

B. DISPLACEMENTS

The displacements are presented graphically in Figures 28 thru 31 and are the normal displacements to the LEM Adapter at circumferential station lines of the idealized structure. These displacements are due to the total loading system for each of the 4 specified conditions investigated.

It should be noted that these curves give the relative radial displacements with respect to the top of the instrument unit since the Adapter structure was simply supported at this location as described in Section II.

C. STRESSES

Stresses are only presented for the total applied loading system for each of the four conditions investigated. The stresses given represent the total longitudinal and circumferential stresses in the inner and outer skins of the sandwich structure as obtained in accordance with the equations.

$$\sigma_o = \sigma_m + \sigma_b$$

$$\sigma_i = \sigma_m - \sigma_b$$

Where σ_o, σ_i are the stresses in the outer and inner skins, and σ_m, σ_b are the membrane and bending stresses described in detail in Section IIIB. For consistancy, the stresses computed midway between the circumferential station lines of the idealized structure are shown in Figures 32 through 39.

V. CONCLUSIONS AND RECOMMENDATIONS

The LEM Adapter of the Apollo vehicle is a relatively complex structure composed of stiffness and sandwich shell elements. All indications are that its structural analysis by means of the discrete element approach as accomplished in this report are realistic. General conclusions deduced from the analysis results and recommendations regarding future analyses are summarized in this section.

Examination and comparison of all the LEM to LEM Adapter attachment loads reveals that the largest of these loads are induced by the End Boost and Hardover Engine conditions. Both of these conditions involve elevated temperature distributions which give rise to approximately identical attachment loads. This is because the average temperatures of the inner and outer walls of the LEM Adapter skin for both conditions are practically of the same magnitude. It should be noted that the End Boost condition involves a relatively large thermal gradient through the sandwich wall of the Adapter, but the corresponding thermal moments do not influence the magnitude of the LEM attachment loads. Such lack of influence results from the LEM attachment points being simply supported, i.e., moments are not transmitted across the attachment points. However, the presence of thermal moments for the End Boost condition help to produce Adapter stresses which are larger than those obtained for the other design conditions.

Comparison of the two sets of results obtained for the two airload orientation situations of the Maximum q_{α} condition revealed that the LEM attachment load levels and directions differ significantly with orientation. However, the computed stress levels in the Adapter are essentially the same. The presence of interface loads at the SM to LEM Adapter juncture and inertia loads contributed little to the LEM attachment loads.

Based on experience gained from the LEM Adapter analysis presented in this report, the following items of work are recommended for the purpose of checking analysis assumption:

1. It was assumed that the LEM Adapter is simply supported at the Adapter to the Instrument Unit interface. Such an assumption would , in general, tend to reduce the LEM attachment loads. Hence, the effect of elastic support condition should be investigated.
2. The validity of the analytically derived LEM symmetric stiffness matrix is in question for the 45° air load orientation analysis condition. because in reality the LEM structure is not symmetric. Hence, the present analysis should be repeated with an experimentally derived LEM stiffness matrix.

REFERENCES

1. P. R. No. 4330060, "Stress and Displacement Analysis of the SM, LEM Adapter and Instrument Unit," Contract No. NAS9-3970, January 1965.

2. Letter from Smith, P., (NASA, Houston) dated March 1965.

3. Letter from Smith, P., (NASA, Houston) dated 1 July 1965.

4. Memorandum from Bone, D., Bune, F., (Grumman Aircraft Engineering Corporation), dated 7 October 1964.

5. Letter from Mueller, W., (Grumman Aircraft Engineering Corporation) dated 18 February 1965.

6. Letter from Cary, J., (Grumman Aircraft Engineering Corporation) dated 17 May 1965.

7. Gallagher, R. H., "A Correlation Study of Methods of Matrix Structural Analysis," Pergamon Press, 1964.

8. Gallagher, R. H., Huff, R., "Derivation of the Force-Displacement Properties of Triangular and Quadrilateral Orthotropic Plates in Plane stress and Bending," Bell Report No. D2114-950005, January 1964.

9. Gellatly, R., Gallagher, R.H., Luberacki, W., "Development of a Procedure for Automated Synthesis of Minimum Weight Structures," FDL-TDR-64-141, October 1964.

10. Letter from Gallagher, R.H. (Bell Aerosystems Company) dated 3 May 1965.

APPENDIX A

BELL GENERAL PURPOSE STRUCTURAL ANALYSIS COMPUTER PROGRAM

The Bell "General Purpose" Matrix Structural Analysis Program, coded for operation on an IBM 7090 computer, is designed to accept the basic information describing a problem, establish its formulation, and perform all computations required for the development of the desired stress and/or displacement results. The basic problem information consists of:

(1) Dimensions of the structure

(2) Load and temperature conditions of interest

(3) Material mechanical properties

(4) Operational controls; i.e., specification of desired printout items, etc.

(5) Designation of the discrete elements

Items (1)-(4) are evident characteristics of any analysis problem. To establish the significance of item (5), the discrete elements, it is first necessary to review briefly the theoretical concepts upon which this method of analysis is based.

This program is formulated in terms of the "displacement" approach to the matrix analysis of structures idealized as systems of connected discrete elements. The points of connection are called "reference" or "node" points. Each class of discrete element (bar, triangular plate, beam segment, etc.) possesses a finite number of connection points, the specific number in a given case being dictated by the number of parameters needed to define the variation of the edge stress systems acting upon the element. A hypothetical element, a rectangular plate segment of a plate component, having four reference points, is shown below.

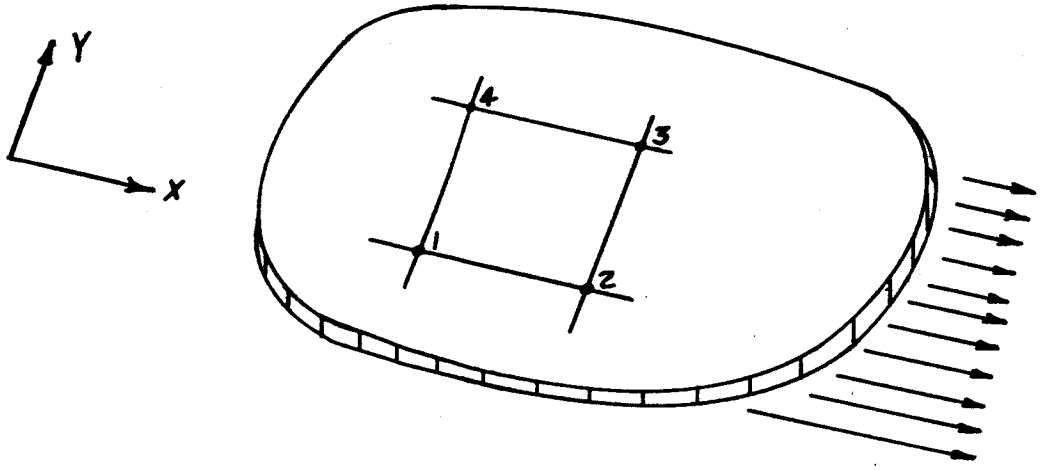

For any such element, it is first necessary to derive relationships between the displacements $\{u\}$ of the boundary points and the forces $\{F\}$ acting at these points. The node point forces are statically equivalent to the stresses that actually exist on the edge areas subtended by the point. On the basis of assumptions as to element deformational behavior, it is possible to establish the desired relationships in matrix form, as

$$\{F\} = [K]\{u\} + \{F^{\alpha}\} \qquad \text{(A-1)}$$

where $[K]$ is the "element stiffness matrix" and $\{F^{\alpha}\}$ represents the terms associated with temperature change, which take the form of "thermal loadings".

General techniques for the derivation of element stiffness properties are to be found in the text "A Correlation Study of Methods of Matrix Structural Analysis", Chapter 3 (Ref. 7).

For the LEM Adapter, five particular types of element behavior are necessary: (1) the quadrilateral plate in plane stress, (2) the quadrilateral plate in bending, (3) the triangular plate in plane stress, (4) the triangular plate in bending, and (5) axial flexural member. The derivation of the triangular and quadrilateral plates in plane stress is found in Reference (7). The derivation of the triangular and quadrilateral plate bending relationships can be found in Reference (8), while those for the axial flexural member can be found in Reference (9)..

The elements are assembled to form the complete analytical model of the structure by joining all elements at their respective juncture points, applying in this process the requirements of juncture point equilibrium and compatibility. Thus, the components of the internal loads $\{F\}$ and external loads $\{P\}$ at each point are related by equilibrium requirements; i.e., $\Sigma F_x = P_x$, etc. The respective coordinate displacements of the nodes of all elements meeting at a given juncture point are equal, a requirement that satisfies compatibility. It is found that the coefficients in the resulting equations that relate the node point forces and displacements can be developed by simply adding the element stiffness coefficients which have subscripts identical to the desired coefficient. The resulting equations are of the form

$$\{P\} = [K]\{u\} + \{P^{\alpha}\} \qquad \text{(A-2)}$$

where the $\{P^{\alpha}\}$ terms are "net" thermal forces at the node points resulting from summation of the element thermal forces $\{F^{\alpha}\}$. Displacement boundary conditions (i.e., the node points that are restrained against displacement) can be imposed, with the effect of reducing the order of Equation (A-2).

The solution of Equation (A-2) for the displacements in terms of the forces is obtained through inversion of the matrix; i.e.,

$$\{u\} = [K]^{-1}\left(\{P\} - \{F^{\alpha}\}\right) = [\delta]\left(\{P\} - \{F^{\alpha}\}\right) \qquad \text{(A-3)}$$

where the set of coefficients $[\delta]$ are the displacement influence coefficients. These are needed if a vibrational analysis is to be performed. The solution for element internal forces (the forces $\{F\}$ in Equation (A-1)) can be affected by multiplying the respective element stiffness matrices by the now-known values of displacement $\{u\}$. Then, in a final step, the element corner forces are transformed into stresses.

Two additional capabilities of the program are utilized in the analysis of the LEM Adapter. Knowing the element stiffness coefficients for the LEM, this matrix may be entered as input. The other additional capability of the program is its ability to treat "oblique" support conditions. It sometimes occurs that a structure is constrained to displace in the direction of axes other than those employed in the definition of the behavior of the structure as a whole (see sketch below).

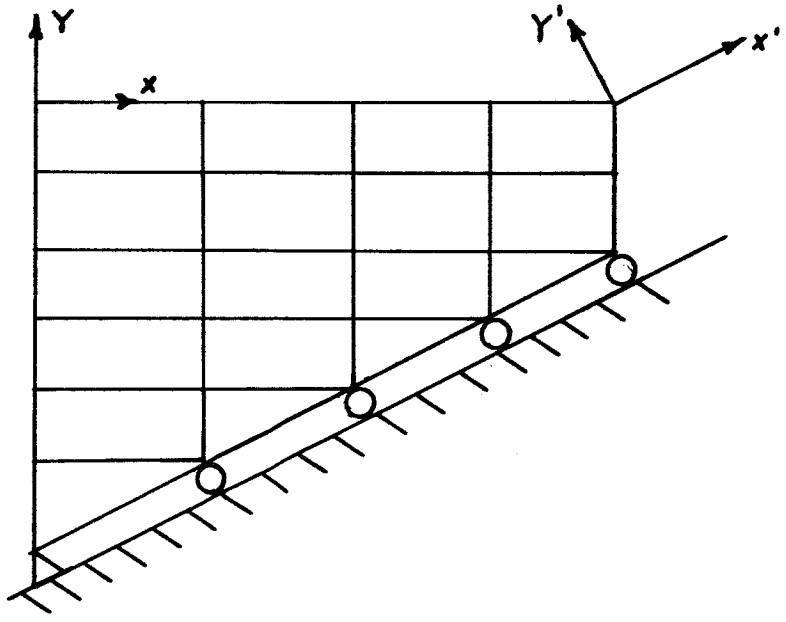

Such conditions can be accommodated simply by specifying, by means of coordinates, the direction of the special x' axis and listing the affected points. The program will then transform all the necessary relationships, such as the stiffness, stress, and thermal load matrices, at all the affected points into equations referred to the special axes. The boundary conditions and applied loads, then are defined with respect to the new system.

From an operational standpoint, the Bell General Purpose Structural Analysis Program consists of three major computational routines:

(1) A library of element stiffness relationships

(2) A routine wherein the master stiffness matrix is calculated, boundary conditions are applied, and the matrix inverted.

(3) A routine which selects information from (1) and the resulting inverse from (2) and calculates stress, displacement, etc.

Routine (1) is the key to the versatility of the program, since the capability to analyze a given type of configuration is dependent upon the availability, in the element library, of relationships for elements of the proper geometric form and behavior. As noted earlier, these elements are for the present case, quadrilateral and triangular plate elements in plane stress and bending, and axial flexural members.

APPENDIX B

LEM STIFFNESS MATRIX

A. INTRODUCTION

As discussed in the body of this report, the LEM is treated as a single discrete element in the analysis of the LEM Adapter and consequently, its stiffness matrix is required for the present analysis. However, flexibility matrices given in Reference (4) for the LEM, cannot be used directly by the Bell General Purpose Structural Analysis Computer Program since acceptable inputs are only stiffness matrices (see Appendix A). The derivation of the necessary LEM stiffness matrices from the flexibility data given in Reference (4), are presented in this appendix for the two airload orientations considered in the analysis. As discussed in detail in Section IIB, since as a simplification, only one half of the entire structure is used in the analysis, the final form of the LEM stiffness matrix is assumed to be symmetric about a diametrical plane for each of the two airload orientations investigated.

B. DETERMINATION OF LEM STIFFNESS MATRIX FOR 0° AIR LOAD ORIENTATION CONDITION

The 0° and 45° airload orientations defined with respect to the LEM structure as given in Reference (4) are shown in Figure B-1. The complete structural characteristics of the LEM structure is presented in Reference (4), in terms of two sets of flexibility coefficients, one set for a symmetric load case and the other for a corresponding anti-symmetric load case.

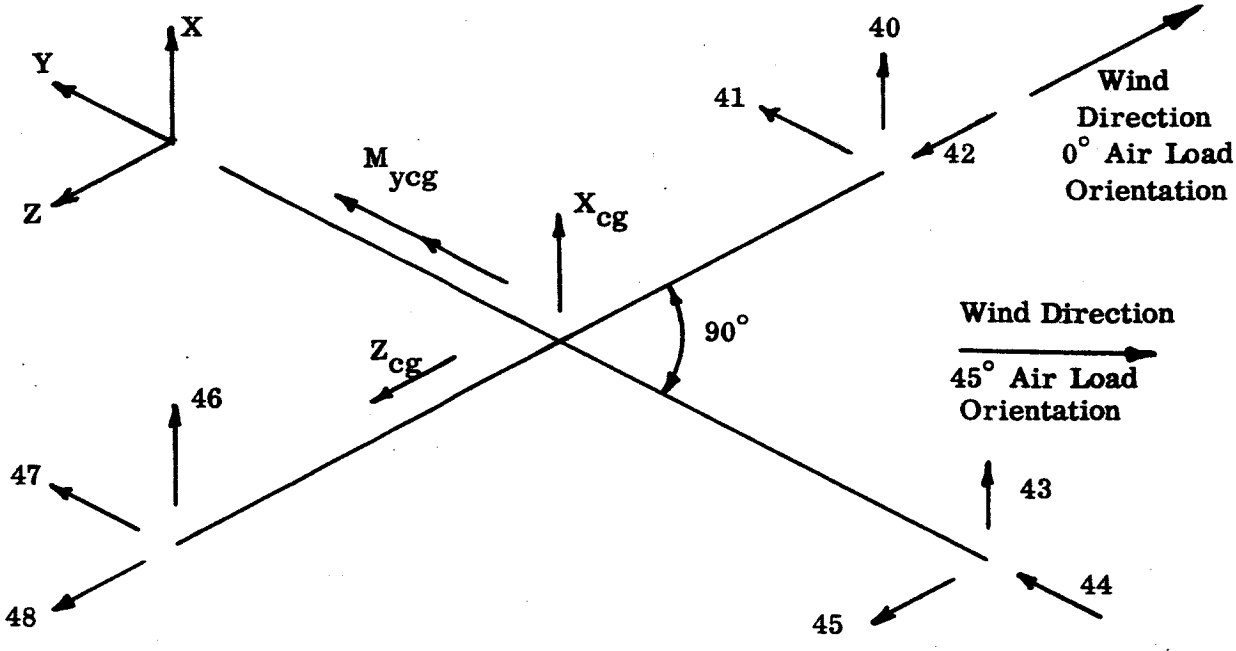

Figure B-1. Idealized LEM Structure Notation of Reference (4)

Since the 0° airload orientation condition coincides with the plane of structural symmetry of the LEM as seen in Figure B-1, the flexibility matrix given in Reference (4) for the symmetric loading case is only of interest and is used in the following manner to determine the required stiffness matrix coefficients.

In general, the flexibility matrix is defined by the expression

$$\{u\} = [f]\{F\} \tag{B-1}$$

where

$\{u\}$ is a column of displacements
$\{F\}$ is the column of applied loads
$[f]$ is the flexibility matrix

The column of forces are first converted to the Bell notation as illustrated in Figure B-2 by the following equation

$$\begin{Bmatrix} F_{40} \\ F_{42} \\ F_{44} \\ F_{48} \\ X_{cg} \\ Z_{cg} \\ M_{ycg} \end{Bmatrix} = [T_s] \begin{Bmatrix} F_{x3} \\ F_{x4} \\ F_{y2} \\ M_{y4} \\ F_{z1} \\ F_{z3} \\ F_{z4} \end{Bmatrix} \tag{B-2}$$

where the transformation matrix $[T_s]$, for the symmetric loading case is given in Reference (5) as

$$[T_s] = \begin{bmatrix} 1 & 0 & 0 & 0 & 0 & 0 & 0 \\ 0 & 0 & 0 & 0 & 0 & 1 & 0 \\ 0 & 0 & 1 & 0 & 0 & 0 & 0 \\ 0 & 0 & 0 & 0 & 1 & 0 & 0 \\ 0 & 2 & 0 & 0 & 0 & 0 & 0 \\ 0 & 0 & 0 & 0 & 0 & 0 & 2 \\ 0 & 0 & 0 & 2 & 0 & 0 & 0 \end{bmatrix} \tag{B-3}$$

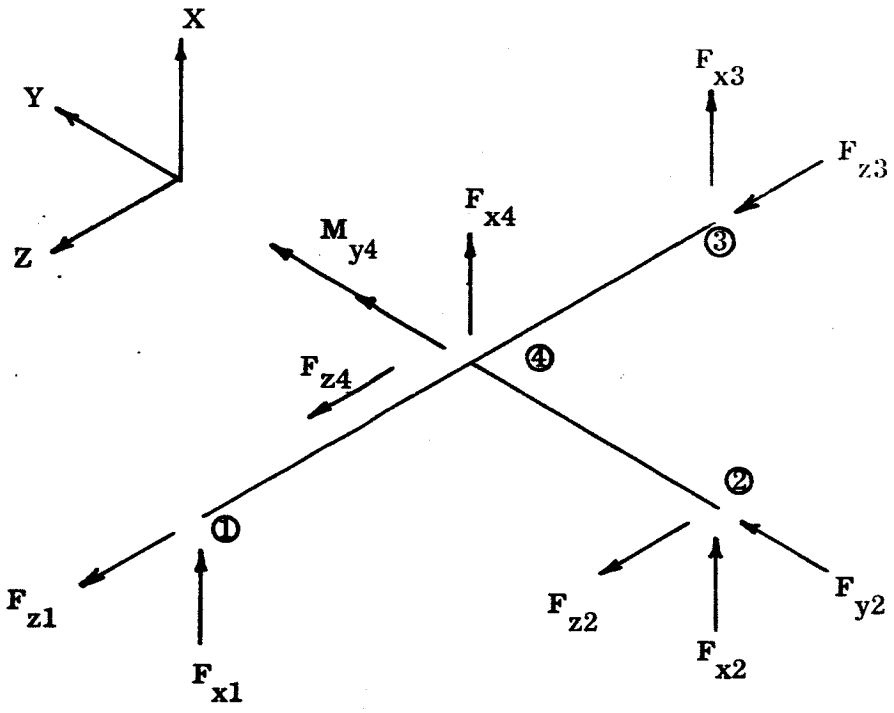

Figure B-2. Idealized LEM Structure, Symmetric Loading Case

In Figure B-2, node points 1, 2 and 3 are the attachment points between the LEM and the Adapter and node point 4 represents the location of the center of gravity (c.g.) of the LEM. The displacements in equation (B-1) are transformed to Bell notation in accordance with the following expression

$$\begin{Bmatrix} u_3 \\ u_4 \\ v_2 \\ \theta_{y4} \\ w_1 \\ w_3 \\ w_4 \end{Bmatrix} = \left[T_s \right]^T \begin{Bmatrix} u_{40} \\ u_{42} \\ w_{44} \\ w_{48} \\ X_{cg} \\ Z_{cg} \\ M_{ycg} \end{Bmatrix} \qquad \text{(B-4)}$$

where $\left[T_s \right]^T$ is the transpose matrix of $\left[T_s \right]$ defined by Equation (B-3). Thus, from the above equations the flexibility matrix, for the symmetric loading case, in Bell notation, is given by

$$\begin{Bmatrix} u_3 \\ u_4 \\ v_2 \\ \theta_{y4} \\ w_1 \\ w_3 \\ w_4 \end{Bmatrix} = \begin{bmatrix} f_s \end{bmatrix} \begin{Bmatrix} F_{x3} \\ F_{x4} \\ F_{y2} \\ M_{y4} \\ F_{z1} \\ F_{z3} \\ F_{z4} \end{Bmatrix} \tag{B-5}$$

where

$$\begin{bmatrix} f_s \end{bmatrix} = \begin{bmatrix} T_s \end{bmatrix}^T \begin{bmatrix} f_1 \end{bmatrix} \begin{bmatrix} T_s \end{bmatrix} \tag{B-6}$$

The matrix $\begin{bmatrix} f_1 \end{bmatrix}$ is the flexibility matrix for the symmetric loading case of the LEM and is given in Reference (4) as

$$\begin{bmatrix} f_1 \end{bmatrix} = 10^{-7} \times \begin{bmatrix} 3083.5 & 90.46 & -56.84 & -57.97 & 362.1 & -44.33 & -4.913 \\ 90.46 & 348.24 & -12.62 & 178.43 & 8.329 & 96.83 & -0.106 \\ -56.84 & -12.62 & 78.31 & 8.867 & -6.423 & 2.627 & 0.0281 \\ -57.97 & 178.43 & 8.867 & 346.92 & -1.478 & 115.97 & -0.1450 \\ 362.1 & 8.329 & -6.423 & -1.478 & 70.02 & -0.4236 & -0.6543 \\ -44.33 & 96.83 & 2.627 & 115.97 & -0.4236 & 77.37 & -0.0579 \\ -4.913 & -0.106 & 0.0281 & -0.1450 & -0.6543 & -0.0579 & 0.0146 \end{bmatrix} \tag{B-6a}$$

Solving equation (B-5) for the forces yields

$$\begin{Bmatrix} F_{x3} \\ F_{x4} \\ F_{y2} \\ M_{y4} \\ F_{z1} \\ F_{z3} \\ F_{z4} \end{Bmatrix} = \begin{bmatrix} K_{1r} \end{bmatrix} \begin{Bmatrix} u_3 \\ u_4 \\ v_2 \\ \theta_{y4} \\ w_1 \\ w_3 \\ w_4 \end{Bmatrix} \tag{B-7}$$

where $\left[K_{1r}\right]$ is the reduced stiffness matrix of the LEM and is determined by inverting the flexibility matrix given by equation (B-6). Thus

$$\left[K_{1r}\right] = \left[f_s\right]^{-1} \tag{B-8}$$

It is evident that from a comparison of the forces in Equation (B-7) and those shown in Figure B-2 indicate that F_{x1}, F_{x2} and F_{z2} are reactions. By writing the appropriate static equilibrium relationships for the LEM, the reactions in terms of the other presumeably known forces can be obtained from

$$\begin{Bmatrix} F_{x1} \\ F_{x2} \\ F_{z2} \end{Bmatrix} = \left[E_s\right] \begin{Bmatrix} F_{x3} \\ F_{x4} \\ F_{y2} \\ M_{y4} \\ F_{z1} \\ F_{z3} \\ F_{z4} \end{Bmatrix} \tag{B-9}$$

where the equilibrium matrix $\left[E_s\right]$, obtained from Reference (5), is given as

$$\left[E_s\right] = \begin{bmatrix} 1.0 & -0.0012 & 0 & -0.00862 & 0 & 0 & 0.0422 \\ -2.0 & -0.9988 & 0 & 0.00862 & 0 & 0 & -0.0422 \\ 0 & 0 & 0 & 0 & -1.0 & -1.0 & -1.0 \end{bmatrix} \tag{B-10}$$

It can be shown that the relationship between the previously defined displacements and the unknown (rigid body) displacements is given by

$$\begin{Bmatrix} u_3 \\ u_4 \\ v_2 \\ \theta_{y4} \\ w_1 \\ w_3 \\ w_4 \end{Bmatrix} = \left[E_s\right]^T \begin{Bmatrix} u_1 \\ u_2 \\ w_2 \end{Bmatrix} \tag{B-11}$$

where $\left[E_s\right]^T$ is the transpose matrix of equation (B-10). Thus the LEM element force displacement relationships for the symmetric loading case depicted in Figure B-2 is given as

$$\begin{Bmatrix} F_{x3} \\ F_{x4} \\ F_{y2} \\ M_{y4} \\ F_{z1} \\ F_{z3} \\ F_{z4} \\ \hline F_{x1} \\ F_{x2} \\ F_{z2} \end{Bmatrix} = \left[\begin{array}{c|c} \left[K_{1r}\right] & \left[K_{1r}\right]\left[E_s\right]^T \\ \hline \left[E_s\right]\left[K_{1r}\right] & \left[E_s\right]\left[K_{1r}\right]\left[E_s\right]^T \end{array}\right] \begin{Bmatrix} u_3 \\ u_4 \\ v_2 \\ \theta_{y4} \\ w_1 \\ w_3 \\ w_4 \\ \hline u_1 \\ u_2 \\ w_2 \end{Bmatrix} \tag{B-12}$$

where $\left[K_{1r}\right]$ and $\left[E_s\right]$ are defined by equations (B-8) and (B-10) respectively.

The above equation defines the appropriate stiffness matrix of the LEM as a discrete element, but the terms in the force and displacement columns must be rearranged in ascending node point notation to be consistent with the input required by the Bell computer program. Thus, after rearranging terms we obtain

$$\begin{Bmatrix} F_{x1} \\ F_{x2} \\ F_{x3} \\ F_{x4} \\ F_{y2} \\ M_{y4} \\ F_{z1} \\ F_{z2} \\ F_{z3} \\ F_{z4} \end{Bmatrix} = \left[\bar{K}_1\right] \begin{Bmatrix} u_1 \\ u_2 \\ u_3 \\ u_4 \\ v_2 \\ \theta_{y4} \\ w_1 \\ w_2 \\ w_3 \\ w_4 \end{Bmatrix} \tag{B-13}$$

where $\left[\bar{K}_1\right]$ is the resulting stiffness matrix. Figure B-3 was drawn to show previously adopted LEM and Adapter reference systems. A comparison of these two systems indicates a rotational difference of 180° with respect to the YZ plane.

Figure B-3

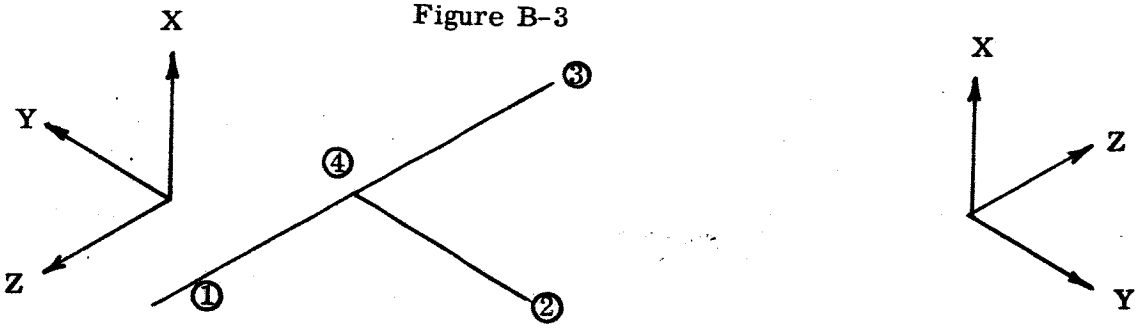

a) LEM Structure and Reference System

b) Adapter Reference System

To be consistent with the reference system used in the analysis of the Adapter, the signs of rows and columns pertaining only to the Y and Z coordinate terms were altered. Finally, after manipulation of equation (B-13), the LEM element force displacement relationships were determined as

$$\begin{Bmatrix} F_{x1} \\ F_{x2} \\ F_{x3} \\ F_{x4} \\ F_{y2} \\ M_{y4} \\ F_{z1} \\ F_{z2} \\ F_{z3} \\ F_{z4} \end{Bmatrix} = \left[K_{s1}\right] \begin{Bmatrix} u_1 \\ u_2 \\ u_3 \\ u_4 \\ v_2 \\ \theta_{y4} \\ w_1 \\ w_2 \\ w_3 \\ w_4 \end{Bmatrix} \qquad \text{(B-14)}$$

where $\left[K_{s1}\right]$ is the required stiffness matrix for the symmetric loading case. This stiffness matrix is presented in the body of the report as Figure 10.

The above presentation gives a complete explanation of the manner in which the LEM stiffness matrix was obtained from a given LEM flexibility matrix (Equation B-6a) and an equilibrium matrix (Equation B-10). However, it must be emphasized that node point 4 (see Figure B-3) is essentially a reference point conveniently located at the c.g. of the LEM structure and the corresponding flexibility coefficients were obtained for node point displacements $u_1 = u_2 = w_2 = 0$. Node point forces F_{x1}, F_{x2} and F_{z2} are therefore unknown reactions.

To determine a stiffness matrix from a flexibility matrix, it is necessary to have available equilibrium equations from which unknown statically determinate reactions can be obtained. These equations were formulated for the LEM structure with the aid of Figure B-2a (see Reference 5). This Figure B-2a gives the relative dimensional location of the LEM node points. Note that terms in the equilibrium matrix reflect these relative dimensions.

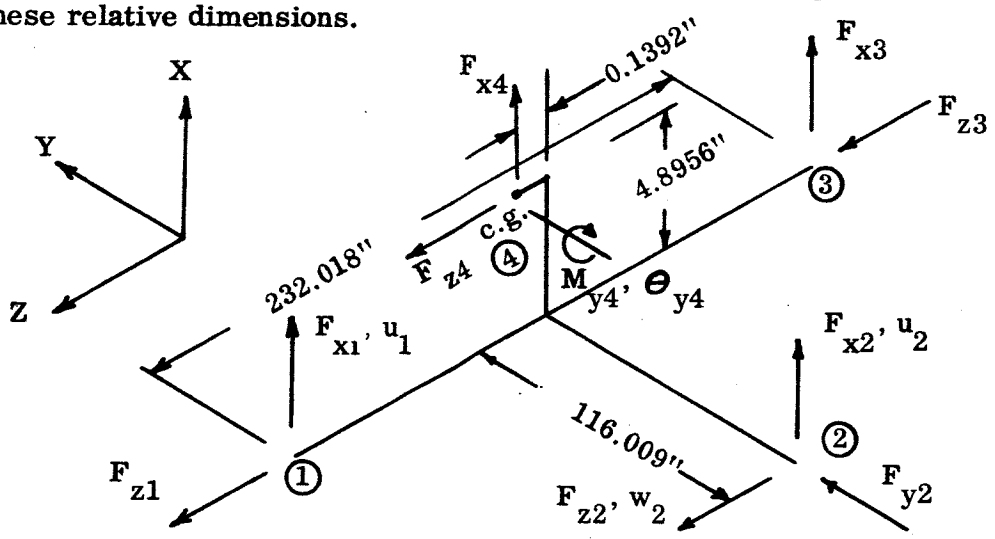

Figure B-2a. Location of LEM Node Points

An examination of the elements in the derived LEM stiffness matrix reveals some relatively large valued stiffness elements. Thus, for example, if all displacements are restrained except θ_{y4}, it is found that the force F_{z4} at the c.g. is given by (see Figure 10)

$$F_{z4} = 801{,}227\ \theta_{y4} \qquad \text{(B-14a)}$$

The force F_{z4} is the reaction in the Z-coordinate axis direction at node number 4 (c.g. location) when an angular rotation of θ_{y4} is imposed. This expression for F_{z4} appears reasonable when it is realized that the moment required to induce the angular rotation θ_{y4} is given by

$$M_{y4} = 405{,}336{,}400\ \theta_{y4} \qquad \text{(B-14b)}$$

It should be cautioned that since the LEM structure is relatively very complex, its representation as an assemblage of bars as sketched throughout this report should not be interpreted literally. Such an interpretation has been found to be misleading.

C. DETERMINATION OF THE LEM STIFFNESS MATRIX FOR 45° AIR LOAD ORIENTATION CONDITION

As depicted in Figure B-1, the 45° airload orientation situation no longer coincides with the LEM plane of symmetry. Thus, the LEM element force-displacement relationships have to be approximated with respect to this 45° orientation utilizing the flexibility matrices given in Reference (4). A brief outline of the steps developed to obtain the final LEM stiffness matrix used in the 45° airload orientation analysis is given in this section.

1. First, by combining the flexibility matrices given in Reference (4) and the appropriate equilibrium equations for the symmetric and antisymmetric loading cases, stiffness matrices for 1/2 the LEM structure are obtained for each of the respective loading cases.
2. Stiffness matrices for the other half of the LEM structure are obtained by the proper substitution of simple transformation expressions into the stiffness matrices derived in item (1).
3. A complete stiffness matrix for the entire LEM structure is then obtained by summing up the four individual matrices determined in items (1) and (2). The resulting stiffness matrix is transformed into a primed reference system employed in the 45° airload orientation analysis.
4. Assuming the LEM structure to be symmetric about the 45° airload direction, the transformed LEM element force-displacement relationships are next subdivided into symmetric and antisymmetric loading cases. Since the symmetric loading case with respect to the 45° airload orientation is only of interest, the element force-displacement relationships obtained for the antisymmetric loading case is discarded and the equations obtained for the symmetric case are used in the 45° airload orientation analysis.

Referring to step 1, the LEM stiffness matrix for the antisymmetric loading case is determined in the same manner as was the stiffness matrix for the symmetric loading case treated in the first part of this Appendix.

Referring to Reference (4), the antisymmetric forces acting on the LEM are related to the Bell notation by the expression

$$\begin{Bmatrix} F_{41} \\ F_{47} \\ Y_{cg} \\ M_{xcg} \\ M_{zcg} \end{Bmatrix} = \left[T_A \right] \begin{Bmatrix} M_{x4} \\ F_{y1} \\ F_{y3} \\ F_{y4} \\ M_{z4} \end{Bmatrix} \qquad \text{(B-15)}$$

where T_A is given for the antisymmetric loading case in Reference (10) as

$$\left[T_A\right] = \begin{bmatrix} 0 & 0 & 1 & 0 & 0 \\ 0 & 1 & 0 & 0 & 0 \\ 0 & 0 & 0 & 2 & 0 \\ 2 & 0 & 0 & 0 & 0 \\ 0 & 0 & 0 & 0 & 2 \end{bmatrix} \tag{B-15a}$$

The corresponding Bell notation is shown below

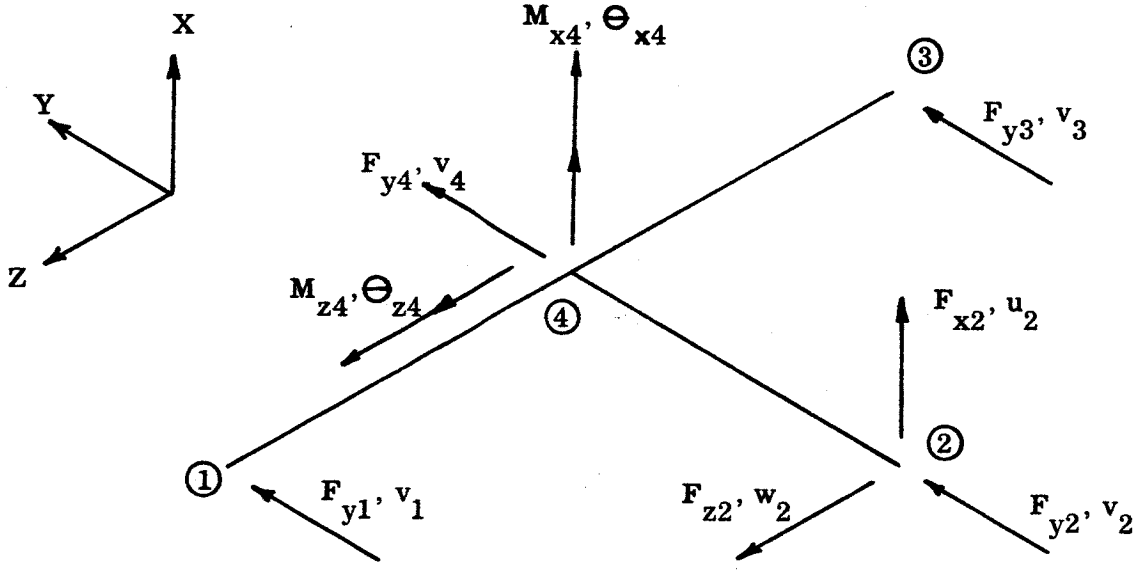

Figure B-4

Node points 1, 2 and 3 are the attachment points between the LEM and the Adapter, and node point 4 is the c.g. of the LEM.

Transforming the forces and displacements of Reference 4 yields the following displacement-force expression in Bell notation as

$$\begin{Bmatrix} \Theta_{x4} \\ v_1 \\ v_3 \\ v_4 \\ \Theta_{z4} \end{Bmatrix} = \left[T_A\right]^T \left[f_A\right] \left[T_A\right] \begin{Bmatrix} M_{x4} \\ F_{y1} \\ F_{y3} \\ F_{y4} \\ M_{z4} \end{Bmatrix} \tag{B-16}$$

The matrix $[T_A]$ is given by equation (B-15a) and $[f_A]$ is the flexibility matrix for the antisymmetric loading obtained from Reference (4) as

$$[f_A] = 10^{-7} \times \begin{bmatrix} 667.8 & -125.2 & 25.48 & 0.6980 & -0.1493 \\ -125.2 & 652.9 & 45.13 & -1.152 & 0.1776 \\ 25.48 & 45.13 & 32.99 & -0.0276 & 0.0296 \\ 0.6980 & -1.152 & -0.0276 & 0.00997 & -0.00108 \\ -0.1493 & 0.1776 & 0.0296 & -0.00108 & 0.00620 \end{bmatrix} \quad \text{(B-16a)}$$

Solving Equation (B-16) for the forces yields

$$\begin{Bmatrix} M_{x4} \\ F_{y1} \\ F_{y3} \\ F_{y4} \\ M_{z4} \end{Bmatrix} = [K_{2r}] \begin{Bmatrix} \theta_{x4} \\ v_1 \\ v_3 \\ v_4 \\ \theta_{z4} \end{Bmatrix} \quad \text{(B-17)}$$

Where $[K_{2r}]$ is the stiffness matrix for the LEM structure depicted in Figure B-4 and is given by

$$[K_{2r}] = \left[[T_A]^T [f_A] [T_A] \right]^{-1} \quad \text{(B-18)}$$

Comparison of the forces given in equation (B-17) and Figure B-4 now indicate that F_{x2}, F_{y2} and F_{z2} are the reations. By rewriting the appropriate static equilibrium relations for the antisymmetric loading, the reactions (or unknown forces) in terms of the known forces are determined from

$$\begin{Bmatrix} F_{x2} \\ F_{y2} \\ F_{z2} \end{Bmatrix} = [E_A] \begin{Bmatrix} M_{x4} \\ F_{y1} \\ F_{y3} \\ F_{y4} \\ M_{z4} \end{Bmatrix} \quad \text{(B-19)}$$

The equilibrium matrix $[E_A]$ for the antisymmetric loading case as obtained from Reference (6) is

$$[E_A] = \begin{bmatrix} 0 & 0 & 0 & -0.04218 & -0.008628 \\ 0 & -1.0 & -1.0 & -1.0 & 0 \\ 0.008628 & -1.0 & -1.0 & -0.001208 & 0 \end{bmatrix} \quad \text{(B-20)}$$

Finally, the element force-displacement equations for the LEM antisymmetric loading case are given by the following matrix equation which is similar to Equation (B-12) for the symmetrical loading case.

$$\left\{\begin{array}{c} M_{x4} \\ F_{y1} \\ F_{y3} \\ F_{y4} \\ M_{z4} \\ \hline F_{x2} \\ F_{y2} \\ F_{z2} \end{array}\right\} = \left[\begin{array}{c|c} & \\ \left[K_{2r}\right] & \left[K_{2r}\right]\left[E_A\right]^T \\ & \\ \hline & \\ \left[E_A\right]\left[K_{2r}\right] & \left[E_A\right]\left[K_{2r}\right]\left[E_A\right]^T \\ & \end{array}\right] \left\{\begin{array}{c} \theta_{x4} \\ v_1 \\ v_3 \\ v_4 \\ \theta_{z4} \\ \hline u_2 \\ v_2 \\ w_2 \end{array}\right\} \qquad \text{(B-21)}$$

Matrices $\left[K_{2r}\right]$ and $\left[E_A\right]$ are defined by Equations (B-18) and (B-20) respectively.

Again, the terms relating to the forces and displacements must be rearranged so that they are compatible with Bell notation. This rearrangement yields the matrix expression

$$\left\{\begin{array}{c} F_{x2} \\ M_{x4} \\ F_{y1} \\ F_{y2} \\ F_{y3} \\ F_{y4} \\ F_{z2} \\ M_{z4} \end{array}\right\} = \left[K_A\right] \left\{\begin{array}{c} u_2 \\ \theta_{x4} \\ v_1 \\ v_2 \\ v_3 \\ v_4 \\ w_2 \\ \theta_{z4} \end{array}\right\} \qquad \text{(B-22)}$$

where $\left[K_A\right]$ is the stiffness matrix for the antisymmetric loading case for one-half the LEM structure.

Using the stiffness matrices derived for the symmetric and antisymmetric loading cases for one-half the LEM structure, the element force-displacement relations for the other half of the LEM structure is determined in the following manner. Figure B-5 depicts the forces for the symmetric and antisymmetric loads on both halves of the LEM structure.

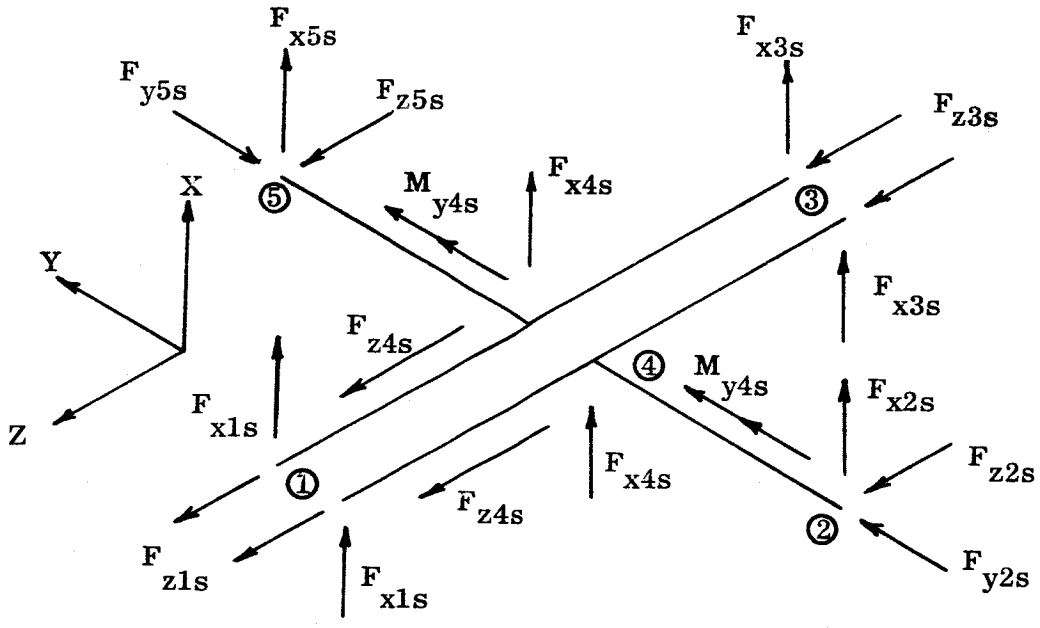

a) Symmetric Loading

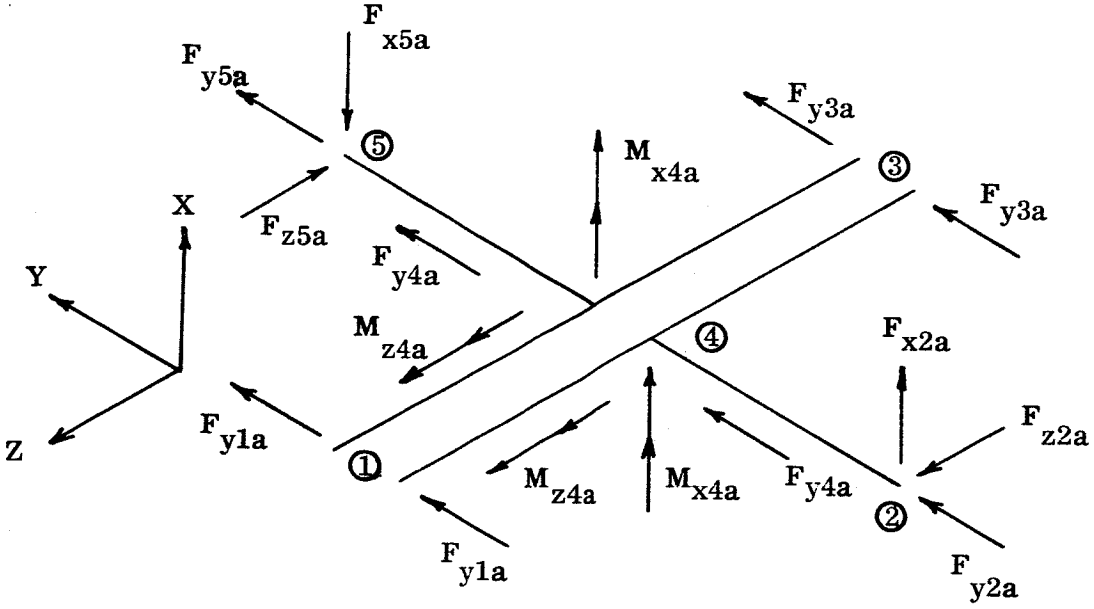

b) Anti-Symmetric Loading

Figure B-5

Node points 1, 2, 3 and 5 shown in Figure B-5 are the attachment points of the entire LEM to the whole Adapter structure and point 4 is again the c.g. of the LEM structure.

The forces and displacements at point 5 and point 2 are related by the following expressions:

$$F_{x2} = F_{x5} \qquad F_{y2} = -F_{y5} \qquad F_{z2} = F_{z5}$$
$$u_2 = u_5 \qquad v_2 = -v_5 \qquad w_2 = w_5 \tag{B-23}$$

for the symmetric loading case

and

$$F_{x2} = -F_{x5} \qquad F_{y2} = F_{y5} \qquad F_{z2} = -F_{z5}$$
$$u_2 = -u_5 \qquad v_2 = v_5 \qquad w_2 = -w_5 \tag{B-24}$$

for the antisymmetric loading case.

Substitution of Equations (B-23) and (B-24) into Equations (B-13) and (B-22) respectively and rearranging, yields the force-displacement relationships for that half of the LEM which contains point 5. Thus, for the symmetric loading case these force-displacement relationships are given by

$$\begin{Bmatrix} F_{x1} \\ F_{x3} \\ F_{x4} \\ F_{x5} \\ F_{y5} \\ M_{y4} \\ F_{z1} \\ F_{z3} \\ F_{z4} \\ F_{z5} \end{Bmatrix} = [K_3] \begin{Bmatrix} u_1 \\ u_3 \\ u_4 \\ u_5 \\ v_5 \\ \theta_{y4} \\ w_1 \\ w_3 \\ w_4 \\ w_5 \end{Bmatrix} \tag{B-25}$$

and for the antisymmetric loading case they are given by

$$\begin{Bmatrix} F_{x4} \\ M_{x4} \\ F_{y1} \\ F_{y3} \\ F_{y4} \\ F_{y5} \\ F_{z5} \\ M_{z4} \end{Bmatrix} = \left[K_4 \right] \begin{Bmatrix} u_4 \\ \theta_{x4} \\ v_1 \\ v_3 \\ v_4 \\ v_5 \\ w_5 \\ \theta_{z4} \end{Bmatrix} \qquad \text{(B-26)}$$

The matrices $\left[K_3 \right]$ and $\left[K_4 \right]$ are the stiffness matrices for that part of the LEM containing point 5 as shown in Figure B-5 .

The complete stiffness matrix of the entire LEM structure is obtained by adding all the individual symmetric and antisymmetric stiffness matrices. Thus, the complete LEM stiffness matrix is obtained from the matrix equation.

$$\left[K_{LEM} \right] = \left[\bar{K}_1 \right] + \left[K_A \right] + \left[K_3 \right] + \left[K_4 \right] \qquad \text{(B-27)}$$

where matrices $\left[\bar{K}_1 \right]$, $\left[K_A \right]$, $\left[K_3 \right]$ and $\left[K_4 \right]$ are defined by Equations (B-13), (B-22), (B-25) and (B-26) respectively.

The forces associated with Equation (B-27) are shown in Figure B-6 .

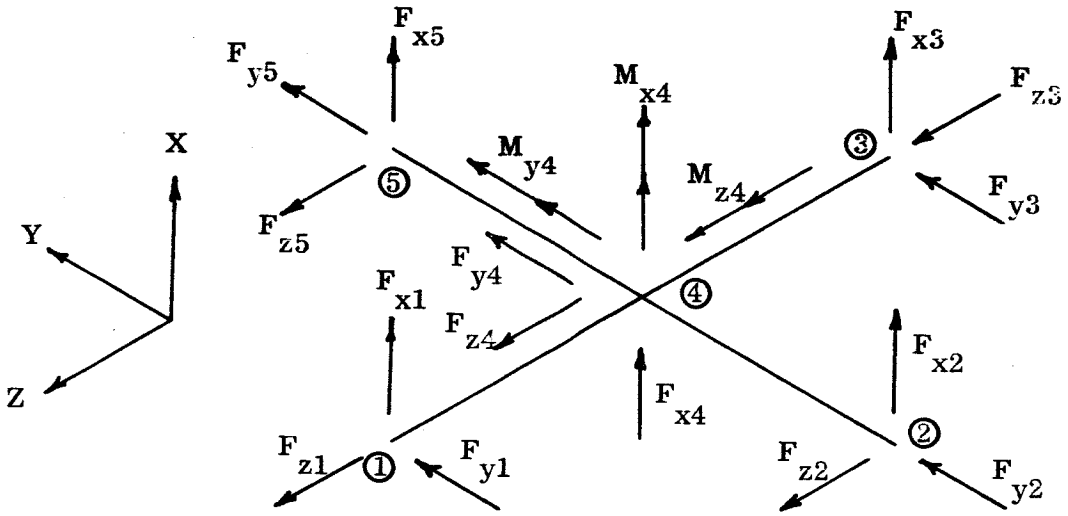

Figure B-6

These forces and corresponding displacements are referred to in the coordinate system adopted for the 0° airload orientation condition analysis. However, to perform the symmetric load analysis for the 45° airload orientation condition, the complete LEM stiffness matrix given by Equation (B-27) must be transformed to a new coordinate reference system. The new reference system is shown as the primed coordinates in Figure B-7. The angle between the two airload directions is denoted, for convenience by β.

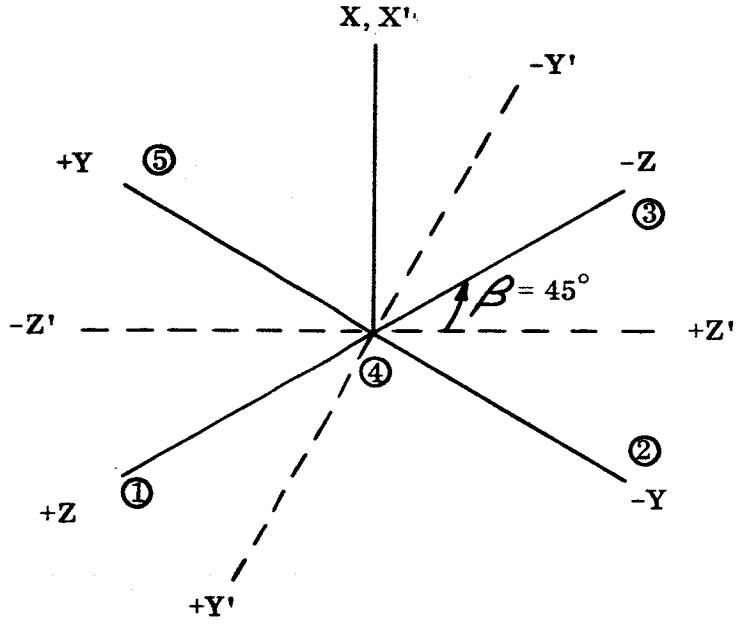

Figure B-7

Thus, the X, Y, Z axes define the 0° airload direction and the X', Y', Z' axes define the 45° airload direction. In addition to these two coordinate axis systems, Figure B-7 also shows the location of the LEM attachment or node points (see Figure B-5). The procedure used to transform the complete LEM stiffness matrix to the new reference system is discussed next.

Referring to Figure B-6 , the forces and moments at all the node points must be first transformed to the X', Y', Z' reference system. Taking node point 2 as an example, the appropriate transformation is obtained with the aid of Figure B-8.

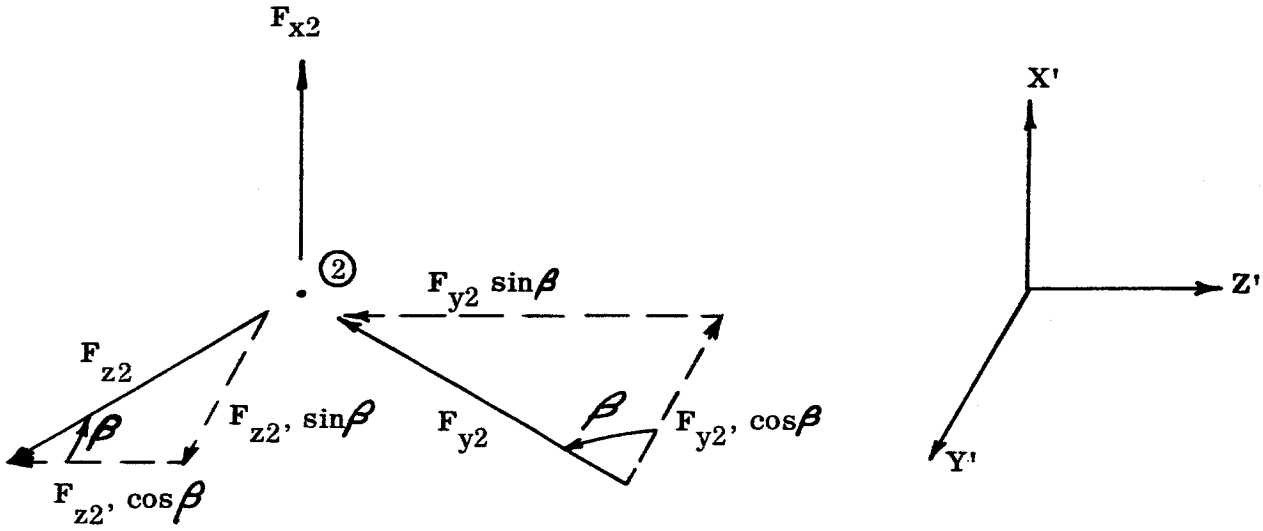

Figure B-8

From Figure B-8 it is noted that

$$\begin{aligned} F'_{x2} &= F_{x2} \\ F'_{y2} &= F_{z2}\sin\beta - F_{y2}\cos\beta \\ F'_{z2} &= -F_{z2}\cos\beta - F_{y2}\sin\beta \end{aligned} \tag{B-28}$$

or in matrix form

$$\begin{Bmatrix} F'_{x2} \\ F'_{y2} \\ F'_{z2} \end{Bmatrix} = \left[T_{PR}\right] \begin{Bmatrix} F_{x2} \\ F_{y2} \\ F_{z2} \end{Bmatrix} \tag{B-29}$$

where the transformation matrix $\left[T_{PR}\right]$ is given by

$$\left[T_{PR}\right] = \begin{bmatrix} 1 & 0 & 0 \\ 0 & -\cos\beta & \sin\beta \\ 0 & -\sin\beta & -\cos\beta \end{bmatrix} \tag{B-30}$$

The transformation matrices required at each node point of the LEM are determined in the manner just described. Once these transformation matrices are defined the element force-displacement relationships for the LEM referred to the primed coordinate axis system is given by

$$\{F'\} = [T][K_{LEM}][T]^T\{u'\} \qquad \text{(B-31)}$$

where

$[K_{LEM}]$ is given by Equation (B-27)

$[T]$ is the expanded form (18 x 18 order) of Equation (B-30)

$[T]^T$ is the transpose of the expanded transformation matrix $[T]$

and

$\{F'\}, \{u'\}$ are the column of forces and displacements in the primed system which coincides with the required 45° airload orientation reference system.

The primed forces in the column matrix $\{F'\}$ in Equation (B-31) are shown in Figure B-9 for the entire LEM. Note again that node points 1, 2, 3 and 5 are the LEM attachment points to the Adapter and node point 4 is the c.g. of the LEM.

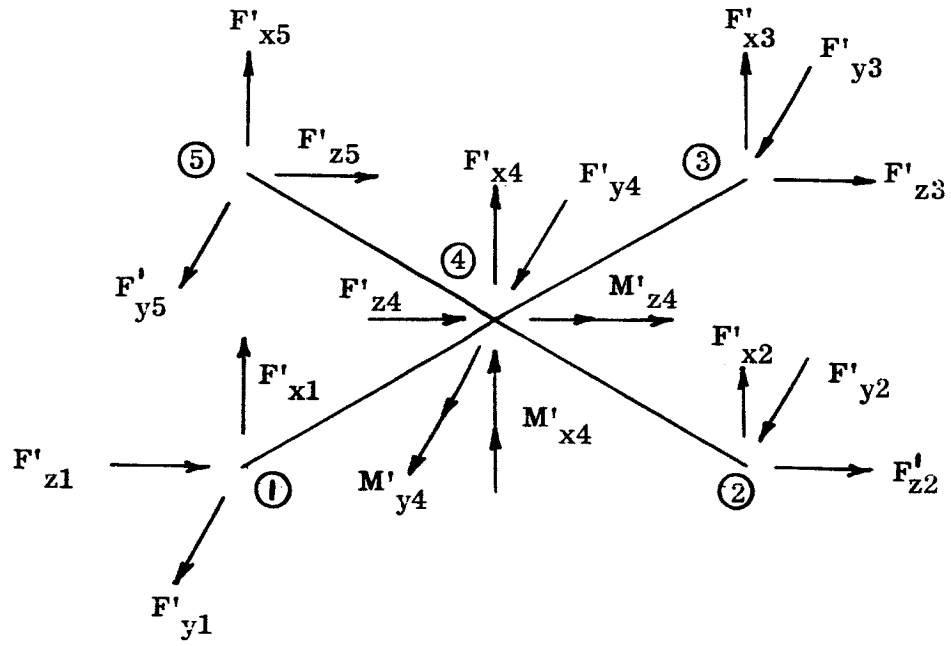

Figure B-9

As stated earlier, only the symmetric loading case for one-half the LEM structure is of interest for the 45° airload orientation condition analysis. The procedure used to obtain this matrix is approximate and is explained in the following portion of this appendix.

The total forces shown in Figure B-9 are first resolved into symmetric and anti-symmetric forces for the entire LEM as illustrated in Figure B-10.

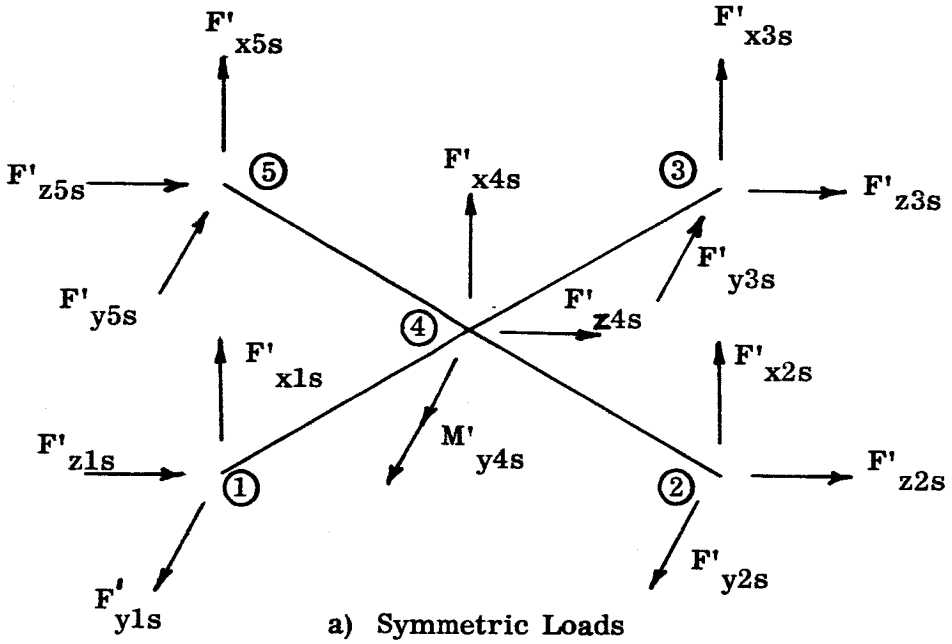

a) Symmetric Loads

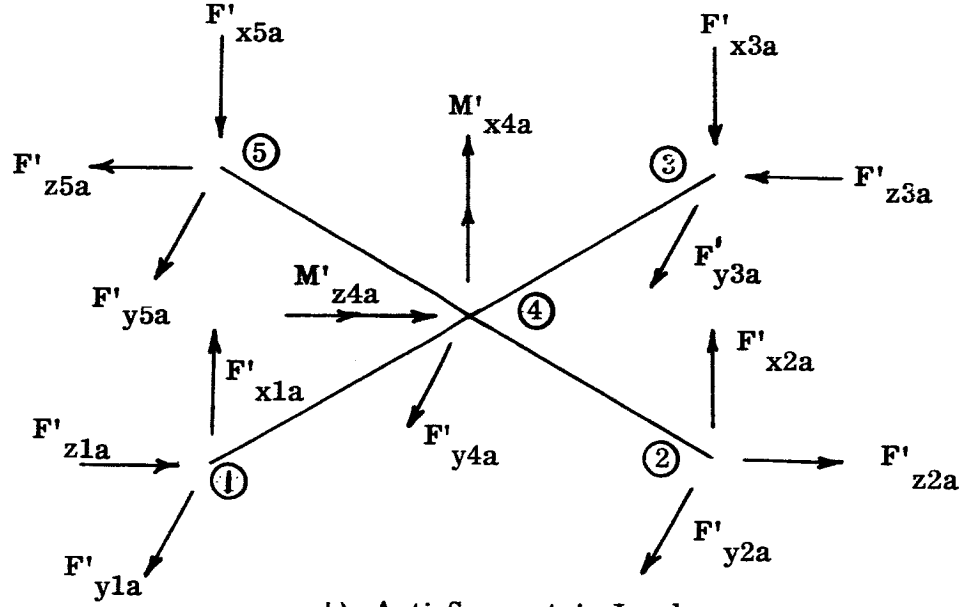

b) Anti-Symmetric Loads

Figure B-10

By equating the total corner forces to the sum of the corresponding unknown symmetric and antisymmetric forces, a sufficient number of equations are formed which yield upon their solution the symmetric loads of interest at node points 1, 2 and 4. Thus, considering node points 1 and 5, the total load in each direction is expressed in matrix notation as

$$\begin{Bmatrix} F'_{x1} \\ F'_{x5} \end{Bmatrix} = \begin{bmatrix} 1 & 1 \\ 1 & -1 \end{bmatrix} \begin{Bmatrix} F'_{x1s} \\ F'_{x1a} \end{Bmatrix}$$

$$\begin{Bmatrix} F'_{y1} \\ F'_{y5} \end{Bmatrix} = \begin{bmatrix} 1 & 1 \\ -1 & 1 \end{bmatrix} \begin{Bmatrix} F'_{y1s} \\ F'_{y1a} \end{Bmatrix} \qquad \text{(B-32)}$$

$$\begin{Bmatrix} F'_{z1} \\ F'_{z5} \end{Bmatrix} = \begin{bmatrix} 1 & 1 \\ 1 & -1 \end{bmatrix} \begin{Bmatrix} F'_{z1s} \\ F'_{z1a} \end{Bmatrix}$$

Solution of Equation (B-32) yields the symmetric and antisymmetric components of the total load as

$$\begin{Bmatrix} F'_{x1s} \\ F'_{x1a} \end{Bmatrix} = \begin{bmatrix} 1/2 & 1/2 \\ 1/2 & -1/2 \end{bmatrix} \begin{Bmatrix} F'_{x1} \\ F'_{x5} \end{Bmatrix}$$

$$\begin{Bmatrix} F'_{y1s} \\ F'_{y1a} \end{Bmatrix} = \begin{bmatrix} 1/2 & -1/2 \\ 1/2 & 1/2 \end{bmatrix} \begin{Bmatrix} F'_{y1} \\ F'_{y5} \end{Bmatrix} \qquad \text{(B-33)}$$

$$\begin{Bmatrix} F'_{z1s} \\ F'_{z1a} \end{Bmatrix} = \begin{bmatrix} 1/2 & 1/2 \\ 1/2 & -1/2 \end{bmatrix} \begin{Bmatrix} F'_{z1} \\ F'_{z5} \end{Bmatrix}$$

Separation of the symmetric load components from Equation (B-33) results in the matrix equation

$$\begin{Bmatrix} F'_{x1s} \\ F'_{y1s} \\ F'_{z1s} \end{Bmatrix} = \left[T_F\right] \begin{Bmatrix} F'_{x1} \\ F'_{x5} \\ F'_{y1} \\ F'_{y5} \\ F'_{z1} \\ F'_{z5} \end{Bmatrix} \tag{B-34}$$

where

$$\left[T_F\right] = \begin{bmatrix} 1/2 & 1/2 & 0 & 0 & 0 & 0 \\ 0 & 0 & 1/2 & -1/2 & 0 & 0 \\ 0 & 0 & 0 & 0 & 1/2 & 1/2 \end{bmatrix} \tag{B-35}$$

The expressions for the symmetric loads acting at node point 2 are derived in the same manner as described above for point 1, thus

$$\begin{Bmatrix} F'_{x2s} \\ F'_{y2s} \\ F'_{z2s} \end{Bmatrix} = \left[T_F\right] \begin{Bmatrix} F'_{x2} \\ F'_{x3} \\ F'_{y2} \\ F'_{y3} \\ F'_{z2} \\ F'_{z3} \end{Bmatrix} \tag{B-36}$$

where $\left[T_F\right]$ is given by Equation (B-35). Finally equating the total forces and moments to the symmetric loads at node point 4 of one-half the LEM structure yields

$$\begin{aligned} F'_{x4s} &= 1/2 \; F'_{x4} \\ M'_{y4s} &= 1/2 \; M'_{y4} \\ F'_{z4s} &= 1/2 \; F'_{z4} \end{aligned} \tag{B-37}$$

Thus, all the symmetric loads acting on one-half the LEM structure can be summarized into the following matrix equation.

$$\left\{F'_s\right\} = \left[T_s\right]\left\{F'\right\} \tag{B-38}$$

where

$\left\{F'_s\right\}$ are the forces associated with the symmetric loading case of interest

$\left\{F'_t\right\}$ are total forces acting on the LEM given by Equation (B-31)

$\left[T_s\right]$ is the transformation matrix formed from elements of Equations (B-35) and (B-37), and is given by

$$\left[\begin{array}{cccccc|cccccc|cccccc} 1/2 & 0 & 0 & 0 & 1/2 & 0 & & & & & & & & & & & & \\ 0 & 1/2 & 1/2 & 0 & 0 & 0 & & & & & & & & & & & & \\ 0 & 0 & 0 & 1/2 & 0 & 0 & & & & & & & & & & & & \\ \hline & & & & & & 1/2 & 0 & 0 & 0 & -1/2 & 0 & & & & & & \\ & & & & & & 0 & 1/2 & -1/2 & 0 & 0 & 0 & & & & & & \\ & & & & & & 0 & 0 & 0 & 0 & 0 & 1/2 & & & & & & \\ \hline & & & & & & & & & & & & 1/2 & 0 & 0 & 0 & 1/2 & 0 \\ & & & & & & & & & & & & 0 & 1/2 & 1/2 & 0 & 0 & 0 \\ & & & & & & & & & & & & 0 & 0 & 0 & 1/2 & 0 & 0 \end{array}\right] \tag{B-39}$$

The symmetric displacements are determined in a manner similar to that employed to obtain the symmetric forces and consequently can be shown to be given by the matrix equation

$$\left\{u'_s\right\} = \left[T_s\right]\left\{u'_t\right\} \tag{B-40}$$

where

$\left\{u'_s\right\}$ are the symmetric displacements for the symmetric loading case of interest

$\left\{u'_t\right\}$ are the total displacements of the total LEM structure for the 45° airload orientation condition

Solving Equation (B-40) for the total displacements yields

$$\left\{u'_t\right\} = \left[T_s\right]^T\left\{u'_s\right\} \tag{B-41}$$

where $[T_s]^T$ is the transpose of the matrix $[T_s]$ defined by Equation (B-39). The element force-displacement relationships for the LEM structure in the primed system given by Equation (B-31) is redefined for convenience as

$$\left\{F'_t\right\} = \left[\bar{K}_2\right]\left\{u'_t\right\} \tag{B-42}$$

Substitution of Equations (B-38) and (B-41) into (B-42) yields the appropriate LEM element force-displacement relationships for the symmetric loading case as

$$\begin{Bmatrix} F_{x1} \\ F_{x2} \\ F_{x4} \\ F_{y1} \\ F_{y2} \\ M_{y4} \\ F_{z1} \\ F_{z2} \\ F_{z4} \end{Bmatrix} = \left[K_{s2}\right] \begin{Bmatrix} u_1 \\ u_2 \\ u_4 \\ v_1 \\ v_2 \\ \theta_{y4} \\ w_1 \\ w_2 \\ w_4 \end{Bmatrix} \tag{B-43}$$

where

$$\left[K_{s2}\right] = \left[T_s\right]\left[\bar{K}_2\right]\left[T_s\right]^T \tag{B-44}$$

The transformation matrix $[T_s]$ is defined by Equation (B-39) and $[\bar{K}_2]$ as defined by Equation (B-42) is the stiffness matrix of the entire LEM structure in the primed system. The matrix $[K_{s2}]$ is the desired symmetric stiffness matrix.

Thus, the LEM element force-displacement relationships given by Equation (B-43) are used in the 45° airload orientation condition analysis and $[K_{s2}]$ is presented in Figure 11 of this report.

It is of interest to note that from a cursory comparison of the elements in the stiffness matrices obtained for the LEM in Figures 10 and 11, indications are that, in general, the LEM is less stiff with regard to the 45° airload orientation condition than for the 0° airload orientation condition. Thus, for example, Equations (B-14a) and (B-14b) derived from Figure 10 are comparable to the following equations derived from Figure 11.

$$F_{z90} = 295{,}804\,\theta_{y90}$$
$$M_{y90} = 206{,}178{,}000\,\theta_{y90} \qquad \text{(B-45)}$$

The 295,804 lb and 206,178,000 in.-lb stiffness coefficients of Equation (B-45) are approximately comparable to 801,227 lb and 405,336,400 in.-lb of Equations (B-14a) and (B-14b).